Functional assessment of myeloid-derived suppressor cells, mesenchymal stromal cells, and regulatory T cells for the control of T-cell function: implications for graft-versus-host disease

Dissertation

der Mathematisch-Naturwissenschaftlichen Fakultät

der Eberhard Karls Universität Tübingen

zur Erlangung des Grades eines

Doktors der Naturwissenschaften

(Dr. rer. nat.)

vorgelegt von

Darina Marlena Siegmund geb. Brosch

aus Überlingen

Tübingen

2018

Gedruckt mit Genehmigung der Mathematisch-Naturwissenschaftlichen Fakultät der Eberhard Karls Universität Tübingen.

Tag der mündlichen Qualifikation:	23.02.2018
Dekan:	Prof. Dr. Wolfgang Rosenstiel
1. Berichterstatter:	Prof. Dr. Dominik Hartl
2. Berichterstatter:	Prof. Dr. Rupert Handgretinger

Danksagung

Zuerst möchte ich mich bei Prof. Dr. D. Hartl, Prof. Dr. R. Handgretinger und Dr. Dr. M. Mezger bedanken, dass Sie mir die Möglichkeit und Ihr Vertrauen für die Anfertigung dieser Doktorarbeit gegeben haben.

Dr. Dr. Markus Mezger danke ich für seine fachliche, methodische und persönliche Unterstützung, sein offenes Ohr bei allen Schwierigkeiten, die vielen hilfreichen Ideen und die exzellente Betreuung! Vielen Dank für dein Engagement während der gesamten Zeit und die sehr gute Zusammenarbeit!

Prof. Dr. Dominik Hartl danke ich für die wissenschaftlichen Anregungen und Ideen, die konstruktive Kritik an meinen Texten, die hilfreichen Tipps und richtungsweisenden Diskussionen, die Möglichkeit zur Teilnahme an der AACR-Konferenz 2017 sowie die Betreuung und Begutachtung meiner Arbeit!

Prof. Dr. Rupert Handgretinger danke ich besonders für die Zweitbetreuung mit zielführenden Diskussionen und Ratschlägen sowie der Begutachtung meiner Dissertation.

Der José Carreras Leukämie-Stiftung danke ich für die finanzielle Unterstützung des Projektes!

Ein großes „Dankeschön“ an Renate Koch, Iris Schäfer und Caroline Baden für die hervorragende technische Unterstützung und die gute Zusammenarbeit!

Vielen Dank an alle Blutspender sowie allen Knochenmarkspendern, die einer Verwendung der Zellen zu Forschungszwecken zugestimmt haben!

Vielen lieben Dank an alle Kolleginnen und Kollegen in den verschiedenen Laboren und Arbeitsgruppen der Kinderklinik für jegliche Hilfe & Unterstützung, den Austausch, die vielen hilfreiche Tipps, die lieben Worte und netten Gesten, wenn es gerade mal wieder nicht nach Plan lief sowie die unzähligen Lacher zwischen Bench und PC. Thanks a lot to everyone!

And thanks to everyone who tried to improve my English and who proof-read my thesis! :-)

Ich möchte mich ganz herzlich bei meinen beiden Familien und meinen Freunden für die Unterstützung sowie für die vielen lieben und motivierenden Worte bedanken!!!

Einen besonderen DANK für so vieles in den letzten Jahren an Benjamin!

List of contents

1 Summary

Unbalanced T-cell responses, such as occurring during graft-versus-host disease (GvHD) in patients after allogenic transplantation, can be fatal. Human mesenchymal stromal cells (MSCs) are already used for the treatment of GvHD, however, their isolation requires a bone marrow puncture and their expansion needs *in vitro* care for several weeks. This study focused on the investigation of different immunosuppressive cell types and on the systematic comparison of their functional capacity to suppress T-cell function, in order to find an alternative for MSCs. Polymorphonuclear myeloid-derived suppressor cells (PMN-MDSCs) and regulatory T cells (Tregs) were isolated by magnetic separation from peripheral blood. In order to investigate the T-cell suppressive capacity of each cell type, cells were co-cultured with stimulated responder cells and after 4-5 days of incubation, T-cell proliferation and secretion of Interferon-γ (IFNγ) were analyzed by flow cytometry and ELISA, respectively. Furthermore, the requirement of cell-to-cell contact was investigated by transwell experiments and the available cell numbers after isolation were assessed, with respect to clinical application.

MSCs, Tregs, and freshly isolated PMN-MDSCs inhibited T-cell proliferation and secretion of IFNγ in a concentration-dependent manner. Thereby, PMN-MDSCs showed the strongest inhibition of T-cell proliferation compared to MSCs and Tregs, but cell number of MDSCs was limited in peripheral blood of healthy donors. Thus, PMN-MDSCs were generated by cytokine induction from peripheral blood mononuclear cells (PBMCs) and from bone marrow mononuclear cells (BMMCs) *in vitro*. BMMC-derived PMN-MDSCs effectively suppressed T-cell proliferation and dampened secretion of IFNγ, while PMN-MDSCs generated from PBMCs showed weaker inhibition. The effects of *in vitro*-generated PMN-MDSCs were partially dependent on cell-to-cell contact, similar to freshly isolated PMN-MDSCs. In order to increase the T-cell suppressive effect at lower cell concentrations, MSCs and freshly isolated PMN-MDSCs, as well as MSCs and BMMC-derived PMN-MDSCs, were combined for the analysis of T-cell suppression and compared with the effect of each cell type alone. MSCs combined with freshly isolated PMN-MDSCs demonstrated no additional effect in this study, whereas MSCs combined with BMMC-derived PMN-MDSCs showed an increased T-cell suppressive effect than each cell type alone. However, the available cell number of BMMC-derived PMN-MDSCs was too low for a clinical application. In another set of experiments, isolated $CD34^+$ hematopoietic stem cells (HSCs) were cultured and stimulated with a mix of cytokines and growth factors to generate MDSCs. The HSC-derived MDSCs

strongly suppressed T-cell proliferation and the secretion of IFNγ in a concentration-dependent manner. The inhibition of IFNγ release by HSC-derived MDSCs was greater than the reduction by freshly isolated PMN-MDSCs or BMMC-derived PMN-MDSCs. In addition, a great expansion of $CD33^+$ MDSCs was detected during HSC-derived generation.

Overall, this study demonstrates a systematical comparison of the T-cell suppressive effect of various immunomodulatory cell types (MSCs, freshly isolated PMN-MDSCs, and six differently *in vitro* generated MDSCs). Freshly isolated as well as generated MDSCs strongly suppressed T-cell proliferation and the secretion of the pro-inflammatory cytokine IFNγ *in vitro.* The HSC-derived MDSCs showed strong suppression of effector T cells and IFNγ release as well as great expansion rates, therefore these cells might represent a novel cellular therapeutic to dampen excessive T-cell responses by adoptive transfer of MDSCs for the management of GvHD.

2 Zusammenfassung

Unkontrollierte Immunantworten der T-Zellen, wie sie bei einer *Graft-versus-Host-Disease* (GvHD) nach allogenen Transplantation auftreten, können zum Tod der Patienten führen. Zur Behandlung der GvHD gibt es unterschiedliche Therapieansätze, unter anderem die Gabe von humanen mesenchymalen Stromazellen (MSCs), da diese Zellen immunsupprimierende Eigenschaften haben. Bei der Verwendung von MSCs sind eine Knochenmarkspunktion beim Spender sowie eine mehrwöchige Expansion der Zellen im Labor notwendig. Im Rahmen dieses Projektes wurden weitere Zellpopulationen mit immunsupprimierenden Eigenschaften untersucht, um diese zu vergleichen und eine therapeutische Alternative für MSCs zu finden. Es wurden polymorphnukleäre, myeloide Suppressorzellen (*myeloid-derived suppressor cells*, PMN-MDSCs) und regulatorische T-Zellen (Tregs) aus den mononukleären Zellen des peripheren Bluts (PBMCs) mit Hilfe von magnetischer Separation isoliert und getestet. Hierzu wurden die Proliferation von T-Zellen nach Ko-Kultivierung mit den immunsupprimierenden Zellen mittels Durchflusszytometrie und die Ausschüttung des pro-inflammatorischen Zytokins Interferon-γ mittels ELISA untersucht. Zusätzlich wurden die Abhängigkeit von direktem Zellkontakt und die verfügbare Zellzahl analysiert.

Sowohl MSCs als auch PMN-MDSCs und Tregs hemmten konzentrationsabhängig die Proliferation der T-Zellen und die Sekretion von Interferon-γ. Frisch isolierte PMN-MDSCs zeigten im Vergleich zu MSCs und Tregs die stärkste Hemmung der T-Zellproliferation mit etwa 95 % Reduktion bei einem Verhältnis allogener, stimulierter PBMCs zu PMN-MDSCs von 1:0,5. Da die Zellzahl von PMN-MDSCs mit rund 0,5 % der PBMCs im Blut von gesunden Spendern für eine klinische Anwendung zu gering war, wurde die Generierung von MDSCs mittels Zytokin-Stimulation zuerst aus mononukleären Zellen des peripheren Bluts und anschließend aus mononukleären Zellen des Knochenmarks untersucht. Diese so generierten Zellpopulationen hemmten ebenfalls konzentrationsabhängig die T-Zell-proliferation und die Freisetzung von Interferon-γ. Die Hemmung der generierten und der frisch isolierten PMN-MDSCs war jeweils bei direktem Zellkontakt stärker ausgeprägt als wenn nur lösliche Faktoren die T-Zellen beeinflussten. Allerdings war trotz dieser unterschiedlichen Ansätze zur Generierung von PMN-MDSCs die Ausbeute für eine therapeutische Anwendung in der Klinik zu gering. Daher wurden auch Kombinationen von verschiedenen immunsupprimierenden Zellen in einem gemeinsamen Ansatz getestet, um einen additiv hemmenden Effekt bei niedrigen Konzentrationen zu erzielen. In dieser Studie war bei einer niedrigen Konzentration von MSCs kombiniert mit frisch isolierten PMN-

MDSCs die Hemmung der T-Zellproliferation geringer als die Hemmung der jeweiligen Zelltypen alleine. Bei der Kombination aus MSCs und Zytokin-induzierten MDSCs aus Knochenmarkzellen wurde ein additiver Effekt in der Hemmung der T-Zellproliferation gemessen, jedoch war die Ausbeute bei der Generierung der MDSCs aus Knochenmark mit etwa 1 % der eingesetzten Zellen immer noch zu gering.

Um eine höhere Zellausbeute zu erreichen, wurde anschließend versucht, MDSCs aus hämatopoetischen Stammzellen ($CD34^+$ HSCs) nach einem bereits publizierten Protokoll (Casacuberta-Serra *et al*. 2017) zu generieren. Die Zytokin-induzierten MDSCs aus $CD34^+$ HSCs zeigten dabei eine starke, konzentrationsabhängige Hemmung der T-Zellproliferation und der Sekretion von Interferon-γ. Bei einem Verhältnis von 1:0,5 der allogenen, stimulierten PBMCs zu MDSCs aus HSCs hemmten MDSCs etwa 90 % der T-Zell-proliferation und etwa 95 % der Interferon-γ-Freisetzung im Vergleich zur unbehandelten Kontrolle. Außerdem wurde eine deutliche Expansion der $CD33^+$ MDSCs von über 70-fachem Zellwachstum bei dieser Generierung gemessen. Die Reinheit der $CD33^+$ MDSCs im entsprechenden Gate war nach der magnetischen Separation über 95 %.

Insgesamt wurden in dem Projekt eine Vielzahl an immunmodulatorischen Zellen (MSCs, frisch isolierte PMN-MDSCs, Tregs und sechs auf unterschiedliche Weise generierte MDSCs) hinsichtlich ihrer hemmenden Wirkung auf T-Zellen untersucht. Zusätzlich zu den bereits zur GvHD-Behandlung angewendeten MSCs zeigen die $CD33^+$ MDSCs aus hämatopoetischen Stammzellen das größte Potenzial für eine klinische Anwendung. Die Daten dieser Studie legen deshalb nahe, dass eine GMP-gerechte Generierung dieser Zellen für eine klinische Anwendung in Betracht gezogen werden kann.

3 Introduction

3.1 Stem cell transplantation

Hematopoietic stem cell transplantation (HSCT) is a potentially curative approach for many malignant and nonmalignant diseases, such as leukemia, lymphoma, neuroblastoma, aplastic anemia, thalassemia and genetic immunodeficiencies (Qian *et al.* 2013). In the early 1960s, the procedure of HSCT was discovered as a cure for hematological cancers (Barriga *et al.* 2012) and in 2015, over 6.000 HSCT were performed in Germany (DRST 2015). There are different purposes for HSCT: 1) To replace the hematopoietic system from the patient with the one of the donor, e.g. in patients with severe blood disorders; 2) to save a cancer patient from the toxic side effects of chemotherapy and/or radiation; 3) to increase the attack to malignant cells by donor's immune cells; and 4) to abolish autoimmunity (Barriga *et al.* 2012). HSCT can be performed with autologous stem cells from the patient itself or with allogenic stem cells from another donor, depending on the patient's disease (Barriga *et al.* 2012). The use of allogenic stem cells is limited by a suitable donor, meaning the matching of highly polymorphic molecules of the major histocompatibility complex (MHC), also called human leukocyte antigens (HLAs), because incomplete matching increases the risk of graft failure or graft-versus-host disease (GvHD) (Geneugelijk *et al.* 2014). Thereby, less than 30 % of patients who require a HSCT have a fully matching family member (Kekre and Antin 2014). Beside the HLA-system, also minor histocompatibility antigens, killer cell immunoglobulin-like receptors (KIRs) that are expressed on immune cells and many other genetic loci are associated with the outcome of HSCT and the development of GvHD (Welniak *et al.* 2007; Ting *et al.* 2013).

In addition, not only bone marrow (BM) can be used as a source of stem cells, but also umbilical cord blood and peripheral blood contains stem cells after mobilization with granulocyte colony-stimulating factor (G-CSF) (Barriga *et al.* 2012; Welniak *et al.* 2007). Studies with stem cells from two unrelated, partially matched umbilical cord blood donors have similar engraftment and overall survival than with grafts from adults (Barriga *et al.* 2012; Welniak *et al.* 2007). Stem cells from umbilical cord blood have the advantages that they are soon available if the cells were stored frozen, the naïve status of immune cells and no morbidity for the donor. In contrast, the disadvantages of these stem cells are very low cell numbers, slower immune reconstitution and the fact that a second graft or transfer of other immune cells is impossible (Barriga *et al.* 2012). Transplantations with stem cells from

peripheral blood avoids BM puncture of the donor and shows improved immune reconstitution; however, compared to umbilical cord blood, it often takes 3-4 months until a donor is available, in which the patient's disease can progress (Barriga *et al.* 2012). For transplantations of stem cells from an unrelated person, the matching of HLA-alleles A, B, C and DRB1 from donor and recipient is associated with improved survival rates (Norkin and Wingard 2017). To decrease time searching for a donor and to increase the pool of available donors, HSCT with haploidentical cells are performed (Handgretinger *et al.* 2007; Norkin and Wingard 2017). In general, conditioning should combat malignant cells and reduce host immune system to avoid graft rejection, while having minimal toxicity and risk of GvHD (Welniak *et al.* 2007). Normally, high-dose myeloablative conditioning consists of one or more cytotoxic drugs and possibly total-body irradiation, whereas reduced-intensity conditioning (RIC) contains lower doses of cytotoxic but also immunosuppressive drugs and occasionally irradiation or depletion of T cells (Welniak *et al.* 2007). In case of haploidentical HSCT, combining RIC prior to HSCT with the depletion of T and B cells in the graft demonstrated low transplant-related mortality and rapid immune reconstitution (Handgretinger *et al.* 2007). By using RIC, HSCT is also possible in older patients or patients with reduced morbidity without increasing the risk of non-relapse mortality (Welniak *et al.* 2007; Martino *et al.* 2006). Another challenge after HSCT is the recipient's treatment to avoid graft rejection or letal infections by the decreased immune system (Welniak *et al.* 2007). After autologous HSCT, two-thirds of deaths are caused by disease relapse, which is less common after allogenic HSCT due to graft-versus-tumor (GvT) reaction (Norkin and Wingard 2017).
Overall, the success of HSCT depends on various factors, such as recipient's primary disease, availability of a donor, graft selection, condition regimen prior to HSCT and maintenance therapy after HSCT (Welniak *et al.* 2007; Norkin and Wingard 2017). However, the increased number of HSCT demonstrates advances gained by basic and clinical research in this field.

3.2 Graft-versus-host disease (GvHD)

The success of HSCT is limited by GvHD, a frequent and severe complication. This medical condition is life-threatening, even lethal for approximately 15 % of patients (Blazar *et al.* 2012) and affects around 70 % of all transplant recipients (Markey *et al.* 2014). GvHD is classically divided into an acute form occurring within the first 100 days after transplantation and a chronic form that develops later. Nowadays, instead of the time of onset, the main criteria for subdividing are the clinical symptoms (Blazar *et al.* 2012), hence an overlap

syndrome is described with typical aspects of both subtypes (Sung and Chao 2013). Acute GvHD is characterized by systemic, strong inflammation and tissue damage, especially in the skin, liver and gastrointestinal (GI) tract (Blazar *et al.* 2012). Typically, first symptoms of acute GvHD appear as skin lesions around the neck and shoulders with a maculopapular rash as well as rashes on palms of hands and soles of feet, but it can get severe with blisters, ulcerates or bullae and desquamation. If the GI tract is affected, the severity will be measured by the volume of diarrhea. In addition, abdominal pain, hematochezia, anorexia, nausea, and vomiting can emerge. The severity of liver damage in patients with acute GvHD is determined by serum bilirubin (Sung and Chao 2013).

In 1997, the severity index was introduced from the Center for International Bone Marrow Transplant Registry for staging and grading of acute GvHD based on clinical symptoms of skin, liver and gastrointestinal tract and the criteria were compared to the former ones from Glucksberg that also contained the functional status (Sung and Chao 2013; Qian *et al.* 2013).
After allogenic HSCT, around 60-80% of long-term survivors suffer from the chronic form of GvHD (Markey *et al.* 2014). Chronic GvHD often shows autoimmune and fibrotic features in several target tissues, such as skin, gut, liver, joints, lungs, and mouth (Blazar *et al.* 2012).
The occurrence of GvHD depends mainly on disease stage and disparities in histo-compatibility antigens between donor and recipient. But also other risk factors are involved, such as conditioning regimen prior to HSCT, graft source, age, donor and recipient sex, type of prophylaxis and prior exposure to viruses (Flowers *et al.* 2011; Calmettes *et al.* 2015). In addition, various genetic polymorphisms affect the risk for GvHD, especially genes encoding for cytokines or chemokines, pharmacogenes and costimulatory molecules (Ting *et al.* 2013).

The pathophysiology of acute GvHD is often described as a circle consisting of three phases (Qian *et al.* 2013; Markey *et al.* 2014; Ferrara *et al.* 2009). Before transplantation takes place, patients receive transplant conditioning with chemotherapy and/or irradiation. This leads to tissue damage and the release of pro-inflammatory cytokines and danger signals, thereby stimulating antigen-presenting cells (APCs) (Qian *et al.* 2013). Damages of the GI tract can also activate the innate immune system by Toll-like receptors detecting bacterial molecules, such as lipopolysaccharide (Sung and Chao 2013). During the second phase of GvHD development, donor T cells are activated by recipient and donor APCs and by cytokines acting as co-stimulatory molecules (Qian *et al.* 2013). After activation in secondary lymphoid organs, T cells proliferate and differentiate into effector T cells (Holtan *et al.* 2014). The

overall balance of different T cell subsets and their secreted cytokines is important for the development of GvHD, however this process is still unclear (Sung and Chao 2013). In the third phase, effector T cells migrate to inflammation sites and cause tissue damage by direct effects to target tissue and by recruiting other immune cells (Sung and Chao 2013). Neutrophils, natural killer (NK) cells, natural killer T (NKT) cells, B cells, macrophages and immunosuppressive cells, e.g. Tregs, T helper 9 cells and MDSCs are probably involved in the pathomechanism of acute GvHD (Holtan *et al.* 2014). All these immune cells can secrete cytokines that boost or damp the disease, and the balance is crucial (Holtan *et al.* 2014). Due to the cytokines, the inflammation can escalate causing further tissue destruction and the cycle of pathogenesis of acute GvHD continues (Holtan *et al.* 2014).
The pathomechanism of chronic GvHD is still not well understood, but due to its characteristic fibrosis, it is probably different from the pathomechanism in acute GvHD (Markey *et al.* 2014).

To prevent the development of GvHD, several strategies are nowadays involved during treatment of HSCT patients: (1) a reduced-intensity conditioning; (2) immunosuppression by combination of drugs, e.g. a calcineurin inhibitor with either mycophenylate mofetil (MMF) or methotrexate (MTX) that both inhibit the synthesis of nucleic acid; (3) T cells are depleted in the graft or by administration of antithymocyte globin or alemtuzumab (anti-CD52 antibody), and (4) blocking of cytokine signaling, e.g. by maraviroc that blocks lymphocyte chemotaxis by CCR5 inhibition (Qian *et al.* 2013; Holtan *et al.* 2014).

Treatment of acute GvHD with grade I is performed by local therapy, but higher grades require systemic immunosuppression with a standard therapy of 1-2 mg/kg corticosteroids, mostly prednisone or methylprednisolone, per day (Qian *et al.* 2013). Only around 50 % of the patients with acute GvHD respond completely to the systemic steroid therapy. The other patients develop a steroid-refractory GvHD, for which no standard therapy is available and a poor prognosis is ascribed to (Holtan *et al.* 2014). Besides new immunosuppressive drugs, many groups are investigating different cell types as therapeutic agents and promising effects in first trials could be detected (Qian *et al.* 2013; Holtan *et al.* 2014).

3.3 Immune system

The immune system is a network of various organs, cells and molecules in living organisms that protects the body against external or internal damage. External damage can be caused by viruses, bacteria, parasites or fungi as well as other harmful substances, e.g. toxins from insects, whereas unusual growth of cells from the organism, so called neoplasm, can cause internal damage to the body. Thereby, it is very important that the body distinguishes between self and nonself molecules (Yatim and Lakkis 2015; Chaplin 2010). The immune system of humans and other mammals is divided into two main categories: the innate and the adaptive immune response. The innate immune response is inherited and starts immediately a relatively non-specific defense against every pathogen. The adaptive immune response needs to be activated by cells from the innate immune system, but the adaptive immune system leads to a specific response and an immunological memory that induces a faster and more specific immune response if the body encounters this pathogen a second time (Chaplin 2010). The innate immune system consists of physical barriers (e.g. skin), bioactive substances (e.g. lysozymes, cytokines, proteins of the complement system) and different cell types (e.g. monocytes/macrophages, neutrophils, basophils and eosinophils). The cells phagocytose pathogens and kill them directly or the cells secrete substances to destroy pathogens (Riera Romo *et al.* 2016). The antigen-presenting cells (APCs) are linking innate and adaptive immune response. Typically dendritic cells (DCs) perform this step by activating cells of the adaptive immune system (Yatim and Lakkis 2015). The adaptive immune system mainly consists of B lymphocytes, which produce immunoglobulin (Ig) and T lymphocytes (Chaplin 2010), which are further described in the following chapter.

3.3.1 Effector T cells

T lymphocytes are part of the adaptive immune system and are generated in thymus, which is referred to by the name “T cells” (Murphy 2011). All T cells express the T-cell receptor (TCR) on their cell surface. There are several different functional and phenotypical subsets of T cells, such as helper, cytotoxic, regulatory, memory and γδ T cells (Chaplin 2010). In this chapter, the focus is set towards helper and cytotoxic T cells, because these cells cause the main effect after activation by a pathogen and that’s why these cell types are also called “effector T cells” (Murphy 2011). The next chapter is focusing on regulatory T cells.

After generation of T cells in the bone marrow, they migrate to the thymus and undergo a process of selection. First, gene rearrangement occurs and the cells express the TCR, most of

them with a pair of α- and β-chain. The α:β TCR normally forms a complex with the CD3 complex that consists of a CD3γε heterodimer, a CD3δε heterodimer and a CD3ζ homodimer. T cells with γ:δ TCR-chains are exported to the periphery. The α:β T cells are then tested for binding of self-molecules presented on MHC molecules in the thymus. T cells that do not recognize self-molecules or binding with high affinity to these antigens are removed by apoptosis. T cells with the appropriate affinity to self-molecules on MHCs are expressing either CD4 or CD8 receptors on the cell surface and they migrate via blood and lymph to the peripheral lymphoid organs, where the naïve T cells become activated by APCs. The antigen is presented as a peptide bound to the MHC molecule, which binds to the TCR/CD3-complex. Thereby, $CD4^+$ T cells only bind to MHC class II molecules, which are exclusively expressed on APCs, whereas $CD8^+$ T cells only bind to MHC class I molecules, which are expressed on almost all cell types. For activation of naïve T cells, also co-stimulation and cytokine stimulation are required, e.g. by binding of B7 molecules of APCs to CD28 on T cells and IL-2. This activation leads to clonal expansion and differentiation to effector T cells depending on the cytokine milieu. These T cells only require binding of their specific antigen bound to MHC molecules and no co-stimulation to perform their function on the host cells (Chaplin 2010; Murphy 2011). $CD4^+$ T cells are also known as helper T cells (Th), because they support the immune response of other cell types. As already mentioned, naïve $CD4^+$ T cells can differentiate into several subsets of T cells and currently, several Th subsets with different functions are known: Th1, Th2, Th9, Th17, Th22, Tregs and follicular helper T cells (Ivanova and Orekhov 2015). In general, Th1 cells are characterized by the expression of the transcription factor T-bet and by the production of IFNγ and tumor necrosis factor (TNF), whereas Th2 cells mainly express the transcription factor GATA-3 and produce IL-4, IL-5, and IL-13 and thereby support the humoral immune response (Ivanova and Orekhov 2015). In most immune reactions, Th1 and Th2 cells are involved at the beginning, but after a while one cell type becomes dominant (Chaplin 2010). This polarization towards one cell type is supported by the fact that the main transcription factors of Th1 and Th2 cells are suppressing each other (Ivanova and Orekhov 2015). Also different subsets of $CD8^+$ T cells are known due to cytokine secretion; however, both types mainly act by perforin- and Fas-dependent cytotoxicity against infected or damaged host cells (Chaplin 2010; Mosmann *et al.* 1997).

In GvHD, the balance between the Th subsets is important for the development as well as its severity and its organ specificity (Henden and Hill 2015). Acute GvHD typically shows a dominance of Th1 cells with high level of the pro-inflammatory cytokines Interferon (IFN)γ

and TNF. Furthermore, the GI tract is mainly affected by Th1-mediated GvHD (Henden and Hill 2015; Markey *et al.* 2014). For example, Toren *et al.* demonstrated that patients of BM transplantation showed an increase of soluble IFNγ from the day of transplantation to the onset of acute GvHD compared to patients without GvHD (Toren *et al.* 1997). Generally, IFNγ is mainly produced by $CD4^+$ Th1 and by $CD8^+$ cytotoxic T cells during the adaptive immune response as well as by NK and by NKT cells during the innate immune response (Schoenborn and Wilson 2007). Th2 and Th17 cells are also contributing to acute GvHD, leading more often to symptoms in lung, liver or skin; however, these cell subsets are more involved in chronic GvHD (Henden and Hill 2015). In general, the balance of surrounding cytokines and thereby the activity of transcription factors is critical for the differentiation or transition of distinct T-cell subsets, and disturbances of this balance can have pathological consequences (Ivanova and Orekhov 2015).

3.3.2 Regulatory T cells

Tregs are a subset of T lymphocytes and play a central role for the immunological self-tolerance as well as the control of undesired immune reactions, such as autoimmune diseases, allergies or after transplantations (Gliwiński *et al.* 2017). The involvement of Tregs in modulating immune reactions is also demonstrated by the lack of functional Tregs in several immunodeficiencies, such as Omenn syndrome, Wiskott-Aldrich syndrome, hyper IgE syndrome and immunodysregulation polyendocrinopathy enteropathy X-linked (IPEX) syndrome (Schmetterer *et al.* 2012).

Two main subsets of Tregs are distinguished: Natural, thymus-derived Tregs and induced Tregs, which are generated in the periphery from naïve $CD4^+$ T cells (Safinia *et al.* 2013). This change to a regulatory phenotype can be induced by antigen stimulation of their T-cell receptor together with immunosuppressive cytokines, such as IL-10 and transforming growth factor (TGF)-ß and/or retinoic acid, or activation by immature dendritic cells (Sojka *et al.* 2008). Furthermore, there is evidence for the ability of natural Tregs to convey suppressive activity to conventional $CD4^+$ T cells, so called infectious tolerance (Jonuleit *et al.* 2002). Natural Tregs present only 1-3 % of total $CD4^+$ T cells in the peripheral blood of healthy individuals (Safinia *et al.* 2013). After development of natural Tregs in the thymus, stimulation with IL-2, TGF-ß and CD28 provides the signals necessary to maintain Tregs in the periphery. Tregs can also expand *in vivo* after antigen stimulation, in contrast to their anergic status *in vitro* (Sojka *et al.* 2008).

Various markers are under discussion for the characterization of human Tregs, but until now, no exclusive marker, that is only specific for Tregs, was found. Most markers are also expressed by activated effector T cells and some others by memory or naïve T cells (Schmetterer *et al.* 2012). Santegoets *et al.* declared in 2015 that the minimal set of required markers for human Tregs consists of expression of CD3, CD4, CD25 and downregulation of CD127 on the cell surface as well as intracellular expression of the transcription factor forkhead box protein 3 (FoxP3). Due to the intracellular localization of FoxP3, this marker cannot be used for isolation or staining of viable Tregs. Further markers are involved in the characterization of Tregs and used to determine subsets of Tregs, such as $FoxP3^{high}CD45RA^{-}$ as activated/TCR-triggered Tregs and $FoxP3^{inter}CD45RA^{+}$ as naïve Tregs or $Ki67^{+}$ Tregs as recently activated and proliferating Tregs (Santegoets *et al.* 2015).

Natural Tregs can suppress activation, proliferation and function of various immune cells, such as $CD4^{+}$ and $CD8^{+}$ effector T cells, B cells, NK and NKT cells as well as APCs (Sakaguchi *et al.* 2010) (Figure 1). Tregs can use a diverse array of suppression mechanisms. Which one they mainly use in a certain situation probably depends on the target cell, the activation status and the environment. Furthermore, the strength of activation of effector cells seems to make them more sensitive or resistant regarding the activity of Tregs (Sojka *et al.* 2008). Most of the studies regarding mechanisms of action of Tregs were performed in mice or with murine Tregs, and only few data from human Tregs is available. Due to the differences between species, the following paragraphs present the knowledge about human Tregs with a main focus on suppression of effector T cells. In general, three types of mechanisms of interaction with other immune cells are described for Tregs: interaction by cell-to-cell contact, by soluble factors, or with the environment, e.g. depletion of factors (Schmetterer *et al.* 2012).

The contact-dependent modes of action mediated by human Tregs are cell lysis via granzyme and perforin secretion as well as mechanisms via surface molecules (CD73, CD39, Fas-ligand (CD95-ligand), and cytotoxic T lymphocyte antigen-4 (CTLA-4)) (Schmetterer *et al.* 2012; Sakaguchi *et al.* 2010). Grossmann *et al.* showed that natural occurring human $CD4^{+}CD25^{+}$ Tregs express high levels of granzyme A, whereas generated adaptive Tregs from purified, CD3/CD46-stimulated $CD4^{+}$ T cells express high levels of granzyme B. Both types of Tregs can kill autologous target cells (e.g. effector T cells) by perforin-dependent cytotoxicity, but independent of the interaction of Fas-receptor (CD95) and Fas-ligand (Grossman *et al.* 2004).

The expression and secretion of granzymes and perforin by Tregs is also involved in the induction of apoptosis of other cell types, e.g. neutrophils (Gliwiński *et al.* 2017).

Strauss *et al*. demonstrated 2009 that Fas-receptors are expressed by around 40 % of human Tregs from healthy individuals and expression increases after stimulation with CD3 antibody and IL-2. Activated Tregs suppressed proliferation of autologous $CD8^+$ T cells, partly by induction of apoptosis via Fas/Fas-ligand pathway, but the suppression of $CD4^+$ T cells was not mediated by Fas-interaction. In murine studies, Tregs also inhibited effector T cells that were resistant to apoptosis (Schmetterer *et al.* 2012). In addition, effector T cells could also induce apoptosis of Tregs with low concentrations of IL-2 during co-culture, while not with high concentrations of IL-2 (Strauss *et al.* 2009). This demonstrates the complex interaction of Tregs and effector T cells and the influence of the surrounding cytokine milieu.

Almost 80 % of human Tregs express CD39 on the cell surface and around 70 % express CD73 intracellularly. Both molecules are ectonucleotidases, which hydrolyze adenosine triphosphate (ATP) to adenosine by co-working. The blockage of CD39 or CD73 reduced the inhibition of T-cell proliferation, demonstrating the immunosuppressive function of adenosine. Due to the high concentration of extracellular ATP in injured tissue, Tregs accumulate at these sites and hydrolyze ATP. The resulting adenosine has anti-proliferative effects, decreases the secretion of pro-inflammatory cytokines, induces anergy of T cells and interferes with DC function (Mandapathil *et al.* 2010).

Human and murine Tregs express constitutively CTLA-4, which is presented at the cell surface after stimulation (Schmidt *et al.* 2012). In mice, CTLA-4 downregulates the expression of CD80 and CD86 on APCs and CTLA-4 increases the expression of indoleamine 2,3-dioxygenase (IDO) in DCs, which subsequently suppresses effector T cells (Schmetterer *et al.* 2012; Schmidt *et al.* 2012). The involvement of CTLA-4 in suppression of effector T cells by human Tregs is still under debate due to discrepancies of experimental results (Schmidt *et al.* 2012). The blocking of CTLA-4 in human Tregs decreased the suppression of T-cell proliferation only in the presence of APCs (Schmidt *et al.* 2011). This suggests that CTLA-4 is involved in some, but not all types of suppression of effector T cells.

Camisaschi *et al.* detected that a subset of human Tregs expresses the surface molecule lymphocyte activation antigen-3 (LAG-3 or CD223), which is further increased in patients with cancer. Studies with murine cells showed that LAG-3 on Tregs binds MHC II on APCs and downregulates the costimulatory molecules and the blocking of LAG-3 reduced T-cell suppression by Tregs (Schmidt *et al.* 2012; Schmetterer *et al.* 2012). Human $LAG\text{-}3^+$ Tregs secrete high levels of IL-10 and TGF-ß, however *in vitro* the suppression of autologous $CD4^+$

T cells required cell-to-cell contact and was not mediated by the cytokines (Camisaschi *et al.* 2010). So, the role of LAG-3 in suppression mediated by human Treg is also not clear.

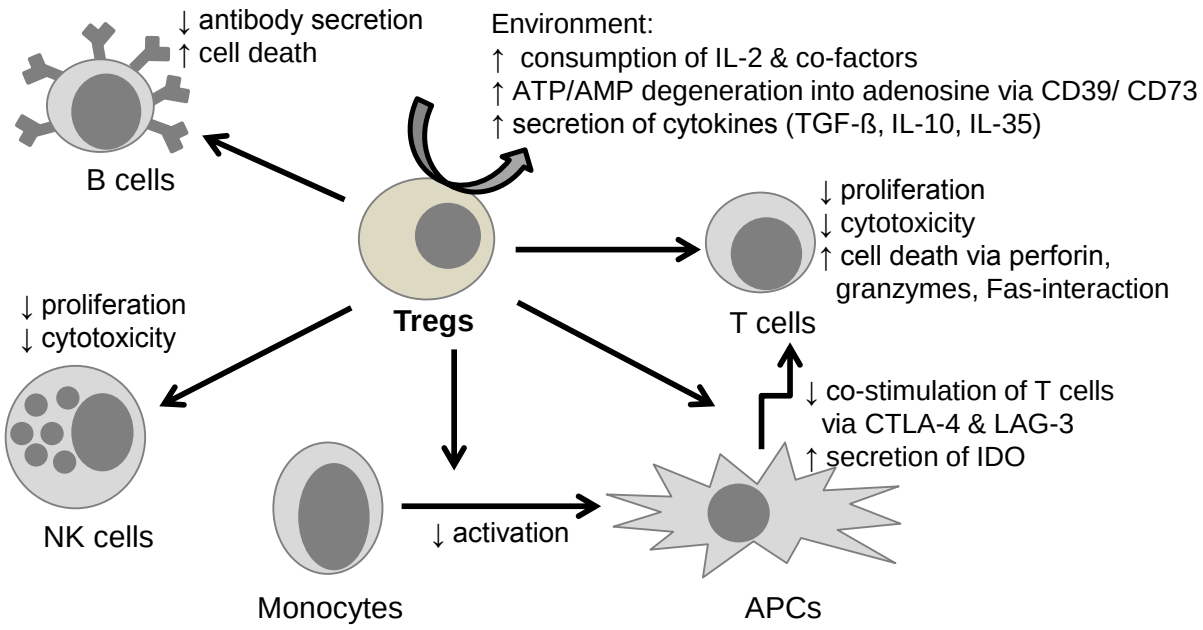

Figure 1: Schematic representation of various immunomodulatory mechanisms mediated by Tregs. Tregs suppress B cells, NK cells, and the development of monocytes into active APCs. The main function of Tregs is the suppression of proliferation, activation and function of effector T cells by effects on effector T cells and on APCs. In addition, Tregs affect the environment by increased consumption of IL-2, release of adenosine after degeneration of complexes, and secretion of cytokines, what in turn also inhibits effector T cells. Chart is adapted from Schmidt *et al*. 2012, Schmetterer *et al.* 2012, Gliwinski *et al.* 2017.

In addition, Tregs secrete cytokines for immunomodulation. Tregs can express TGF-ß in a membrane-bound and a soluble form (Nakamura *et al.* 2004); however, there are evidences that Tregs often do not express TGF-ß by themselves. Instead Tregs induce TGF-ß production in other cell types (Sojka *et al.* 2008). On the one side, several studies showed that TGF-ß deficiency in mice leads to autoimmune diseases and the blocking of TGF-ß reduced the suppression of T-cell proliferation and B-cell mediated antibody production *in vitro* (Nakamura *et al.* 2004). On the other side, studies from different groups did not detect the requirement of TFG-ß in the suppression of effector T cells by Tregs (Schmidt *et al.* 2012; Sojka *et al.* 2008). Probably, TGF-ß is involved in T-cell suppression by Tregs, but not as a major mechanism (Nakamura *et al.* 2004; Schmidt *et al.* 2012).

Similar to TGF-ß, the study results regarding the involvement of IL-10 are also quite controversial depending on the T-cell activation and the experimental settings. IL-10 seems to be more important in inflammation than in autoimmunity and the respective development of T cells in the lymph nodes (Asseman *et al.* 2003; Schmidt *et al.* 2012).

The group of Vignali reported that the inhibitory cytokine IL-35 is also involved in Treg-mediated suppression of T-cell proliferation and function in mice (Collison *et al.* 2007). Human Tregs do not express and secrete IL-35 constitutively; however, long-term activation increases its expression (Schmidt *et al.* 2012).

Furthermore, Tregs can modulate their direct environment. Pandiyan *et al.* reported that murine Tregs induce apoptosis in effector T cells by consumption of IL-2 due to their high expression of CD25 (Pandiyan *et al.* 2007). But Tregs can also inhibit the response of T cells, which are deficient in IL-2 receptors (Sojka *et al.* 2008). The consumption of IL-2 and following induction of apoptosis by Tregs remains controversial with inconsistent results depending on experimental settings, such as species, concentration of IL-2, stimulation of the cells and time frame (Schmidt *et al.* 2012).

Additionally, different groups reported that Tregs express the same transcription factors as effector T cells (such as T-bet, GATA-3), which leads to a suppression of these effector T cells, probably by competition for limiting factors (Schmidt *et al.* 2012).

Several other suppressive mechanisms of Tregs are described, such as high levels of cAMP which is transferred into effector T cells, rapid suppression of TCR-signalling, competition of APC stimulation via higher avidity to MHC than effector T cells, modulation of APCs (e.g. via IDO, interleukins) or other immune cells, which also suppress immune reactions (Schmetterer *et al.* 2012; Schmidt *et al.* 2012; Gliwiński *et al.* 2017).

In compensation to the diverse spectrum of suppression mechanisms by Tregs, effector T cells have different strategies to escape the inhibition, mainly by strengthening the activation of effector T cells by increasing antigen dose or co-stimulation (Sojka *et al.* 2008). Besides, pro-inflammatory cytokines can negatively regulate Treg function, e.g. by tumor necrosis factor-α (TNF-α), IL-6 or Toll-like receptor activation (Sojka *et al.* 2008).

Due to the diverse array of suppressive mechanisms of Tregs, researchers examined the potential of Tregs for adaptive cell therapy in preclinical *in vitro* and animal studies with encouraging results for patients with excessive immune reactions. For the translation to clinical studies with humans, many questions and new problems emerged regarding isolation of a pure and functional active Treg population without contaminations of effector T cells, the stability of Tregs, the possibilities to expand Tregs *ex vivo*, the influence of immuno-suppressive drugs on Tregs, the site and timing of Treg injection as well as the doses required for humans (Safinia *et al.* 2013). Many different clinical studies testing adoptive transfer of Tregs are currently ongoing, which target immunosuppression in prophylaxis and/or therapy

of GvHD after HSCT or solid organ transplantation as well as autoimmune diseases or allergies. Most clinical trials regard GvHD, e.g. there are over 10 completed or ongoing studies with freshly isolated Tregs and 4 studies with expanded Tregs (Gliwiński *et al.* 2017). These studies differ in various aspects, such as the use of allogenic or autologous Tregs, polyclonal or antigen-specific cells, which are freshly isolated or *ex vivo* expanded with many different protocols regarding cell origin, isolation, expansion, doses, time and so on, which makes a comparison difficult (Gliwiński *et al.* 2017; Brunstein *et al.* 2011; Di Ianni *et al.* 2011; Trzonkowski *et al.* 2009). Trzonkowski *et al.* described in the first study with two humans that transfer of Tregs is in principle safe. They detected a reduced requirement of immunosuppression for the patient with chronic GvHD and transient improvement in the patient with acute GvHD (Trzonkowski *et al.* 2009). Brunstein and colleagues reported reduced incidence of acute GvHD without an impact on the graft-versus-tumor effect, but it was not possible to administrate the targeted dose of expanded Tregs to all patients and later an increased incidence of viral infections was noticed (Gliwiński *et al.* 2017; Brunstein *et al.* 2011). The group around Di Ianni and Martelli detected reduced incidence of GvHD and leukemia relapses after infusion of freshly isolated Tregs prior to HSCT (Di Ianni *et al.* 2011; Martelli *et al.* 2014). Overall, administration of Tregs is well tolerated with good immunosuppressive functions in some diseases, which emphasizes the need of further studies (Gliwiński *et al.* 2017).

3.3.3 Myeloid-derived suppressor cells

Myeloid-derived suppressor cells are a diverse cell population of the myeloid cell lineage regarding their phenotype and morphology. MDSCs are functionally defined by their T-cell suppressive capacity and they are further subdivided into three subsets: monocytic (M-) MDSCs, polymorphonuclear (PMN-) MDSCs and early-stage (e-) MDSCs. In humans, M-MDSCs are $CD11b^-$, $CD14^+$, $HLA\text{-}DR^{low/-}$, $CD15^-$ and PMN-MDSCs are $CD11b^+$, $CD66b^+$ or $CD15^+$, $CD14^-$ of the PBMC fraction after density centrifugation. The myeloid cell surface antigen CD33 can also be used instead of the marker CD11b. eMDSCs are negative for all lineage markers (CD3, CD14, CD15, CD19, CD56), $HLA\text{-}DR^-$ and $CD33^+$. Due to the large overlap of phenotypic markers with other cell types, functional assessment of the suppressive activity is always necessary to identify MDSCs (Bronte *et al.* 2016).

Under healthy conditions, MDSCs are a rare population of around 0.5 % of human PBMCs. However, a strong accumulation of MDSCs was described in individuals under pathological

conditions, such as various cancer types, trauma, autoimmune diseases, infections, transplantations, etc. (Gabrilovich and Nagaraj 2009). Furthermore, in patients with solid tumors a significant association between high levels of MDSCs and poor overall survival was found (Zhang, Ma, *et al.* 2016).

Different suggestions regarding the origin of MDSCs are currently under discussion. The classical "two-signal model" or "emergency myelopoiesis" was pronounced by Gabrilovich and Nagaraj in 2009. During normal myelopoiesis, hematopoietic stem cells differentiate first into a common myeloid progenitor and then into an immature myeloid cell (IMC) in the bone marrow. This first step of growth and expansion is initiated by growth factors and cytokines, such as granulocyte/macrophage colony-stimulating factor (GM-CSF), stem-cell factor (SCF) and interleukin-6 (IL-6), which activate the Janus kinase (JAK) and the signal transducer and activator of transcription 3 (STAT3) transcription factor. Under normal conditions, IMCs migrate to the periphery and further differentiate into macrophages, dendritic cells and/or granulocytes. Under pathological conditions, this differentiation of IMCs is blocked by pro-inflammatory stimulation (e.g. interferons, signaling of Toll-like receptors (TLRs) and S100A8/A9 proteins) and thereby IMCs accumulate. Due to that activation signal, the transcription factor nuclear factor kappa-light-chain-enhancer of activated B-cells (NFκB) is activated leading to the generation of immunosuppressive MDSCs (Gabrilovich and Nagaraj 2009; Millrud *et al.* 2017). Studies in mice have contributed to the hypothesis of extramedullary myelopoiesis in which the activation of TLRs leads to the differentiation of IMCs into MDSCs in the periphery (Millrud *et al.* 2017).

An opposed idea is based on the reprogramming of pro-inflammatory monocytes into immunosuppressive M-MDSCs under inflammatory conditions. Repeated activation of TLRs by damage- or pathogen-associated molecular patterns (DAMPs/PAMPs) and specific cytokines (such as IL-6, IL-10, and TNF) activate the transcription factors STAT3 and NFκB leading to the downregulation of surface molecules (such as TLRs, HLA, and co-receptors) and thus, the generation of MDSCs (Millrud *et al.* 2017).

Several different mechanisms are described for the immunosuppressive activity of MDSCs (Figure 2). Each MDSC subset can use various suppressive mechanisms, but each cell uses not all of them to the same extend at the same time point; this depends on the activation of MDSCs and the underlying disease (Gabrilovich 2017). Many of these mechanisms are described only for murine MDSCs and it is not clear if these mechanisms are used by human MDSCs in the same way. In general, the main mechanisms of murine MDSCs are arginase 1

and inducible nitric oxide synthase (iNOS) targeting the metabolism of L-arginine, reactive oxygen species (ROS) and the induction of IDO (Zhao *et al.* 2016). Both murine MDSC subsets are producing high levels of arginase-1. Further, M-MDSCs are mainly expressing nitric oxide (NO) and only limited amounts of ROS, while PMN-MDSCs are producing high levels of ROS and low levels of NO in mice (Gabrilovich and Nagaraj 2009).

Both subsets of MDSCs require the amino acid L-arginine for protein synthesis, as all other cells do. Human MDSCs express intracellular high levels of the enzyme arginase 1, which catabolizes L-arginine and leads to a depletion of this amino acid in the environment (Rodríguez and Ochoa 2008). Thus, surrounding T cells are deficient in L-arginine, which results in a reduced expression of CD3ζ chain of the T-cell receptor (TCR) and an arrest in G0/G1 phase of the cell cycle; in addition, deprivation of L-arginine activates Tregs (Dilek *et al.* 2012).

Another enzyme, which uses L-arginine as a substrate, is iNOS, which is also expressed by MDSCs. The generation of NO by iNOS induces apoptosis of T cells and it inhibits the transcription and expression of MHC class II molecules in antigen-presenting cells (APCs) (Gabrilovich and Nagaraj 2009). Hence, MDSCs suppress the proliferation of T cells by two enzymes affecting the metabolism of L-arginine.

It was shown for MDSCs from cancer patients that they also produce high levels of ROS, which contribute to their immunosuppressive function (Gabrilovich and Nagaraj 2009). A chemical reaction of NO with superoxide anion leads to peroxynitrite, which can be produced by murine MDSCs. This can induce tolerance in antigen-specific $CD8^+$ T cells by nitration of the surface molecules on the T cells. This nitration disrupts the binding of TCRs and the MHC molecules, making the T cells not sensitive to antigen stimulation towards specific peptides (Nagaraj *et al.* 2010) Studies with human prostate carcinomas indicate that peroxynitrite is also involved in T-cell suppression in humans (Bronte *et al.* 2005) and this peroxynitrite could be produced by MDSCs.

Furthermore, murine MDSCs interfere with T-cell activation by cysteine/cystine deprivation. T cells cannot produce the amino acid cysteine, so that they cannot be activated and proliferate without an uptake of cysteine from the extracellular space. Normally, macrophages and dendritic cells produce more cysteine than these cells require and secrete it to the environment. During antigen presentation, these APCs are in close contact with T cells and thereby provide T cells with cysteine. If MDSCs are present during antigen-presentation, murine MDSCs sequester cysteine and limit the availability of cysteine, which inhibits T-cell activation (Ostrand-Rosenberg 2010; Srivastava *et al.* 2010).

Naïve T cells migrate to lymph nodes and inflammatory sites to become activated and the membrane molecule L-selectin (CD62L) is involved this homing process. Murine MDSCs produce constitutive the ADAM metalloproteinase domain 17, which cleaves L-selectin and thereby disturbing T cell trafficking and activation in tumor-bearing mice (Hanson *et al.* 2009; Ostrand-Rosenberg 2010).

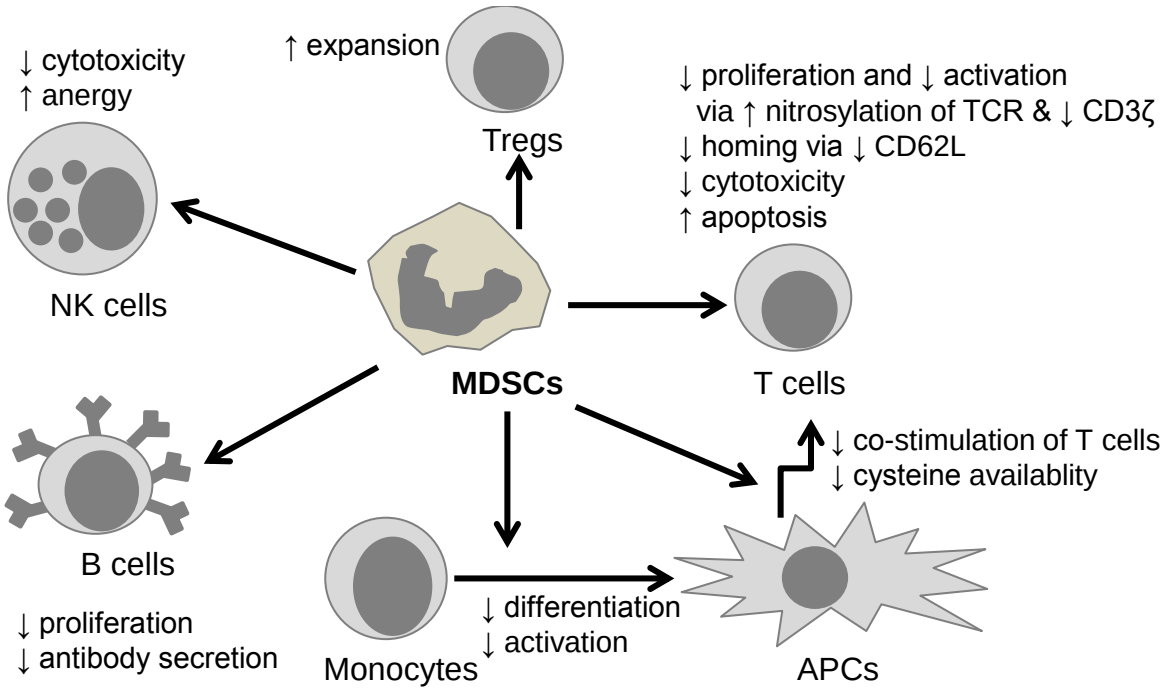

Figure 2: Scheme of immunomodulatory mechanisms mediated by MDSCs. Immune reactions of NK cells and B cells are suppressed by MDSCs, whereas the generation of Tregs is increased. MDSCs reduce differentiation and activation of APCs as well as their cysteine supply and their co-stimulation of effector T cells. MDSCs suppress T-cell function by various mechanisms decreasing T-cell proliferation, activation, homing, cytotoxicity and increasing apoptosis. Chart is adapted from Dilek *et al.* 2012 and Ostrand-Rosenberg & Sinha 2009.

A further enzyme, the heme oxygenase-1 (HO-1) contributes to the suppression of T-cell function by endotoxin-induced murine MDSCs, because its inhibition reduced the production of IL-10 and restored T-cell proliferation and IFNγ secretion. $CD11b^+$ MDSCs from LPS-treated mice express high levels of HO-1 and their transfer to untreated mice delayed skin graft rejection compared to mice without this cell transfer (De Wilde *et al.* 2009; Dilek *et al.* 2012).

Human MDSCs also express the enzyme IDO, which catalyzes the oxidation of the amino acid L-tryptophan and the expression of IDO is upregulated in patients with breast cancer. The degradation of tryptophan leads to local starvation and thus to an inhibition of T-cell proliferation and CD3ζ chain expression (Zhao *et al.* 2016).

In murine studies, MDSCs suppress NK-cell function by the membrane-bound TGF-ß1 molecule. It leads to downregulation of the expression of the receptor NKG2D, a decrease of the cytotoxicity of NK cells and the production of IFNγ. Further, murine MDSCs induce anergy in NK cells (Zhao *et al.* 2016)

The studies regarding the induction of Tregs showed contradictory results and it is not completely clear if there is an association between expansion of MDSCs and Tregs during tumor progression. Human MDSCs from patients with hepatocellular carcinoma induced Tregs, when co-cultured with $CD4^+$ T cells (Hoechst *et al.* 2008). However, other groups could not find a correlation between MDSCs and expansion of Tregs (Gabrilovich and Nagaraj 2009).

In vitro studies with human MDSCs in our laboratory demonstrated that MDSCs suppress B-cell proliferation and thereby antibody secretion. This MDSC-mediated inhibition of B cells involved several mechanisms, such as arginase-1, NO, ROS and B-cell death (Lelis 2017).

Several groups described different protocols to generate MDSCs *in vitro*, mostly murine MDSCs out of bone marrow (BM) cells. For stimulation, mainly GM-CSF was used alone or in addition with either granulocyte colony-stimulating factor (G-CSF), IL-6, IL-13, IFNγ or a combination of factors (Lechner *et al.* 2010; Ribechini *et al.* 2010). The protocols vary between the used cytokines and stimulatory factors, concentrations, time intervals and selection methods at the end. For the generation of human MDSCs, the use of PBMCs, isolated $CD14^+$ monocytes, umbilical cord blood cells, BM cells and $CD34^+$ hematopoietic stem cells were described (Lechner *et al.* 2010; Höchst *et al.* 2013; Marigo *et al.* 2010; Casacuberta-Serra *et al.* 2017; Zoso *et al.* 2014). In several studies with animal models, these *in vitro* generated MDSCs were investigated for the use as cellular therapies against pathological conditions. The murine MDSCs reduced GvHD lethality after BM transplantation in several studies; thereby different mechanisms have been detected, such as arginase-1 and turning of T cells towards type 2 T cells (Highfill *et al.* 2010; Messmann *et al.* 2015; Zhou *et al.* 2010). However, one group detected that transferred MDSCs lose their immunosuppressive function under inflammatory conditions due to inflammasome induction (Koehn *et al.* 2015). Consequently, further studies are required in order to better characterize the function of human MDSCs and to investigate their potential for GvHD treatment.

3.3.4 Mesenchymal stromal cells

Mesenchymal stromal cells (MSCs), also referred to as multipotent mesenchymal stem cells, were first described in detail by Friedenstein *et al.* in the late 1960s as fibroblast-like cells from the bone marrow with the ability to differentiate into other cell types, such as osteoblasts and chondroblasts (Friedenstein *et al.* 1968). Due to this ability, MSCs were intensively investigated in the last 50 years.

In humans, MSCs are a rare cell population found in various tissues, such as bone marrow (0.01 to 0.001 % of the nucleated cells), umbilical cord blood, placenta, and adipose tissue (Bernardo *et al.* 2009). Investigations of the precise compartment of MSCs in the tissues mentioned above indicated the stromal compartment (Horwitz *et al.* 2005); however, Crisan *et al*. described that MSCs originate from perivascular cells, which surround the blood vessel (Crisan *et al.* 2012; Crisan *et al.* 2008). MSCs can be isolated by their plastic adherence and expanded *in vitro*. The cells have a typically fibroblastic appearance in cell culture and keep their ability to differentiate into a variety of cell types, such as adipocytes, chondrocytes, and osteocytes. Human MSCs are further characterized by the expression of CD73, CD90, CD105, and HLA-ABC, and the absence of CD45, CD34, and HLA-DR (Bernardo *et al.* 2009; Müller *et al.* 2008; Dominici *et al.* 2006).

MSCs interact with various cell types of the innate and adaptive immune system by direct cell-to-cell contact and by secretion of soluble factors (Uccelli and de Rosbo 2015) (Figure 3). The effect of MSCs towards B cells seems to be contradictory depending on the experimental settings. Human MSCs can inhibit B-cell proliferation and the differentiation of B cells into plasma cells, and thereby the antibody production. However, this inhibition was only detected when T cells were included in the co-culture of MSCs with sorted and CpG stimulated B cells (Rosado *et al.* 2015). Furthermore, adipose tissue-derived MSCs support the development of regulatory B cells, which secrete the anti-inflammatory IL-10 (Franquesa *et al.* 2015; Uccelli *et al.* 2008). Rasmusson *et al*. demonstrated that the effect of MSCs on the activation of B cells and the antibody secretion depends on the stimulation of B cells (Rasmusson *et al.* 2007; Uccelli and de Rosbo 2015). The source of MSCs, the presence or absence of helper cells, such as T cells, the stimulation of cells, and the cell-to-cell contact seem to affect the interaction of MSCs and B cells. Nevertheless, the majority of studies detected an inhibition of B-cell proliferation and differentiation (Uccelli and de Rosbo 2015).

Several groups reported that MSCs interact with DCs by various mechanisms depending on cell-to-cell contact and on soluble factors. Human MSCs reduced the differentiation and

maturation of human DCs from monocytes and from $CD34^+$ HSCs, partially mediated by soluble factors, such as prostaglandin E2, IL-6, IL-10 and M-CSF (Bernardo *et al.* 2009). Direct contact between MSCs and human DCs renders the actin distribution in the cytoskeleton in the DCs, so that no stable immunological synapse is formed with T cells, reducing T-cell activation (Aldinucci *et al.* 2010). Chiesa *et al*. detected that in the presence of MSCs, murine DCs downregulate the expression of activation markers (e.g. CD80, CD86, and MHC class I molecule) and the secretion of cytokines (Chiesa *et al.* 2011). The interaction between MSCs and precursors of DCs as well as with mature DCs leads to suppression of T-cell activation, and thereby T-cell functions.

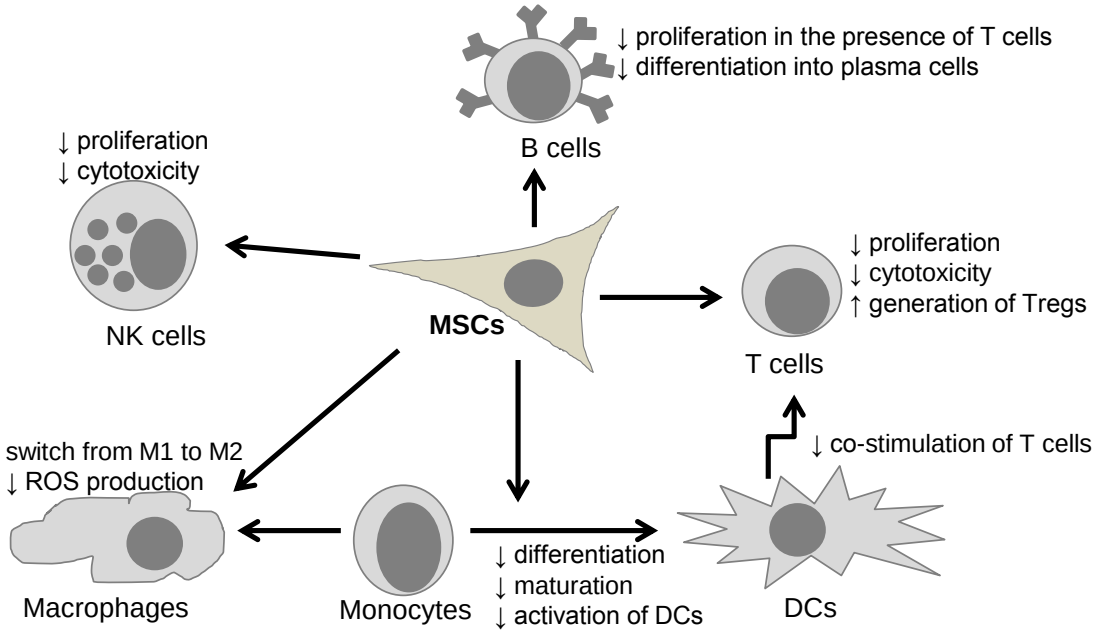

Figure 3: Schematic representation of various immunomodulatory effects of MSCs on other cells of the immune system. MSCs inhibit immune reactions by mediating suppressive effects on B cells, NK cells, macrophages, as well as the development of monocytes into active DCs. Furthermore, MSCs suppress proliferation, activation and function of effector T cells and MSCs increase the generation of Tregs. Chart is adapted from Bernardo *et al*. 2009.

MSCs derived from placenta interact with macrophage differentiation under inflammatory conditions by inducing the conversion of activated pro-inflammatory M1 macrophages to an anti-inflammatory M2 phenotype. This effect was induced by direct cell-to-cell contact and by soluble molecules (Abumaree *et al.* 2013). In a feedback loop, MSCs also secrete TNF-stimulated gene 6 protein (TSG-6), which leads to a reduction of pro-inflammatory molecules by the macrophages. Furthermore, MSCs suppress the production of ROS in macrophages (Uccelli and de Rosbo 2015).

Sotiropoulou *et al*. detected that human NK cells showed an altered phenotype and a decrease of proliferation, secretion of cytokines, and cytotoxic potential towards HLA class I-

expressing target cells after exposure to MSCs (Sotiropoulou *et al.* 2006). MSC-mediated suppression of NK-cell function was reported by several studies, whereas only one group measured an improved NK-cell function after contact with human MSCs or their soluble factors (Cui *et al.* 2016; Amorin *et al.* 2014). However, activated human NK cells can lyse MSCs (Sotiropoulou *et al.* 2006).

In 2002, Di Nicola and colleagues demonstrated for the first time that human MSCs suppress proliferation of T cells after stimulation with cellular or nonspecific mitogenic stimuli (Di Nicola *et al.* 2002). Several different mechanisms are described how MSCs affect T cells and their effector functions. It was shown that after contact with MSCs, human T cells undergo cell cycle arrest in G0 phase and not apoptosis (Di Nicola *et al.* 2002; Glennie *et al.* 2005). On the one side, lymphocytes need to be activated so that MSCs suppress the proliferation of T cells, on the other side, human MSCs support T-cell survival under quiescent conditions (Haddad and Saldanha-Araujo 2014; Benvenuto *et al.* 2007). MSCs can prevent cell death of T cells by downregulation of Fas ligand on the T-cell surface (Benvenuto *et al.* 2007). Regarding expression of activation markers of T cells, such as CD25, CD38, and CD69, there are contrary results of the effect of MSCs depending of the enrichment and stimulation of T cells (Castro-Manrreza and Montesinos 2015). In various experimental settings, MSCs decreased T-cell proliferation using PBMCs or isolated T cells by cell-to-cell contact and soluble factors (Castro-Manrreza and Montesinos 2015). MSCs express several integrins, intracellular adhesion molecules (ICAM-1, ICAM-2) and vascular cell adhesion protein (VCAM-I) to bind T cells with high affinity (Haddad and Saldanha-Araujo 2014). In addition, MSCs express programmed cell death-ligand 1 (PD-L1) and HLA-G1, which are involved in direct cell-to-cell interaction with T cells (Castro-Manrreza and Montesinos 2015).

Over 30 different soluble factors are described to be released by MSCs for the interaction with T cells, such as IDO, prostaglandin E2, IL-10, TGF-ß1, NO, hepatocyte growth factor, and HLA-G5 (Castro-Manrreza and Montesinos 2015). Galectin-1 has immunomodulatory effects on T cells as secreted molecule and bound on the cell surface (Gieseke *et al.* 2010). It is controversial whether the inhibitory effect on T-cell proliferation is mainly dependent on cell-to-cell contact or not. Different outcomes are found for the secretion of IFNγ depending on the source of MSCs, the lymphocyte population, and the environmental factors. For example, an inflammatory milieu with high IFNγ levels increased the immunosuppressive capacity of MSCs towards T cells (Castro-Manrreza and Montesinos 2015).

It was also shown that MSCs induce the generation of Tregs, that depended on direct cell-to-cell contact with purified $CD4^+$ T cells, but not if MSCs and PBMCs are co-cultured (Uccelli

and de Rosbo 2015). Melief *et al*. detected that MSCs induce Tregs from human PBMCs *in vitro* by the secretion of TGF-ß1 and by promoting the differentiation of monocytes towards anti-inflammatory macrophages (Melief *et al.* 2013). Furthermore, MSCs lead to the conversion of Th17 cells to Tregs (Uccelli and de Rosbo 2015). In addition, MSCs stimulate the generation of regulatory T type 1 (Tr1) cells, which are $IL10^{+}IFN\gamma^{+}CD4^{+}$, by secretion of prostaglandin E_2 and IDO (Hsu *et al.* 2013). Moreover, MSCs inhibit differentiation, proliferation, and function of pro-inflammatory Th17 cells (Uccelli and de Rosbo 2015).

Due to their potential of differentiation, their migration and homing mechanisms, their secretion of trophic factors and their immunoregulatory ability, MSCs are tested in over 450 clinical trials of cell-based therapies according to the US National Institutes of Health. Most of these studies are still phase I or II, so demonstrating safety and therapeutic efficiency (Squillaro *et al.* 2016). The objectives of the treatments in these studies are numerous with around 20 % in regenerative medicine of bone and cartilage diseases, 15 % in cardiovascular diseases and 17 % in neurological diseases; also autoimmune and inflammatory diseases as well as hematological pathologies and GvHD are targeted (Squillaro *et al.* 2016). Concerning GvHD, MSCs were analyzed for prevention and treatment of acute as well as chronic GvHD. The infusion of MSCs seems to be feasible and safe, as no severe side effects were detected in various studies (Castro-Manrreza and Montesinos 2015; Amorin *et al.* 2014). One important aspect for the safety of MSCs is that MSCs express no HLA II molecules and low amounts of HLA I molecules and thereby allowing administration of MSCs without taking care of HLA-matching between donor and recipient (Le Blanc *et al.* 2008; Balan *et al.* 2014). Several studies showed good response rates and increased overall survival of patients with GvHD after MSC administration compared to historical or simultaneous control groups (Bernardo and Locatelli 2016). Introna *et al*. observed that the rate of complete response was higher in children than in adults, but the overall response rate was not different (Introna *et al.* 2014). However, some clinical trials detected only in a few patients an improvement by the treatment with MSCs (Müller *et al.* 2008; Castro-Manrreza and Montesinos 2015). Furthermore, it is not clear if MSC infusion increases the risk of infectious complications (Balan *et al.* 2014). The conflicting results are probably due to high variations between disease stages, sources of cell isolation and methods of *in vitro* expansion, cell numbers and timing of administration, among others. Thus further clinical tests, especially randomized phase III studies with large and comparable cohorts of patients are required to determine the efficiency of MSCs for the treatment of GvHD.

3.4 Aim of the study

Graft-versus-host disease is a severe complication after transplantation of hematopoietic stem cells or organs from an allogenic donor. This uncontrolled immunological reaction is characterized by alloreactive T cells, which cause a strong inflammation and life-threating tissue damage in the patients (Ferrara *et al.* 2009). Cell-based approaches to diminish the T-cell reaction are promising therapeutic options that are under investigation for clinical treatment of GvHD. Several cell types are known to decrease T-cell function, including MSCs, Tregs and MDSCs (Gabrilovich and Nagaraj 2009; Di Nicola *et al.* 2002; Schmetterer *et al.* 2012). However, so far, it is not known, which cell type provides the greatest capacity for the control of T-cell function. The main aim of this study was to systematically compare the T-cell suppressive effect of different cell types. To address this question, *in vitro* assays with co-cultures of PBMCs containing stimulated T cells were performed with previously isolated immunomodulatory cells in different ratios. After incubation of 4-5 days, the proliferation of $CD4^+$ and $CD8^+$ T cells was measured by flow cytometric analysis of the dilution of a fluorescence dye. The secretion of IFNγ was also determined by enzyme-linked immunosorbent assay (ELISA) of the supernatants from the co-cultures.

To detect, if cell-to-cell contact is required for the inhibition of T-cell proliferation and IFNγ secretion, transwell experiments were performed, in which immunomodulatory cells and the stimulated PBMCs were separated by a semipermeable membrane.

For clinical application, the cell number is very important to achieve similar cell ratios in a patient as during *in vitro* assays. This raised the question, if the cell yield of MDSCs could be increased by generation. Thus, I investigated the generation of MDSCs by cytokine stimulation during cell culture of PBMCs and of BMMCs. To ensure that the generated cells are cytokine-induced MDSCs, first a characterization of the expression of surface markers was performed by flow cytometric analysis. After magnetic separation of these $CD33^+$ MDSCs, the suppressive effect of these cytokine-induced MDSCs was examined by the previously described *in-vitro* assays regarding T-cell proliferation and the release of IFNγ during co-culture was measured by ELISA.

In order to further increase cell yield of cytokine-induced MDSCs, $CD34^+$ HSCs were used for their generation. These generated MDSCs from $CD34^+$ HSCs were also characterized by flow cytometry to ensure the phenotype of MDSCs. To evaluate the suppressive effect of MDSCs generated from $CD34^+$ HSCs, the $CD33^+$ MDSCs were selected by magnetic separation and afterwards, the inhibition of T-cell proliferation as well as IFNγ secretion was analyzed as previously described.

Overall, the functional capacities of various immunomodulatory cells (MSCs, Tregs, freshly isolated PMN-MDSCs and six different cytokine-induced MDSCs) were systematically compared with each other regarding the suppression of T-cell proliferation as well as the inhibition of IFNγ secretion and the available cell yield.

4 Materials and methods

For better reading, all symbols of trademarks and copy rights as well as legal entities, such as GmbH or Co. KG and places of company headquarters are just mentioned at the first naming of a product.

4.1 Materials

Equipment	Manufacturer
Assistent Rotating Mixer RM 5	Karl Hecht GmbH & Co. KG, Sondheim, Germany
autoMACS® Pro Separator	Miltenyi Biotec GmbH, Bergisch Gladbach, Germany
AxioCam MR	Carl Zeiss AG, Oberkochen, Germany
Axioskop20 and Axiovert 135 microscope	Carl Zeiss
Centrifuges: Rotixa 50 RS and Rotina 420R Bench-top centrifuge Micro 22R	Andreas Hettich GmbH & Co. KG, Tuttlingen, Germany
Clean bench HERAsafe	Heraeus Holding GmbH, Hanau, Germany
CliniMACS Prodigy®	Miltenyi Biotec
ELISA/Microplate Reader ELX800	BioTek Instruments, Inc., Winooski, VT, USA
Eos 550D camera	Canon Deutschland GmbH; Krefeld, Germany
FACSCalibur™	BD Biosciences, Becton, Dickinson and Company, Franklin Lakes, NJ, USA
Freezer (-20° C)	Liebherr-International Deutschland GmbH, Biberach an der Riß, Germany
Freezer (-80° C)	Forma Scientfic, Egelsbach, Germany
Incubator Hera cell	Heraeus Holding GmbH
Inverted Microscope IX50	Olympus, Hamburg, Germany
Liquid nitrogen storage	Cryoson GmbH, Westerngrund, Germany
Magnetic stirrer	Thermo Fisher Scientific, Inc. Waltham, MA, USA
MiniMACS™ Separator	Miltenyi Biotec
Mr. Frosty® Cryo 1°C Freezing Container	Nalgene, Thermo Fisher Scientific, Inc.
Multichannel pipettes: MULTIMATE and Discovery Comfort	HTL, Warsaw, Poland
Neubauer counting chamber	La Fontaine International GmbH, Waghaeusel, Germany
pH meter: Model pH538	Wissenschaftlich-technische Werkstätte, Weilheim, Germany
Pipette controller: Pipetboy acu 2	Integra Biosciences GmbH, Fernwald, Germany

Equipment	Manufacturer
Pipettes: Discovery Comfort Eppendorf research Plus	HTL Eppendorf AG, Hamburg, Germany
Refrigerator (4° C)	Liebherr
Rotating tube mixer	Karl Hecht
Shaker Polymax1040 and Titramax1000	Heidolph Instruments GmbH & Co. KG, Schwabach, Germany
Vortex shaker MS1	IKA-Werke-GmbH & Co KG, Staufen, Germany
Water Bath Model 1012	Gesellschaft für Labortechnik, Burgwedel, Germany

Table 1: List of equipment

Consumables	Manufacturer
Cell culture flasks (25 cm^2, 75 cm^2, 175 cm^2)	Greiner Bio-One GmbH, Frickenhausen, Germany
Cell culture plates (24-well)	Corning Incorporated, Corning, NY, USA
Cell culture plates (U-bottom, 96-well)	Greiner Bio-One
Cryo vial (2 ml): cryo.S™	Greiner Bio-One
Disposable pipettes (5 ml, 10 ml, 25 ml)	Corning Incorporated
Disposal Bags	Brand GmbH & Co KG, Wertheim, Germany
HTS Transwell®-96 well (0.4 µm pore size, polycarbonate membrane)	Corning Incorporated
Luer-Lok™ Syringe (60 ml)	BD Plastikpak™, Becton, Dickson & Company
LD and MS Columns for MACS®- separation	Miltenyi Biotec
Microplates (flat-bottom, 96-well)	Corning Incorporated
Pipette tips (10 µl)	ULPlast Universal Laboratory Plasticware Warsaw, Poland
Pipette tips (200 µl, 1000 µl)	Sarstedt AG & Co.
Polypropylene tubes (15 ml)	Greiner Bio-One
Polypropylene tubes (50 ml)	Greiner Bio-One
Polystyrene (FACS) tubes (5 ml)	Sarstedt AG & Co, Nümbrecht, Germany
Reagent reservoir	Multimed Biotechnologiekontor GmbH, Giengen, Germany
Safe-Lock tubes (0.5 ml, 1.5 ml, 2 ml)	Eppendorf
Safety Multifly® Needle 21G x ¾’’TW	Sarstedt AG & Co.
Sterile filter	Sartorius AG, Göttingen, Germany
Syringe (10 ml)	B. Braun Melsungen AG, Melsungen, Germany

Table 2: List of consumable material

Chemicals, reagents & solutions	Manufacturer
autoMACS™ Pro Washing Buffer	Miltenyi Biotec
autoMACS™ Running Buffer	Miltenyi Biotec
Biocoll Separating Solution (1.077 g/ml)	Biochrom AG, Berlin, Germany
Detachin	Genlantis, San Diego, CA, USA
Dimethylsulfoxid (DMSO)	WAK- Chemie Medical GmbH, Steinbach, Germany
Dulbecco's modified eagle's medium (DMEM) (3.7 g/l $NaHCO_3$, 1g/l glucose, w/o L-glutamine)	Biochrom AG
Dulbecco's phosphate buffered saline (PBS)	Sigma-Aldrich Inc., Merck KgaA, Darmstadt, Germany
Ethanol	Merck KgaA, Darmstadt, Germany
FACS Clean® / Rinse® / Flow®	BD Biosciences
Fetal bovine serum (FBS)	Gibco, Thermo Fisher Scientific
FoxP3 Staining Buffer Set	Miltenyi Biotec
Heparin natrium 100 I.E./ml and 5000 I.E./ 0.2 ml	Sintetica GmbH, Münster, Germany Ratiopharm GmbH, Ulm, Germany
Irradiated human platelets	University of Tübingen, blood donor center, Tübingen, Germany
L-glutamine (200 mM)	Biochrom
MACS® BSA Stock Solution	Miltenyi Biotec
CliniMACS® PBS/EDTA Buffer	Miltenyi Biotec
Penicillin/Streptomycin (10.000 U/ml, 10.000 µg/ml)	Biochrom
Propidium iodide	BD Biosciences
Reagent Additive 1 (Normal goat serum)	R&D Systems
RPMI-1640 (Roswell park memorial institute medium) (2.0 g/l $NaHCO_3$, w/o L-glutamine)	Biochrom
Trypane blue solution (0.4 %)	Sigma-Aldrich Inc.
TrypLE Select™	Life Technologies, Thermo Fisher Scientific
Trypsin/ EDTA solution in PBS (0.05 %/ 0.02 % w/v)	Biochrom
Tween® 20	Carl Roth GmbH & Co. KG, Karlsruhe, Germany

Table 3: List of chemicals, reagents and solutions

Kits and separation reagents	Manufacturer
Anti-FITC MicroBeads	Miltenyi Biotec
CD33 MicroBeads, human	Miltenyi Biotec
$CD4^+CD25^+$ Regulatory T Cell Isolation Kit (human)	Miltenyi Biotec

Kits and separation reagents	Manufacturer
CliniMACS® CD34 Complete Kit	Miltenyi Biotec
Dead Cell Removal Kit	Miltenyi Biotec
DuoSet® Ancillary Reagent Kit 2	R&D systems, Minneapolis, MN, USA
IFN-γ DuoSet® ELISA	R&D systems
Vybrant™ CFDA SE Cell Tracer Kit (CFSE)	Life technologies, Thermo Fisher Scientific

Table 4: List of kits and separation reagents

Stimulation reagents and cytokines	Manufacturer
Anti-human CD3 antibody: Orthoclone® OKT3 (in 5.1 and 5.2) or Purified NA/LE Mouse Anti-Human CD3 (clone: HIT3a) (in 5.3 and 5.4)	Janssen-Cilag GmbH, Neuss, Germany or BD Pharminen™, Becton, Dickinson and Company
Human Fms-related tyrosine kinase 3 (Flt3)-Ligand, research grade	Miltenyi Biotec
Human GM-CSF (Leukine)	Genzyme, Cambridge, MA, USA
Human IL-3, research grade	Miltenyi Biotec
Human IL-6, research grade	Miltenyi Biotec
Proleukin®S as human Interleukin 2	Novartis Pharma GmbH, Nürnberg, Germany
Human stem cell factor (SCF), research grade	Miltenyi Biotec
Human thrombopoietin (TPO), research grade	Miltenyi Biotec

Table 5: List of stimulation reagents and cytokines

Self-mixed media & buffers	Composition
Block buffer (ELISA)	PBS with 1 % BSA
Complete RPMI medium	RPMI-1640 medium with 10 % heat-inactivated FBS, 2 mM L-glutamine, 100 IU/ml penicillin, 100 µg/ml streptomycin
Donor-specific medium	RPMI-1640 medium containing 10 % donor-specific human serum, 2 mM L-glutamine, 100 IU/ml penicillin and 100 µg/ml streptomycin
FACS buffer	PBS with 2 % FBS
Freezing medium	FBS with 10 % DMSO
gMDSC medium	StemMACS HSC Expansion Media XF (human) with 50 IU/ml penicillin, 50 µg/ml streptomycin, 50 ng/ml human SCF, 10 ng/ml human TPO, 50 ng/ml human Flt3-Ligand, 40 ng/ml human IL-6, 40 ng/ml human GM-CSF and where indicated 20 ng/ml human IL-3
MSC medium	DMEM (1g/l glucose) with 100 IU/ml heparin natrium, 10^8/ml irradiated human platelets, 2 mM L-glutamine, 100 U/ml penicillin, 100 µg/ml streptomycin
Wash buffer (ELISA)	PBS with 0,05 % Tween® 20

Table 6: List of self-mixed media and buffers with detailed composition

Specificity*	Isotype	Clone	Fluoro-chrome	Dilution	Manufacturer
CD3	mouse IgG1	SK7	FITC	1:50	BioLegend®, San Diego, CA, USA
CD3	mouse IgG2a	BW264/56	PerCP	1:50	Miltenyi Biotec
CD4	mouse IgG2a	VIT4	APC, PerCP	1:50	Miltenyi Biotec
CD4	Mouse IgG1	RPA-T4	PE	1:50	BioLegend
CD4	REA Control S	REA623	FITC	1:25	Miltenyi Biotec
CD8a	mouse IgG1	HIT8a	APC	1:50	BioLegend
CD11b	rat IgG2b	M1/70.15.11.5	PE, APC	1:50	Miltenyi Biotec
CD14	mouse IgG2a	TÜK4	APC	1:20	Miltenyi Biotec
CD14	mouse IgG2b	MΦP9	FITC	1:20	BD Biosciences
CD15	mouse IgG1	W6D3	PE	1:50	BioLegend
CD16	mouse IgG1	3G8	PerCP	1:50	BioLegend
CD19	mouse IgG1	SJ25C1	PE	1:50	BioLegend
CD25	mouse IgG1	3G10	PE	1:10 or 1:25	Miltenyi Biotec
CD25	mouse IgG1	M-A251	PE	1:10	BioLegend
CD33	Mouse IgG1	AC104.3E3	PE	1:25	Miltenyi Biotec
CD34	mouse IgG2a	AC136	FITC	1:31	Miltenyi Biotec
CD45	mouse IgG2a	5B1	FITC	1:50	Miltenyi Biotec
CD45	REA Control S	REA747	PerCP-Vio700	1:25	Miltenyi Biotec
CD56	mouse IgG2a	MEM-188	FITC	1:50	BioLegend
CD66b	REA Control S	REA306	FITC, PE, APC	1:25	Miltenyi Biotec
CD66b	mouse IgM	G10F5	FITC	1:25	BD Biosciences
CD73	mouse IgG1	AD2	PE	1:35	BD Biosciences
CD90	mouse IgG1	DG3	PE	1:50	Miltenyi Biotec
CD105	mouse IgG1	43A4E1	FITC	1:33	Miltenyi Biotec
CD127	mouse IgG2a	MB15-18C9	FITC	1:10	Miltenyi Biotec
CD184/ CXCR4	mouse IgG2a	12G5	APC	1:20	Miltenyi Biotec
CD192/ CCR2	mouse IgG2a	K036C2	APC	1:25	BioLegend
CD195/ CCR5	mouse IgG2a	2D7/CCR5	PE	1:20	BD Biosciences
FoxP3	mouse IgG1	3G3	APC	1:10	Miltenyi Biotec
HLA-ABC	mouse IgG1	G46-2.6	PE	1:10	BD Biosciences
HLA-DR	mouse IgG2a	AC122	PerCP	1:50	Miltenyi Biotec
HLA-DR	mouse IgG2a	AC122	FITC	1:100	BioLegend

Table 7: List of fluorochrome-labeled antibodies

* All used antibodies are anti-human antibodies.

Isotype	Clone	Fluorochrome	Manufacturer
Mouse IgG1	IS5-21F5	PE, APC	Miltenyi Biotec
Mouse IgG1	MOPC-21	FITC	BioLegend
Mouse IgG2a	S43.10	FITC, APC, PerCP	Miltenyi Biotec
Mouse IgG2b	IS6-11E5.11	FITC, PE	Miltenyi Biotec
Mouse IgM	IS5-20C4	FITC	Miltenyi Biotec
Rat IgG2b	ES26-5E12.4	PE, APC	Miltenyi Biotec
REA Control S	REA293	PE, APC, PerCP-Vio700, VioBrightFITC	Miltenyi Biotec

Table 8: List of isotype controls

Software	Manufacturer
BD CellQuest™ Pro software	BD Biosciences
Eos Utility software	Canon Deutschland
Gen5™ All-In-One Microplate Reader Software	BioTek Instruments, Inc.,
Windows	Microsoft Corporation, Redmond, WA, USA
GraphPad Prism® 6.0	GraphPad Software Inc., La Jolla, CA, USA

Table 9: List of softwares

Further, we used heparinized peripheral blood of healthy volunteers or buffy coats from the Blood bank Tübingen, Germany and excessive material of standard bone marrow biopsies and of $CD34^+$ HSCs from the University Children's Hospital, Tübingen, Germany.

4.2 Methods

All experiments were performed in a standardized laboratory with safety level S1.

4.2.1 Isolation and first expansion of human MSCs

Human MSCs were derived from excessive material of standard bone marrow biopsies. Excess material was used after informed consent in accordance with the Declaration of Helsinki and approval by the Institutional Review Board of the University Children's Hospital Tübingen (approval 338/2013 B02). MSCs were initially cultivated in the GMP facility at the Department of General Paediatrics, Haematology/Oncology in Tübingen using animal serum-free medium as described previously (Müller *et al.* 2008; Müller *et al.* 2006). In brief, 10-15 ml BM aspirates of healthy donors were resuspended in DMEM medium (1 g/l glucose) supplemented with 100 IU/ml heparin natrium, 1 mM L-glutamine and 10^8/ml irradiated human platelets. After 2-3 days of incubation at 37° C and 10 % carbon dioxide (CO_2), non-adherent cells were removed. MSCs were expanded over a period of 3-4 weeks and harvested using TrypLE Select. Microbial analyses was performed regularly and the purity of MSCs (>95 %) was defined by flow cytometry on the basis of CD73, CD105, CD45, as well as CD3, CD19 and CD14 to exclude T cells, B cells and monocytes, respectively.

4.2.2 Cell culture of human MSCs

MSCs were cultured in MSC medium at 37° C and 10 % CO_2. Cell density and appearance of cells was regularly checked by microscopy. If cell density was over 95 % confluence, MSCs were passaged. Therefore, medium was discarded and cells were washed once with phosphate-buffered saline (PBS). Depending on the flask size, a defined volume of trypsin solution was added (Table 10) and cells were incubated for up to 5 min at 37° C.

Flask size (cm^2)	Trypsin solution (ml)	Media (ml)
25	1	7
75	2	13
175	3	25

Table 10: Flask size with suitable volumes of trypsin solution and media

To stop the cleavage of adhesion molecules by trypsin, at least double the volume of media was added and the cell suspension was transferred into 15 ml tube for centrifugation at 350 g, 10 min at room temperature (RT). Supernatant was completely removed, the cell pellet was resuspended in 1-3 ml media and the cell number was determined.

After isolation and expansion, human MSCs can be stored frozen for longer periods in liquid nitrogen. Therefore, MSCs were detached from the cell culture flasks by incubation with trypsin solution and once washed with PBS. Afterwards, up to $5 \cdot 10^6$ cells were resuspended in 1 ml freezing media and 1 ml cell suspension was transferred into a cryo vial. The tubes were placed inside a Mr. Frosty Cryo 1°C Freezing Container and frozen overnight at -80° C. Afterwards, the cryo vials were stored in liquid nitrogen.

For thawing of MSCs, the cryo vials were warmed up at 37° C in the water bath and directly transferred into a 50 ml tube containing pre-warmed media. After one washing step with media, the cells were seeded in new cell culture flasks with around 30 % confluence. On the following day, media was exchanged and cells were cultured as described above.

4.2.3 Counting of living cells

During seeding, cell titer was defined using a Neubauer counting chamber and trypan blue solution. This staining color can just enter into dying or dead cells without an intact cell membrane, staining those blue and not the viable cells. Thereby, staining with trypan blue solution shows viability of the cells and increases the visibility of the living cells in the cell suspension. The Neubauer chamber is a special glass slide with a graved grid in the center (Figure 4), covered by another thin glass slide.

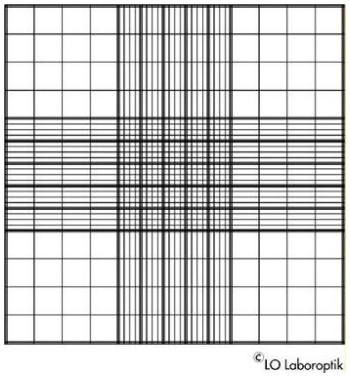

Figure 4: Grid of a Neubauer improved chamber.

Chart is taken from LO-Laboroptik GmbH
(http://www.zaehlkammer.de/deutsch/neubauer.improved.html; 04.12.2017 at 1:35 pm).

Before counting, trypan blue was diluted 1:10 with PBS to a 0.04 % working solution. The cell suspension was diluted in an appropriated ratio with the trypan blue dilution and 10 µl of this mixture was directly transferred into the Neubauer chamber. Only the light shining, living cells (n) were counted in the squares of the four outer quadrants in the corners of the grid under the microscope. Due to the size of the Neubauer chamber and the dilution of the cell

suspension, the concentration of living cells per ml suspension can be calculated by the following formula:

$$\frac{cells}{ml} = \frac{n}{4} \times dilution\ factor\ \times 10^4$$

Afterwards, the cell suspensions were adjusted to the desired concentration for cell culture or the following experiments.

4.2.4 Isolation of mononuclear cells

PBMCs were prepared from heparinized peripheral blood of healthy volunteers or buffy coats (Blood bank Tübingen, Germany) and BMMCs from excessive material of standard bone marrow biopsies (for ethical approval: see 4.2.1). Mononuclear cells can be isolated by density gradient centrifugation and Biocoll separating solution, which is a hydrophilic polysaccharide solution with a density of 1.077 g/ml. First, blood or BM aspirates were diluted with PBS at least in a 1:1 ratio. For larger sample volumes, 50 ml conical tubes with 20 ml Biocoll separating solution were prepared. For smaller volumes, 15 ml conical tubes with 4 ml Biocoll separating solution were used. The diluted sample was slowly overlayed onto the Biocoll separating solution and centrifuged at 500 g for 25 min at RT without brake. After centrifugation, granulocytes and aggregated erythrocytes are at the bottom of the tube due to their high density, covered by the Biocoll separating solution. Onto this solution follows an interphase layer of mononuclear cells that mainly consisting of lymphocytes and monocytes in case of blood separation, and on top is the diluted plasma fraction of the sample (Figure 5).

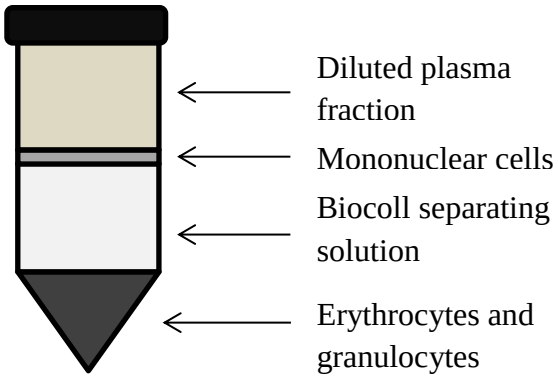

Figure 5: Isolation of mononuclear cells. After centrifugation, different cells are found in different positions in the tube according to their density.

The interphase of PBMCs was collected and transferred into fresh tubes. Cells were washed twice by filling the tubes with RPMI-1640 medium, centrifugation at 400 g for 10 min at RT

and discarding the supernatant. Before further experiments or cell culture were started, cell number and viability were measured (see 4.2.3).

4.2.5 *In vitro* generation of cytokine-induced MDSCs

To increase the cell yield, different protocols of *in vitro* generation of MDSCs from various cell types were tested by stimulation with different cytokines.

4.2.5.1 Generation of MDSCs from PBMCs or BMMCs

PBMCs or BMMCs were isolated by density gradient centrifugation (see 4.2.3) from buffy coats or excessive material of standard bone marrow biopsies, respectively. The cell viability and numbers were determined (see 4.2.3) and the cell density was adjust to $5 \cdot 10^5$ PBMCs/ml or $3 \cdot 10^5$ BMMCs/ml in a volume of 50 ml in 75 cm^2 cell culture flasks. Cells were cultured with RPMI-1640 medium supplemented with 10 % heat-inactivated fetal bovine serum (FBS), 2 mM L-glutamine, 100 U/ml penicillin and 100 µg/ml streptomycin at 37° C and 5 % CO_2. Cells were stimulated with 10 ng/ml granulocyte-macrophage colony-stimulating factor (GM-CSF) alone or in combination with 10 ng/ml human Interleukin-6 (IL-6). Media and supplements were exchanged every 3-4 days. Therefore, the cell suspension was transferred into tubes, centrifuged at 400 g, 10 min at RT, supernatant discarded, the cell pellet suspended in fresh medium, cytokines added as on the first day and cell suspension transferred back into the flask with the attached cells. After incubation for 7 days, cell suspension and adherent cells were collected by incubation for 5-10 min with 1 ml Detachin per flask. Cells were then washed once with PBS and afterwards, the cell titer and viability were checked (see 4.2.3). For functional assays, cytokine-induced MDSCs were isolated with human CD33 MicroBeads, as described in 4.2.6.4.

4.2.5.2 Generation of MDSCs from CD34⁺ hematopoietic stem cells

Human $CD34^+$ HSCs were derived from excessive material of apheresis products of healthy donors after mobilization of HSCs with granulocyte colony-stimulating factor. $CD34^+$ HSCs were isolated in the GMP facility at the Department of General Paediatrics, Haematology/Oncology of the University Children's Hospital Tübingen. Isolation was performed by using magnetic cell separation with CliniMACS CD34 Complete Kit and a CliniMACS device from Miltenyi Biotec and purified $CD34^+$ cells were cryopreserved in liquid nitrogen until no further clinical application was required and the cells could be used for experimental settings.

Purified $CD34^+$ cells were thawed by warming up the cells at 37° C in the water bath and directly transferred into a fresh tube containing 5 ml pre-warmed StemMACS HSC Expansion Media XF (human). After centrifugation at 350 g for 10 min at RT, supernatant was discarded, the cell pellet resuspended in 1 ml StemMACS HSC Expansion Media XF (human) and the cell titer determined (see 4.2.3). The cell concentration was adjusted to 250.000 cells per ml with gMDSC medium containing 50 IU/ml penicillin, 50 µg/ml streptomycin, 50 ng/ml SCF, 10 ng/ml TPO, 50 ng/ml Flt3-Ligand, 40 ng/ml IL-6, 40 ng/ml GM-CSF and where indicated 20 ng/ml IL-3. According to the publication of Casacuberta-Serra *et al.* 2017, the $CD34^+$ cells were seeded in a round-bottom 96-well plate with 50.000 cells in a volume of 200 µl per well and cultured at 37 °C and 5 % CO_2. To maintain cell density, the cells were transferred to 24-well plate after 7 days with a volume of 500 µl per well and on day 15, cells were transferred to 12-well plate with a volume of 1000 µl per well. If the cells proliferated fast and the media turned yellow, fresh gMDSC medium was added on day 10 and/or day 17 in the ratio 1:3. After 20 days, cells were harvested by collecting all cells from each well and were counted (see 4.2.3) followed by dead cell removal (see 4.2.6.3) and $CD33^+$ selection (see 4.2.6.4). Afterwards, characterization by flow cytometry and T-cell suppression assay was performed.

4.2.6 Magnetic cell separation

This method is based on the specific binding of antibodies conjugated with magnetic nanoparticles, which retain the bound cells in suspension inside a column in a magnetic field. The used MACS MicroBeads from Miltenyi Biotec are described as non-toxic, super-paramagnetic particles with a diameter of 50 nm, which do not activate the bound cells. The MACS Columns are filled with a matrix of ferromagnetic spheres. The area between the spheres inside the columns is larger than the cells, thereby allowing them to flow through without getting stressed or activated (Miltenyi Biotec GmbH 2017).

All separations were performed according to the manufacturer's protocols, which are described in detail below. The volumes mentioned in the protocols are suitable for up to 10^7 PBMCs. If higher cell numbers were used, the volumes were scaled up accordingly to the increased cell numbers; however for lower cell numbers, no down-scaling was recommended. The autoMACS Pro Separator was always prepared by running a washing program before use. If not indicated otherwise, all centrifugation steps were performed at 300 g, 10 min at RT and only MACS buffer was used. Before the collected cells were further used, the cell viability and titer was checked by staining with trypan blue solution (see 4.2.3). In addition,

the purity of all isolated cells was analyzed by flow cytometry: for the $CD66b^+$ separation, >95 % of the cells were $CD66b^+$ PMN-MDSCs, and the purity of $CD33^+$ cells and of $CD4^+CD25^+$ Tregs was >90 % of the contained cells.

4.2.6.1 Isolation of CD66b⁺ PMN-MDSCs

After isolation of PBMCs from blood (see 4.2.3), PBMCs were first stained with Fluorescein isothiocyanate (FITC) mouse anti-human CD66b antibody from BD Biosciences and later separated with anti-FITC MicroBeads from Miltenyi Biotec by positive selection. The desired PBMC number was transferred into a 15 ml conical tube, centrifuged, and the supernatant was discarded. The cell pellet (of up to 10^7 PBMCs) was resuspended in 100 µl PBS and 20 µl anti-human CD66b FITC-conjugated antibody solution was added. After mixing, the cells were incubated for 20 min at RT in the dark. The unbound antibodies were washed away by adding 1-2 ml buffer, centrifugation, and discarding the supernatant. The cell pellet was resuspended in 90 µl buffer, mixed with 10 µl anti-FITC MicroBeads, and incubated for 15 min at 4° C in the refrigerator. After washing with 1-2 ml buffer, the supernatant was completely removed and the pellet was resuspended in 500 µl buffer (for up to 10^8 PBMCs). The sample was placed in the tube rack of the autoMACS Pro Separator in row A and two new 15 ml tubes were placed in row B and C (Table 11).

Row	Tube containing …
A	Sample
B	Negative fraction containing unlabeled cells
C	Positive fraction containing labeled cells

Table 11: Tube rack of autoMACS Pro Separator

For separation, the program "Posseld2" was started, by which the cell suspension passes twice a MACS column inside the autoMACS Pro Separator and this program is optimized for positive selection of the labeled fraction. After selection, the labeled fraction containing the $CD66b^+$ PMN-MDSCs was collected in row C and the negative fraction was in row B.

4.2.6.2 Isolation of CD4⁺CD25⁺ regulatory T cells

The $CD4^+CD25^+$ Regulatory T Cell Isolation Kit (human) from Miltenyi Biotec was used to isolate Tregs in a two-step process. First, the depletion of non-$CD4^+$ cells was performed,

followed by the positive selection of $CD4^+CD25^+$ T cells.

After isolation of PBMCs from buffy coats (see 4.2.3), the desired cell number was transferred into a 15 ml conical tube, centrifuged, and the cell pellet was resuspended in 90 µl buffer per 10^7 PBMCs. First, 10 µl of $CD4^+$ T Cell Biotin-Antibody Cocktail was added to the cell suspension, mixed well, and incubated for 5 min at 4° C. Then, 20 µl Anti-Biotin MicroBeads were added, again well mixed, and incubated for 10 min at 4° C. For depletion, the volume of the sample amount to minimum 500 µl, so if necessary, buffer was added. The sample tube was placed in row A of the tube rack, and two labeled 15 ml tubes were placed in row B and C for the cell fractions (Table 11). The program "Depl05" is optimized for collection of the unlabeled cell fraction and with labeling of unwanted cells by surface markers with low expression. After "Depl05" selection, the negative fraction in row B, containing the unlabeled $CD4^+$ T cells, was collected for further procedures. After centrifugation and discarding the supernatant, the cell pellet was resuspended in 90 µl MACS buffer, 10 µl CD25 MicroBeads were added, mixed and incubated at 4° C for 15 min. Cells were washed with 1-2 ml buffer, centrifuged, the supernatant was discarded, and the pellet resuspended in 500 µl buffer (for up to 10^8 PBMCs at the beginning; for higher cell numbers, the volume was scaled up). The tube containing the sample was again placed in row A in the tube rack, two new tubes were placed in rows B and C (Table 11), and program "Posseld2" for the positive selection was started at the autoMACS Pro Separator. Afterwards, the labeled $CD4^+CD25^+$ regulatory T cells in row C were collected and counted (see 4.2.3) before using them in the following experiments.

4.2.6.3 Dead cell removal

After cell culture of $CD34^+$ HSCs to generate MDSCs (see 4.2.5.2), cells were collected and cell titer and viability checked by trypan blue staining (see 4.2.3). If many cells were dead in the cell suspension, the Dead Cell Removal Kit from Miltenyi Biotec was performed to reduce the amount of dead cells and thereby increasing cell yield of the following isolation of $CD33^+$ MDSCs. First, 20-fold Binding Buffer Stock Solution was diluted with sterile, double distilled water to a 1-fold Binding Buffer. The collected cells were centrifuged at 300 g for 10 min at RT and the supernatant was completely removed. The cell pellet was resuspended in 100 µl Dead Cell Removal MicroBeads per 10^7 total cells. The cell suspension was mixed well and incubated for 15 min at RT. In the meantime, one MACS Column MS per sample was placed in the magnetic field of a MiniMACS Separator and the column was prepared by rinsing with 500 µl 1-fold Binding Buffer. After incubation time, cell suspension was

resuspended with 500 µl 1-fold Binding Buffer and the cell suspension was applied onto the MACS Column. The MACS Column was rinsed four times with 500 µl 1-fold Binding Buffer. The total effluent containing the living cells was collected and further isolation of $CD33^+$ MDSCs was performed (see 4.2.6.4).

4.2.6.4 Isolation of CD33+ MDSCs after in vitro generation

After cell culture of 7 days and detachment of PBMCs or BMMCs (see 4.2.5.1), the cell number of the cytokine-induced PMN-MDSCs was determined (see 4.2.3). The generated MDSCs from $CD34^+$ HSCs (see 4.2.5.2) were also collected, and if required, the Dead Cell Removal Kit was performed, and the cell number was determined. The volumes of the protocol were adjusted according to the cell number.

All cells from one donor were pooled, centrifuged at 400 g, 10 min at RT, and the supernatant was discarded. The cell pellet was resuspended in 80 µl of MACS buffer, mixed with 20 µl CD33 MicroBeads per 10^7 cells and incubated for 15 min at 4° C. After washing the cells with 1-2 ml MACS buffer and complete removal of the supernatant, the pellet was resuspended in 500 µl buffer (for up to 10^8 total cells) and placed in row A in the tube rack of the autoMACS Pro Separator (Table 11). Two new tubes were placed in row B and C for the different fractions. Again, the program "Posseld2" was started for the positive selection, and afterwards the labeled $CD33^+$ cells were collected in row C.

4.2.7 Flow cytometry

Flow cytometry is a laser-based technology to analyze the size and granularity of cells as well as the specific binding of fluorochrom-labeled antibodies to cellular antigens. For analysis the cells are in suspension and one cell at a time passes a light beam and thereby scatters the light. Sensors (or photo multiplying tubes) detect the intensity of the scattered light and the computer further registers and analyzes the data. The detected forward scatter (FSC) represents the cell size, whereas the right-angle scatter, better known as sideward scatter (SSC), correlates with the internal density (granularity) of the cell. Furthermore, by the use of several lasers, filters and detectors also the fluorescence signal of antibodies bound to cellular antigens can be detected. If cells are first labeled with specific fluorochrom-conjugated antibodies and later pass the light beam inside a flow cytometer, the fluorophore absorbs light energy and emits light at a longer wavelength. Due to the filters, each sensor only detects the fluorescence signal at a specific wavelength and converts the energy of the light into voltage.

Thereby, multiple parameters of a single cell can be measured with flow cytometry at the same time. It is also possible to separate cells based on different fluorescence signals in a so called fluorescence-activated cell sorter (FACS). However, this abbreviation is colloquial used instead of flow cytometry (Luttmann *et al.* 2008).

During all preparations for flow cytometry, a washing step was performed by addition of 2 ml FACS buffer to the cells in each 5 ml FACS tube, followed by centrifugation at 400 g, for 5 min at RT and discarding the supernatant.

4.2.7.1 Cell surface staining for characterization of the cell type

First, cells were isolated and if required, cultured and harvested as described above. Afterwards, cells from one donor were pooled in one FACS tube and washed with 2 ml FACS buffer. In the meantime, all antibodies and isotype controls were pipetted to the bottom of labeled FACS tubes and placed in the dark. The cell pellet was resuspended with 50 µl FACS buffer per scheduled approach and from this cell suspension was 50 µl volume transferred to each FACS tube containing antibodies or isotype controls. Cells were incubated with antibodies for 15 min at RT or 30 min at 4° C in the dark. After incubation, the cells were washed with FACS buffer and supernatant was discarded. One sample was stained with 1 µl propidium iodide (PI) 2 min before acquisition to analyze cell viability. Propidium iodide, a membrane impermeable dye, only binds DNA of cells with damaged cell membranes and only PI-negative, living cells were considered for analysis. Flow cytometric analysis was performed with FACSCalibur and Cell Quest Pro Software. MSCs were stained with anti-human CD34-FITC, CD45-FITC, CD73- Phycoerythrin (PE), CD90- PE, CD105-FITC, CD271-PE and HLA-ABC-PE. Freshly isolated PMN-MDSCs were stained with anti-human CD11b-Allophycocyanin (APC), CD14-APC, CD16-PerCP, CD33-PE, CD66b-PE, CXCR4-APC and HLA-DR Peridinin chlorophyll (PerCP). Cytokine-induced $CD33^+$ MDSCs derived from PBMCs, from BMMCs or from $CD34^+$ HSCs were stained with anti-human CD3-PerCP, CD11b-APC, CD14-FITC, CD16-PerCP, CD19-PE, CD33-PE, CD56-FITC, CD66b-FITC, HLA-DR PerCP, CXCR4-APC, CCR5-PE, and CCR2-APC. For all antibodies, the cells were also stained with the appropriate isotype control in the same concentration as the respective antibody. All experiments were performed at least three times in independent experiments.

4.2.7.2 Intracellular staining for characterization of the $CD4^+CD25^+$ Tregs

The $CD4^+CD25^+$ Tregs were isolated from PBMCs by magnetic cell separation (see 4.2.6.2) and the cell surface staining was performed with anti-human CD45RA-FITC, CD3-PerCP,

CD4-APC, CD25-PE, and CD127-FITC as described above (see 4.2.7.1). Intracellular staining of the transcription regulator FoxP3 was performed with use of FoxP3 Staining Buffer Set and Anti-FoxP3 antibody conjugated with APC from Miltenyi Biotec. Before staining, the working concentrations of all reagents were prepared freshly. The Fixation/ Permeabilization Solution 1 was diluted with Fixation/ Permeabilization Solution 2 in the ratio 1:4 and the ten-fold stock of Permeabilization Buffer was diluted with deionized water in the ratio 1:10. After staining with the antibodies binding to the cell surface and one washing step, cells were incubated with 1 ml cold Fixation/Permeabilization Solution per tube for 30 min at 4° C in the dark. Afterwards, cells were washed once with FACS buffer and once with 1 ml Permeabilization Buffer. Cell pellets were resuspended and anti-FoxP3 antibody or its isotype control antibody was added. For antibody binding, cells were incubated at 4° C for 30 min in the dark, followed by one washing step with Permeabilization buffer. After discarding the supernatant, flow cytometry was performed with FACSCalibur and Cell Quest Pro Software. To analyze cell viability, one sample was stained with 1 µl PI for 2 min immediately before acquisition. The characterization staining was performed three times in independent experiments.

4.2.7.3 Flow cytometric analysis of T-cell suppression assay

After incubation of the T-cell suppression assay (see 4.2.8) and collection of supernatants for IFNγ detection (see 4.2.9), cells were harvested by scratching the bottom of the plate and transferring the solution into FACS tubes. Cells were washed once with 2 ml PBS. After addition of 1 µl anti-human CD4 antibody labeled with PE and 1 µl anti-human CD8a APC-antibody per tube, cells were incubated at RT for 10 min in the dark, followed by a washing step. Immediately before acquisition, 1 µl PI was added to each tube for 2 min to analyze cell viability. Flow cytometric analysis was performed with FACSCalibur and Cell Quest Pro Software. During acquisition and analysis, the cells of interest were selected by gating of the cell population as shown in Figure 6.

Briefly, the first gating step was exclusion of cell debris by the density plot of forward and sideward scatter (FSC/SSC plot). By staining with PI, non-viable cells were excluded and only PI-negative, living cells were considered for analysis. The T-cell proliferation was determined by the percent of cells that divided during co-culture and this cell division was detected by the fluorescence intensity of carboxyfluorescein succinimidyl (diacetate) ester (CFSE). This was measured separately for $CD4^+$ and $CD8^+$ T cells by gating cells with high

fluorescence signals for PE or APC, respectively. Polyclonal T-cell proliferation was normalized to responder PBMCs without any immunomodulatory cells as 100 %,

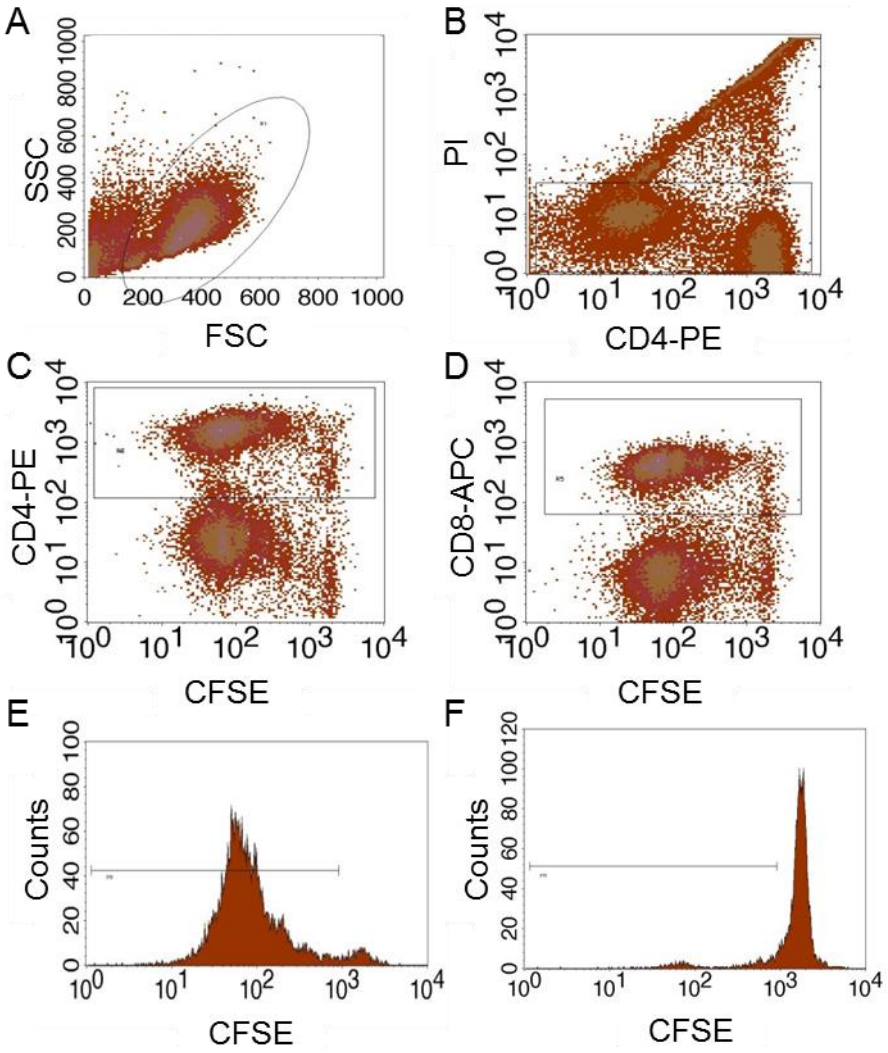

Figure 6: Gating strategy of T-cell suppression assay. (A) First, cell debris was excluded in the dotplot showing forward and sideward scatter. (B) The living cells were selected by exclusion of dead, PI-positive cells. (C+D) $CD4^+$ and $CD8^+$ T cells were separated by staining with surface antibodies. (E+F) T-cell proliferation was analyzed by the CFSE staining. Representative histograms for a positive control with stimulated responder PBMCs (E) and a negative control with unstimulated PBMCs (F) are shown.

4.2.8 T-cell suppression assay

Responder PBMCs were obtained from healthy volunteers and isolated according to 4.2.4. By staining cells with Vybrant CFDA SE Cell Tracer Kit containing carboxyfluorescein succinimidyl (diacetate) ester (CFSE), it is possible to detect cell proliferation by serial halving of the intensity of the fluorescence signal with each cell division (Lyons 2000).

Between 10-20·10^6 PBMCs were transferred to a 15 ml tube, at least 5 ml PBS were added and centrifugation was performed at 400 g for 10 min at RT. In the meantime, 1 µl CFSE dye

was diluted in 5,625 ml PBS and well mixed. The supernatant from the cells was discarded; the pellet was resuspended in 1 ml PBS and carefully 1 ml CFSE solution was added. For staining, the cells were incubated for 10 min at 37° C at 5 % CO_2. The reaction was stopped by addition of 4 ml pre-warmed FBS and 2 min later 6 ml RPMI-1640 medium. Cells were centrifuged at 350 g for 5 min, supernatant removed and the cell pellet resuspended in 1 ml donor-specific media. The cell number was determined (see 4.2.3). Responder PBMCs were stimulated with 100 IU/ml Interleukin-2 and 1 µg/ml anti-human CD3 antibody (clone OKT3 in chapter 5.1-5.2, and clone HIT3a in chapter 5.3-5.4).

According to standardized methods, 60 000 responder PBMCs were co-cultured in a 96-well flat-bottom plate with 10.000 (ratio 1:0.16), 15.000 (ratio 1:0.25), or 30.000 (ratio 1:0.5) immunomodulatory cells per well at 37° C and 5 % CO_2. For each approach, the volume per well was equalized by addition of donor-specific medium. As a positive control, stimulated responder PBMCs without immunomodulatory cells were used, and as a negative control, unstimulated PBMCs were analyzed. In case of co-culture with MSCs, these cells were seeded one day in advance (see 4.2.2). Medium was removed from MSCs directly before responder PBMCs were added. If not indicated otherwise, all experiments were performed in an allogenic setting.

Where indicated, responder PBMCs and immunosuppressive cells were separated by a semipermeable membrane with 0.4 µm pores in a transwell plate in order to investigate if cell-to-cell contact is required. In transwell experiments, responder PBMCs and immuno-modulatory cells were seeded in two ratios (1:0.16 and 1:0.5) without cell-to-cell contact. Due to the bigger volume of the transwell plate, the cell numbers and volumes were doubled.

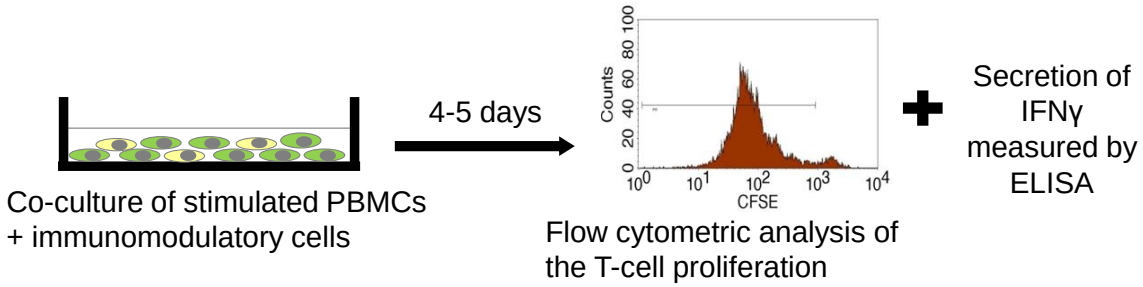

Figure 7: Schematic procedure of T-cell suppression assay. Responder PBMCs were isolated, stained CFSE solution and stimulated with anti-human CD3 antibody and IL-2. Responder PBMCs were co-cultured with previously isolated immuno-modulatory cells in different ratios. After 4-5 days of incubation, the supernatants were collected and stored frozen until analysis of the released IFNγ followed. The cells were harvested, stained with anti-human CD4 and CD8 antibodies and T-cell proliferation measured by flow cytometric analysis.

Where indicated, two types of immunomodulatory cells were co-cultured with stimulated responder PBMCs. In these cases, 60.000 responder PBMCs were incubated with two times

10.000 or 30.000 immunomodulatory cells, changing the ratios of responder PBMCs to all immunomodulatory cells to 1:0.33 or 1:1, respectively.

After co-culture for 4-5 days, 75 µl supernatant from each well were collected and frozen at -80° C for analysis of IFNγ secretion (see 4.2.9). Cells were harvested and stained with anti-human CD4 PE and CD8a APC to determine polyclonal T-cell proliferation as described in 4.2.7.3. All experiments were at least performed three times in independent experiments. Except experiments investigating MSCs combined with freshly isolated PMN-MDSCs were performed only on two days, whereby one time several donors of immunosuppressive cells were used.

4.2.9 Cytokine analysis

IFNγ is an important cytokine for innate and adaptive immune response with pleiotropic functions. It is secreted by several cell types of both types, such as mainly by NK, NKT and T cells, but also APCs and B cells. IFNγ plays a central role in the host defense against intracellular pathogens, such as viruses, and transformed tumor cells. The cytokine IFNγ has immunomodulatory effects, such as activation of macrophages, upregulation of MHC class I and II expression and antigen presentation as well as increased differentiation of naïve $CD4^+$ T cells into Th1 effector cells. Furthermore, IFNγ is involved in the regulation of T-cell proliferation (Wang and Yang 2014; Schoenborn and Wilson 2007).

The secretion of IFNγ during co-culture of stimulated PBMCs with immunomodulatory cells was measured by using enzyme-linked immunosorbent assay (ELISA). ELISA is a biochemical immunoassay to measure the presence and amount of a substance in a fluid sample by using specific antibodies and a color change due to an enzymatic reaction. The IFN-γ DuoSet ELISA is based on a sandwich immunoassay and was performed according to manufacturer's protocol.

Supernatants from T-cell suppression assays were taken on day 4 or 5 and stored at -80° C until cytokine analysis. Human IFNγ standard from the kit was reconstituted by adding 0.5 ml reagent diluent to each vial of lyophilized, recombinant human IFNγ, 15 min gentle shaking and then 15,4 µl IFNγ standard with 984,6 µl reagent diluent were mixed and stored at -80° C. The mouse anti-human IFNγ capture antibody was solved with 0.5 ml PBS, the biotinylated goat anti-human IFNγ detection antibody was reconstituted with 1.0 ml reagent diluent, both were 15 min gently mixed, aliquot and stored at -20° C until use.

The human IFNγ capture antibody was diluted to the working concentration of 4.0 µg/ml with PBS and immediately 100 µl per well were used for coating the microtiter plate. The plate

was sealed and incubated overnight at RT with the IFNγ-specific capture antibody (Figure 8). The next day, unbound antibodies were removed by aspirating each well and washing with wash buffer three times. For each washing step, wash buffer was added to each well and the liquid was completely removed by inverting the plate over the sink and blotting it against clean paper towels. Afterwards, a blocking step was performed to decrease unspecific binding of other molecules by adding 300 µl blocking buffer to each well and incubating at RT for at least 1 hour. In the meantime, standards and supernatants were thawed at RT. A serial dilution of the reconstituted human IFNγ standard was prepared with reagent diluent by always transferring 500 µl to the next tube. The supernatants were diluted with reagent diluent in 1:3 or 1:5 ratio to adjust their concentration to the standard concentrations.

After blocking, the washing procedure was repeated three times. Then, 100 µl of prepared samples, standards or reagent diluent as a blank were added per well. The plate was covered with an adhesive strip and incubated for 2 hours at RT allowing the secreted IFNγ to bind to the capture antibody (Figure 8). During incubation time, the reconstituted human IFNγ detection antibody was thawed at RT, diluted to the concentration of 200 ng/ml with reagent diluent containing 2 % of heat-inactivated normal goat serum. After washing three times to remove unbound supernatants, 100 µl of prepared detection antibody was added per well, covered, and again incubated for 2 hours at RT.

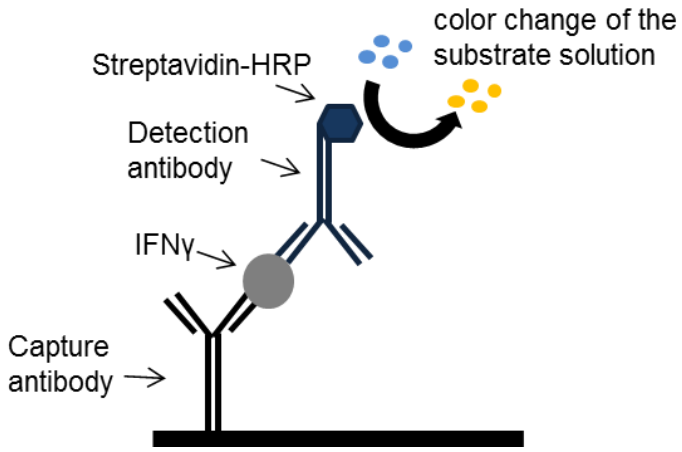

Figure 8: Principle of ELISA. First, the capture antibody bins to the microplate. IFNγ binds to this antibody during incubation with the supernatants from the T-cell suppression assay. The detection antibody binds to IFNγ and next, the Streptavidin- horseradish peroxidase (HRP) binds to this antibody. By addition of the substrate solution, an oxidation occurs and the bound IFNγ turns blue, followed by a color change after adding the stopping solution. The graphic is adapted from the manufactrer's web page: www.rndsystems.com/resources/technical/duoset-elisa-development-systems-assay-principle.

Afterwards, the plate was again washed three times as described above. The Streptavidin-horseradish peroxidase (HRP) was diluted to the lot-specific working concentration using reagent diluent. To each well 100 µl of the working dilution of Streptavidin-HRP were added. The plate was covered and incubated at RT for 20 min in the dark. The Streptavidin-HRP

binds to the biotin-conjugated detection antibody and catalyzes later the oxidation of the substrate solution leading to color development. After incubation, the washing procedure was repeated three times. The substrate solution was prepared by mixing color reagent A containing H_2O_2 with color reagent B containing tetramethylbenzidine in a 1:1 ratio. Addition of 100 µl substrate solution to each well and incubating for 20 min at RT in the dark leads to development of blue color (Figure 8). The intensity of the blue color is proportional to the bound content of IFNγ. The oxidization was stopped by adding stopping solution (2 mol/liter sulfuric acid), again leading to a color change from blue to yellow. The optical density of the differently colored samples was measured at 450 nm and at 570 nm in the microplate reader. Using the Gen5 Software, the blank only contained the reagent diluent and its value was regarded as zero optical density, thus the blank value was subtracted from all sample values. Afterwards, the measurement at 570 nm was subtracted from the data at 450 nm for correction of optical imperfections of the plate. The standard curve was generated with the software as a four parameter logistic curve-fit. The average of all duplicates was calculated and the value of the samples multiplied by the dilution factor. To normalize the different levels of IFNγ due to donor dependency, the IFNγ values were also normalized to the value of the control. The calculated values were further analyzed by GraphPad Prism 6.0 software for statistical analysis (see 4.2.10).

4.2.10 Statistical analysis

Data are reported as means ± standard deviations (SD). Statistical analysis was performed by using GraphPad Prism 6.0. Differences between the groups were determined by a Mann-Whitney test regarding non-Gaussian distribution. In all tests, a p value ≤ 0.05 was considered to be significant (* $p \leq 0.05$, ** $p \leq 0.01$, *** $p \leq 0.001$).

5 Results

5.1 Comparison of T-cell suppressive effect of freshly isolated PMN-MDSCs, MSCs, and CD4+CD25+ Tregs

After HSCT the transplanted alloreactive T cells from the donor can cause GvHD by an immunological reaction against cells of the recipient. One treatment option for GvHD could be a cell transfer of immunomodulatory cells, such as MSCs, PMN-MDSCs or Tregs. However, until now, it is not clarified which cell type is the most suitable one for this application.

5.1.1 Characterization of MSCs, freshly isolated PMN-MDSCs as well as Tregs

Before a functional assessment of the different cell types regarding the suppression of T-cell function was measured, a phenotypic characterization of each cell type was performed to ensure that the correct cells were used.

MSCs were isolated and *in vitro* expanded (see 4.2.1 and 4.2.2). The MSCs showed plastic adherence and a fibroblastic appearance during cell culture (Figure 9). By staining of MSCs with fluorochrom-labeled antibodies and flow cytometric analysis (see 4.2.7.1), the expression of phenotypic cell surface molecules was examined. MSCs demonstrated the expression of the surface markers CD73, CD90, CD105, HLA-ABC, whereas CD45, HLA-DR as well as CD34 were absent, as seen in Figure 9 by the representative histograms.

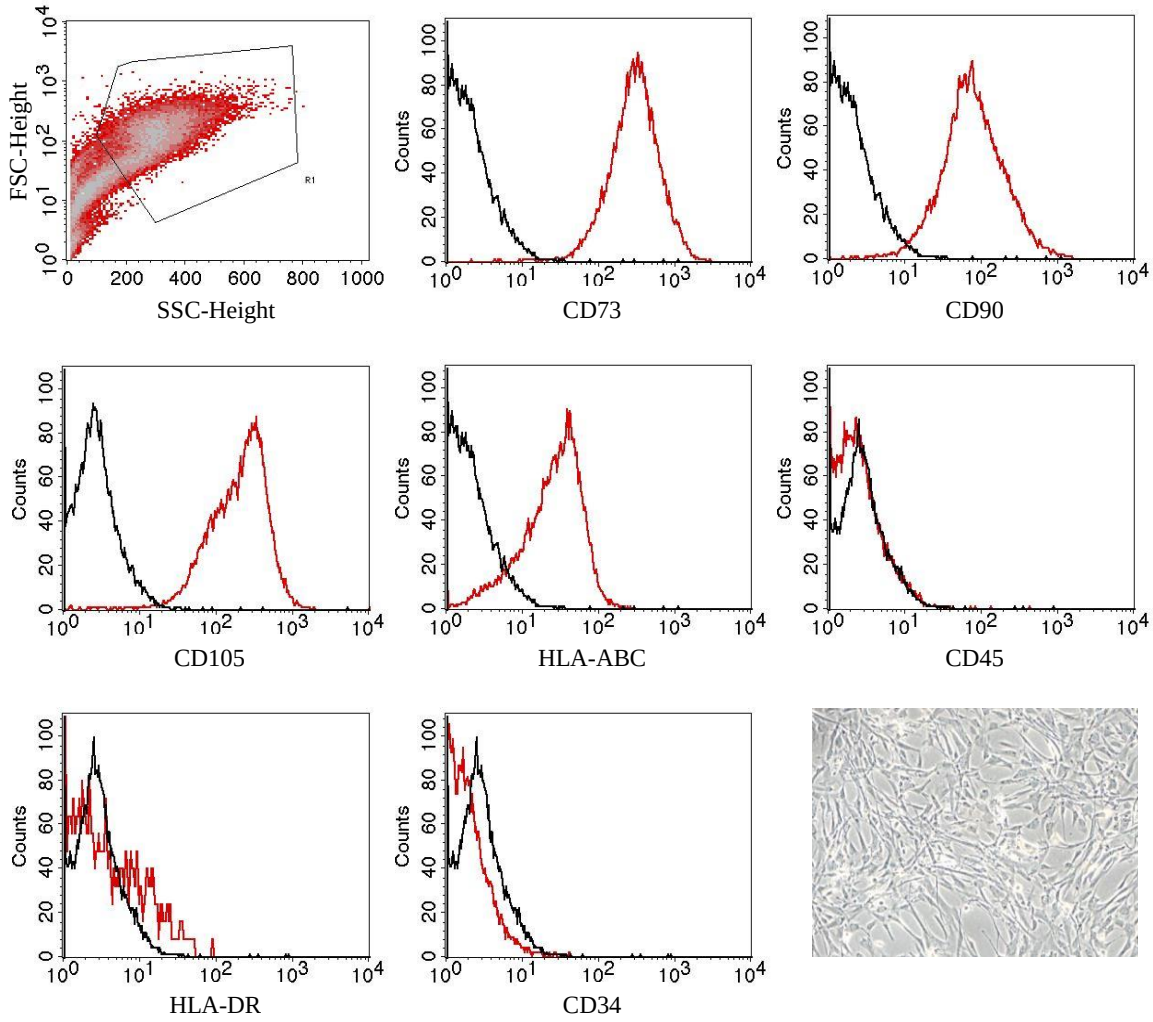

Figure 9: Characterization of MSCs. Human MSCs were isolated, cultured and cell morphology was analyzed at 20-fold original magnification by microscopy. The immunophenotype of MSCs was confirmed as $CD73^+$, $CD90^+$, $CD105^+$, $HLA\text{-}ABC^+$, $CD45^-$, $HLA\text{-}DR^-$, and $CD34^-$. Representative histograms are shown with surface markers in red and isotype controls in black.

PMN-MDSCs were isolated from blood by density centrifugation and magnetic separation of $CD66b^+$ cells (see 4.2.4 and 4.2.6.1). After staining of the freshly isolated PMN-MDSCs with fluorochrom-labeled antibodies, the expression of surface molecules was determined by flow cytometric analysis (see 4.2.7.1). Freshly isolated PMN-MDSCs demonstrated by their SSC^{high} position in the forward/sideward scatter dot plot that PMN-MDSCs have a high granularity. Further, PMN-MDSCs showed a high expression of CD66b, CD33, CD11b, and CD16, an intermediate expression of CXCR4, but no HLA-DR and CD14 (Figure 10).

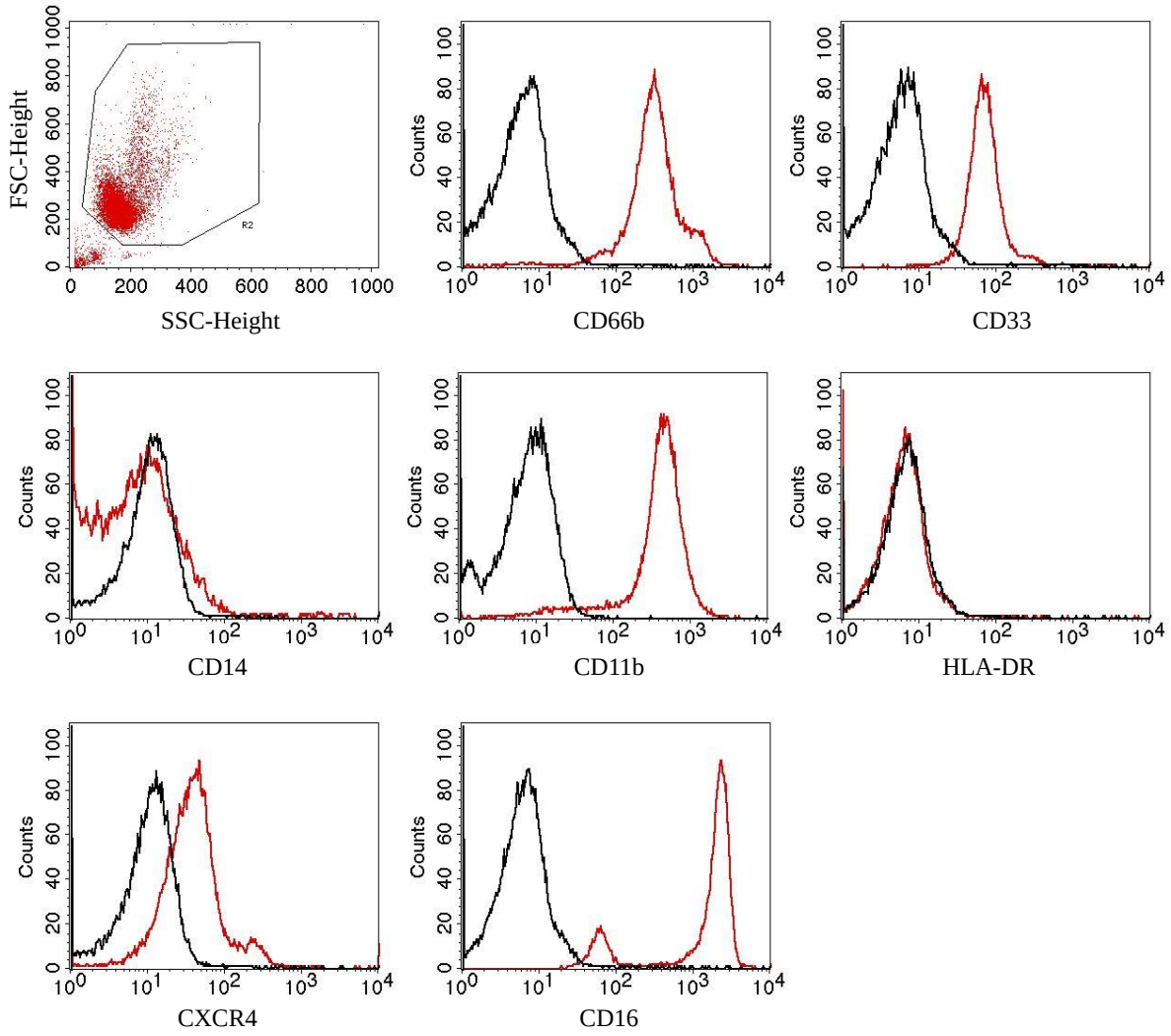

Figure 10: Characterization of freshly isolated PMN-MDSCs. PMN-MDSCs were obtained from PBMC fraction by magnetic separation with anti-human CD66b-FITC antibodies and anti-FITC MicroBeads. The immunophenotype of PMN-MDSCs was determined as SSC^{high}, $CD66b^{+}$, $CD33^{+}$, $CD11b^{+}$, $CXCR4^{+}$, $CD16^{+}$, $CD14^{-}$, and $HLA\text{-}DR^{-}$. Representative histograms are shown with surface markers in red and isotype controls in black.

Tregs were also isolated from PBMCs by magnetic separation of $CD4^{+}CD25^{+}$ cells (see 4.2.4 and 4.2.6.2). Surface molecules and the intracellular transcription factor FoxP3 were stained with fluorochrom-labeled antibodies for the phenotyping of Tregs (see 4.2.7.1 and 4.2.7.2). Isolated Tregs showed a distinct population in the forward/sideward scatter dot plot with a high expression of the surface markers CD3, CD4, CD25 and the absence of CD127. Further, the transcription factor FoxP3 was highly expressed intracellular and a small population of Tregs also expressed CD45RA on the cell surface (Figure 11).

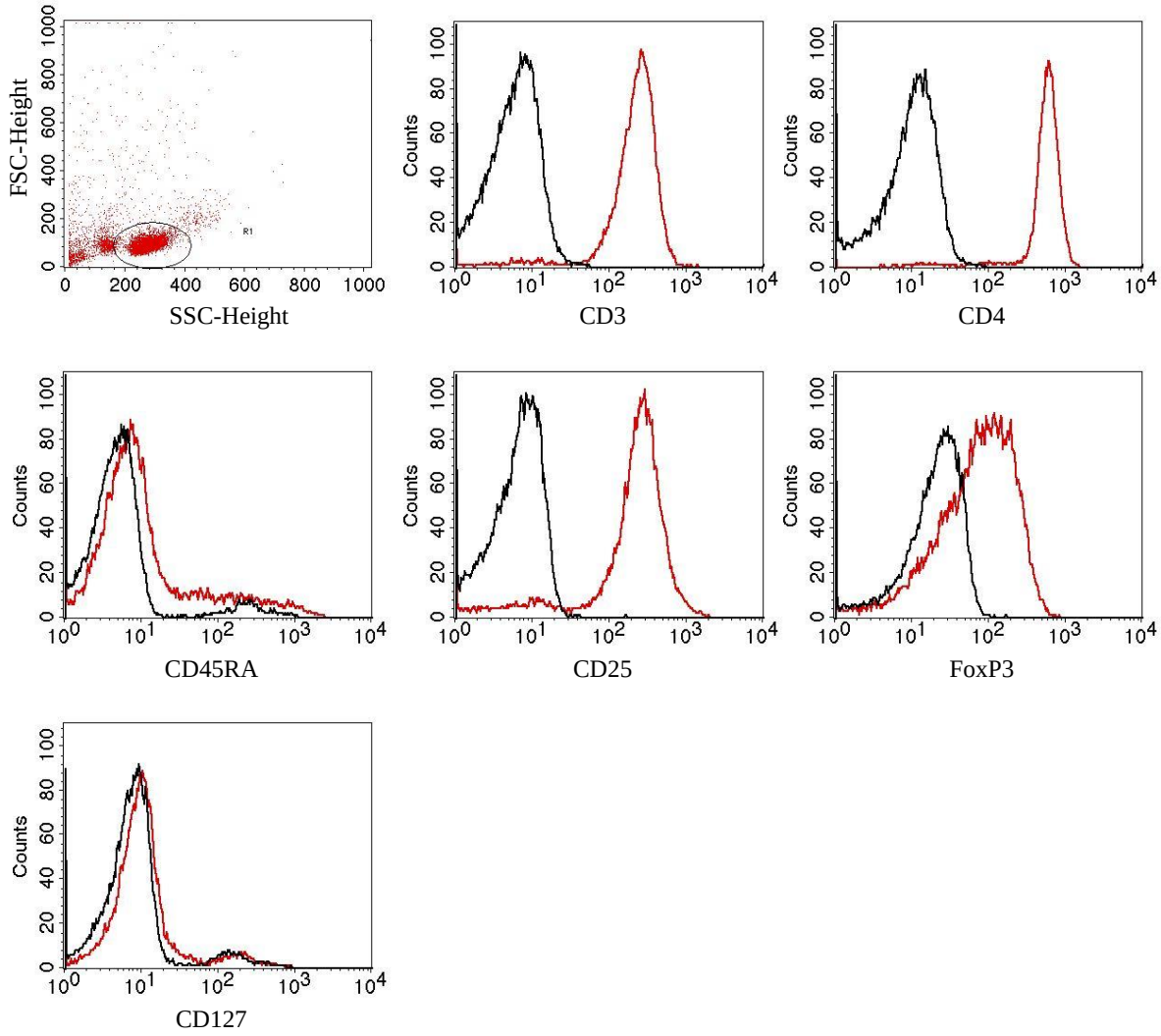

Figure 11: Characterization of regulatory CD4$^+$ CD25$^+$ T cells. Tregs were isolated from the PBMC fraction by using CD4$^+$CD25$^+$ Regulatory T Cell Isolation Kit. Tregs were identified as CD3$^+$, CD4$^+$, CD25$^+$, FoxP3$^+$, CD127$^-$, and CD45RA^{low}. Typical histograms are presented with cell markers in red and isotype controls in black.

5.1.2 Functional assessment of T-cell suppressive effect of freshly isolated PMN-MDSCs, MSCs, and CD4$^+$CD25$^+$ Tregs

To assess the T-cell suppressive potential of MSCs, freshly isolated PMN-MDSCs or Tregs, we systematically performed CFSE assays in which stimulated allogenic responder PBMCs were co-cultured with immunomodulatory cells and after 4-5 days of incubation, the poly-clonal T-cell proliferation was measured by flow cytometric analysis. As seen in Figure 12, the stimulated responder PBMCs without any immunomodulatory cells regarded as a positive control showed a strong T-cell proliferation, whereas unstimulated responder PBMCs without any other cells regarded as a negative control showed only one peak of undivided T cells as a result of no proliferation.

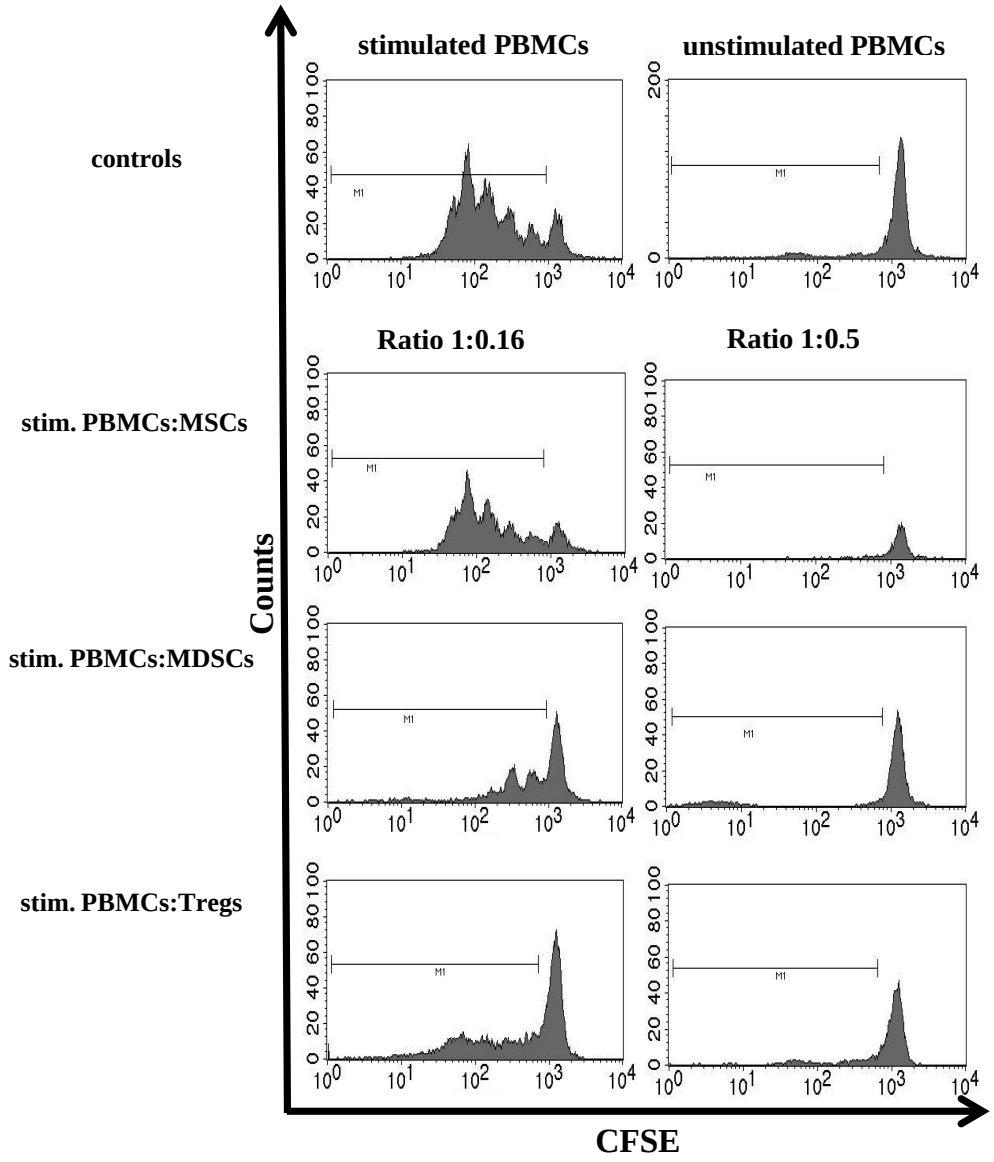

Figure 12: Representative histograms polyclonal T-cell proliferation assay. Responder PBMCs were isolated, labelled with CFSE and stimulated with anti-human CD3 antibody and IL-2 to induce polyclonal T-cell proliferation. The stimulated responder PBMCs were co-cultured with allogenic MSCs, MDSCs, or $CD4^+CD25^+$ Tregs in different ratios for 4-5 days at 37 °C and 5 % CO_2. Stimulated PBMCs without immunomodulatory cells and unstimulated PBMCs were used as controls. After incubation, the proliferation of $CD4^+$ and $CD8^+$ T cells was analyzed by flow cytometry. Representative histograms from $CD8^+$ T cells are shown in the ratios 1:0.16 and 1:0.5.

The representative histograms in Figure 12 indicate that each MSCs, PMN-MDSCs and Tregs inhibited the $CD8^+$ T-cell proliferation. Comparing the two cell ratios, more suppression of the T-cell proliferation was seen with a higher amount of immunomodulatory cells.

To investigate the suppressive potential of different immunomodulatory cells, CFSE co-culture assays was systematically performed to analyze polyclonal T-cell proliferation and the release of IFNγ was checked by enzyme-linked immunosorbent assay (ELISA).

Stimulated responder PBMCs without other cells were set to 100 % as positive control in Figure 13, showing the results of the other conditions in percent compared to this control. The addition of MSCs, freshly isolated PMN-MDSCs or $CD4^+CD25^+$ Tregs led to a decrease of both $CD4^+$ and $CD8^+$ T-cell proliferation, respectively (Figure 13 A). Each immunomodulatory cell type suppressed T-cell proliferation in a dose-dependent manner comparing the different ratios. At a ratio of 1:0.16, the proliferation was around 45.4 ± 22.5 % for $CD4^+$ and 42.5 ± 18.9 % for $CD8^+$ T cells with MSCs, 33.9 ± 24.2 % and 26.8 ± 20.0 % for $CD4^+$ and $CD8^+$ T cells with freshly isolated PMN-MDSCs, and 39.9 ± 20.1 % for $CD4^+$ and 39.9 ± 19.1 % for $CD8^+$ T cells with $CD4^+CD25^+$ Tregs. Accordingly, the data of each immunomodulatory cell type demonstrated variance between different experiments, which was greater at lower concentrations of immunomodulatory cells.

At a ratio of 1:0.5, 85.8 % of $CD4^+$ and 83.9 % of $CD8^+$ T-cell proliferation were inhibited by MSCs, 96.3 % of $CD4^+$ and 94.3 % of $CD8^+$ T-cell proliferation were inhibited by freshly isolated PMN-MDSCs, and 91.5 % of $CD4^+$ and 88.8 % of $CD8^+$ T-cell proliferation were inhibited by Tregs. Comparing the suppression at the 1:0.5 ratio, freshly isolated PMN-MDSCs suppressed both $CD4^+$ and $CD8^+$ T-cell proliferation significantly stronger than MSCs (p=0.009 and p=0.002, respectively) and $CD4^+CD25^+$ Tregs (p=0.008 and p=0.04, respectively) (Figure 13 A).

In vitro expanded MSCs, freshly isolated PMN-MDSCs and freshly isolated Tregs strongly suppressed the release of IFNγ during co-culture with stimulated PBMCs compared to the level of IFNγ of the positive control only containing stimulated PBMCs, which was set to 100 %. All three immunomodulatory cell types acted in a dose-dependent manner. Thereby, freshly isolated PMN-MDSCs and freshly isolated Tregs revealed a greater variance in the reduction of IFNγ secretion between different experiments than expanded MSCs, again especially at lower concentrations of immunomodulatory cells. At a ratio of 1:0.5, the level of IFNγ was at 1.3 ± 1.4 % with MSCs, at 10.4 ± 9.7 % with PMN-MDSCs, or at 3.6 ± 3.9 % with Tregs compared to 100 % in the untreated control of stimulated PBMCs. Overall, MSCs showed a significantly greater inhibition of IFNγ secretion than PMN-MDSCs (p=0.01) and Tregs (p=0.05) (Figure 13 B).

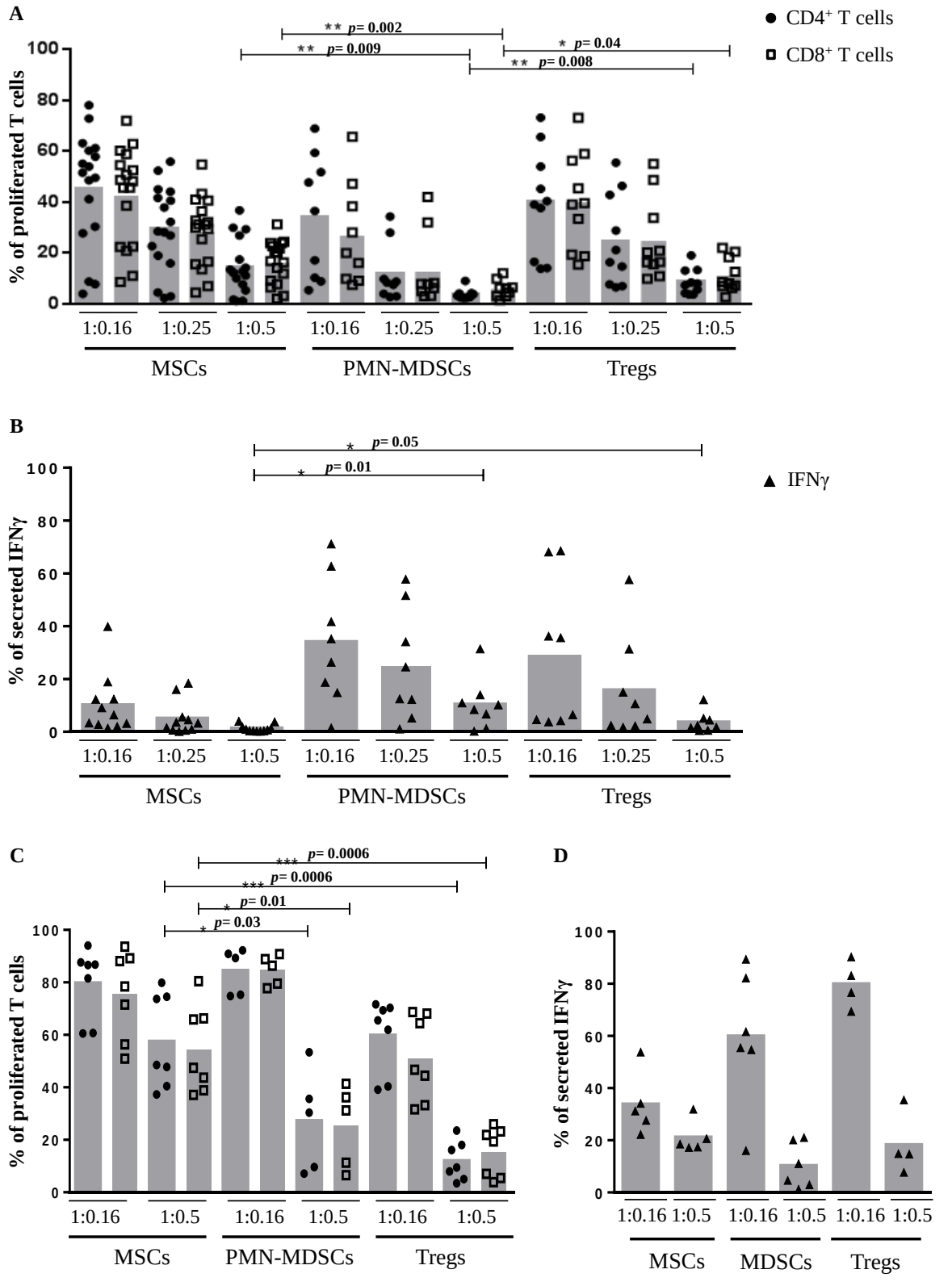

Figure 13: Suppressive effects on T-cell proliferation and secretion of Interferon-γ by MSCs, polymorphonuclear MDSCs and CD4$^+$CD25$^+$ Tregs. (A) Responder PBMCs were labeled with CFSE, stimulated with anti-human CD3 antibody and IL-2 to induce polyclonal T-cell proliferation, and cultured in different ratios of 1:0.16, 1:0.25 or 1:0.5 with the indicated immunomodulatory cells. After 4 days of incubation, the proliferation of T cells was analyzed by flow cytometry. Each donor of responder PBMCs is presented by ● for CD4+ and by □ for CD8+ T cells. MSCs of 9 different donors, PMN-MDSCs of 7 donors and CD4+CD25+ Tregs of 6 donors were examined. (B) After co-culture the supernatants were collected and the secretion of IFNγ was determined by ELISA. Each ▲ indicates the level of IFNγ from a single donor of responder PBMCs after co-culture with the indicated cell type from assays as in Figure 13 A. (C) PBMCs and

immunomodulatory cells were used in ratios of 1:0.16 and 1:0.5 and the cells were separated by a semipermeable membrane in a transwell system during T-cell suppression assay. Each donor of responder PBMCs is presented by ● for CD4+ and by □ for CD8+ T cells. MSCs of 4 different donors, PMN-MDSCs of 5 donors and CD4+CD25+ Tregs of 4 donors were examined. (D) The supernatants of the stimulated PBMCs were collected after 4 days incubation in a transwell system and the release of IFNγ was analyzed by ELISA. Each ▲ indicates the level of IFNγ from a single donor of responder PBMCs after co-culture with the indicated cell type. All measurements were normalized to the control of untreated PBMCs as 100 %.

In order to analyze if cell-to-cell contact is required for the inhibitory effect, stimulated PBMCs and immunomodulatory cells were separated by a semipermeable membrane in a transwell system (Figure 13 C+D). Regarding cell proliferation as shown in Figure 13 C, MSCs only slightly suppressed T-cell proliferation, also in a dose-dependent manner, indicating that cell-to-cell contact was required for effective inhibition after polyclonal T-cell stimulation. Freshly isolated PMN-MDSCs also inhibited T-cell proliferation in this experimental setting, whereby the higher concentration of PMN-MDSCs had a much stronger effect than the lower one. Furthermore, a suppression of T-cell proliferation by $CD4^+CD25^+$ Tregs was also detected in the transwell system. Comparing the ratio 1:0.5, the T-cell suppressive effect of PMN-MDSCs and Tregs, respectively were significantly higher than the inhibition of T-cell proliferation by MSCs (Figure 13 C). As seen in Figure 13 D, the secretion of IFNγ was also suppressed without direct cell-to-cell contact by MSCs, PMN-MDSCs and $CD4^+CD25^+$ Tregs, respectively. Compared to the slight effect of MSCs towards T-cell proliferation in this experimental setting, the level of secreted IFNγ was clearly decreased. At the ratio 1:0.5, PMN-MDSCs and Tregs distinctly inhibited the release of IFNγ.

5.1.3 Functional assessment of freshly isolated PMN-MDSCs in an autologous and an allogenic setting

For patients with GvHD, a cell transfer of immunomodulatory cells could be a treatment option. After a HSCT, in most cases the transplanted T cells from the donor cause the GvHD. But, even after allogenic HSCT, the use of immunomodulatory cells from the same donor as the HSC would lead to an autologous setting of activated effector T cells and the immunomodulatory cells. Therefore, the inhibitory effect of PMN-MDSCs was compared in an autologous experimental setting containing stimulated PBMCs from the same blood donor and the suppression in an allogenic setting containing stimulated PBMCs from another person by T-cell suppression assay and analysis of the secretion of IFNγ.

As seen in Figure 14 A, freshly isolated PMN-MDSCs suppressed T-cell proliferation in a dose-dependent manner in the autologous and allogenic setting. At the ratio 1:0.5, 87.0 % of $CD4^+$ and 88.9 % of $CD8^+$ T-cell proliferation were inhibited by freshly isolated PMN-

MDSCs in the autologous setting, compared to 96.3 % inhibition of $CD4^+$ and 94.3 % inhibition of $CD8^+$ T-cell proliferation in the allogenic setting. This demonstrates that PMN-MDSCs suppressed T-cell proliferation slightly better in an allogenic than autologous setting, but not significantly different and in the same range as MSCs and Tregs. The inhibitory effect of PMN-MDSCs showed more variance between different experiments in the autologous setting than in the allogenic setting.

Additionally, freshly isolated PMN-MDSCs suppressed the secretion of IFNγ in both settings in a similar, concentration-dependent range (Figure 14 B).

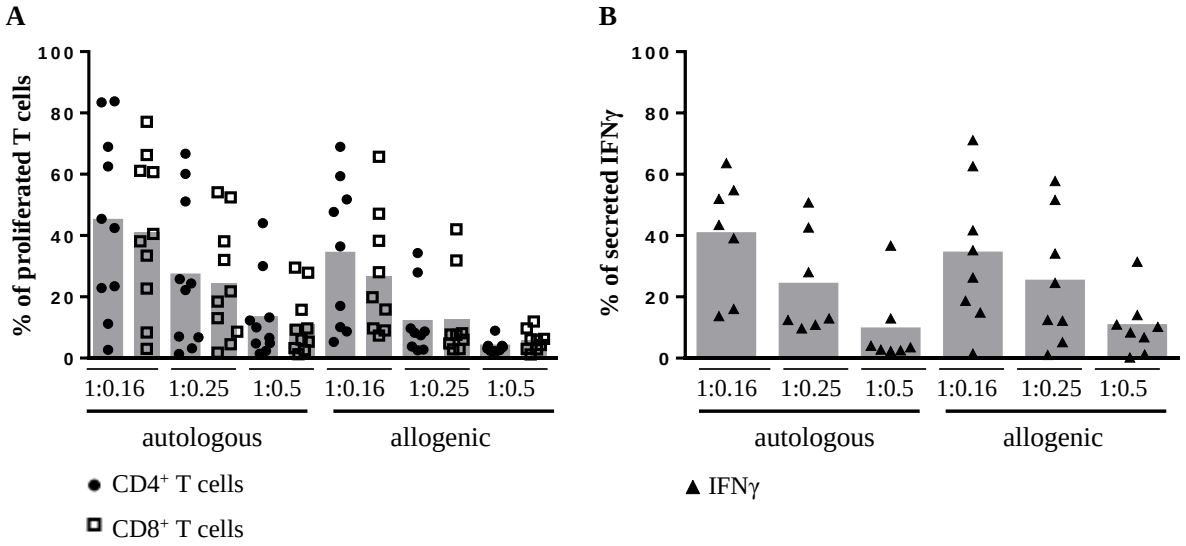

Figure 14: Comparison of the T-cell suppression by autologous and allogenic PMN-MDSCs. (A) Responder PBMCs were labelled with CFSE, stimulated with anti-human CD3 antibody and IL-2. PMN-MDSCs were isolated by magnetic separation with CD66b antibodies and appropriate MicroBeads. Stimulated PBMCs were cultured in different ratios of 1:0.16, 1:0.25 or 1:0.5 with PMN-MDSCs from either the autologous or an allogenic donor as indicated. After 4 days of incubation, the proliferation of T cells was analyzed by flow cytometry. Each donor of responder PBMCs is presented by ● for $CD4^+$ and by □ for $CD8^+$ T cells. (B) Supernatants from the co-cultured PBMCs with PMN-MDSCs were collected after 4 days and were assessed for IFNγ levels by ELISA. Each ▲ indicates the level of IFNγ from a single donor of responder PBMCs.

5.1.4 Functional assessment of MSCs and PMN-MDSCs from the same donor in an autologous and an allogenic setting

To further compare the inhibitory effect of MSCs and PMN-MDSCs, we isolated these two cell types from the same donor and analyzed their T-cell suppressive capacity in an autologous and an allogenic setting. As seen in Figure 15 A showing an autologous setting, freshly isolated PMN-MDSCs suppressed on average the $CD4^+$ and $CD8^+$ T-cell proliferation slightly more than MSCs, however not significantly more because T-cell proliferation of one donor was not inhibited neither by PMN-MDSCs nor by MSCs. The detailed comparison of $CD4^+$ and $CD8^+$ T-cell proliferation at a specific ratio, e.g. 1:0.25, shows that in a single donor $CD4^+$ T cells are more suppressed by immunomodulatory cells, whereas in another

donor $CD8^+$ T cells are more inhibited. In addition, the secretion of IFNγ was inhibited in a dose-dependent manner by autologous freshly isolated PMN-MDSCs and by autologous MSCs (Figure 15 B). Also in the supernatants from the co-cultured cells of the donor with almost no effect on T-cell proliferation, a clear decrease of the level of IFNγ was detected.

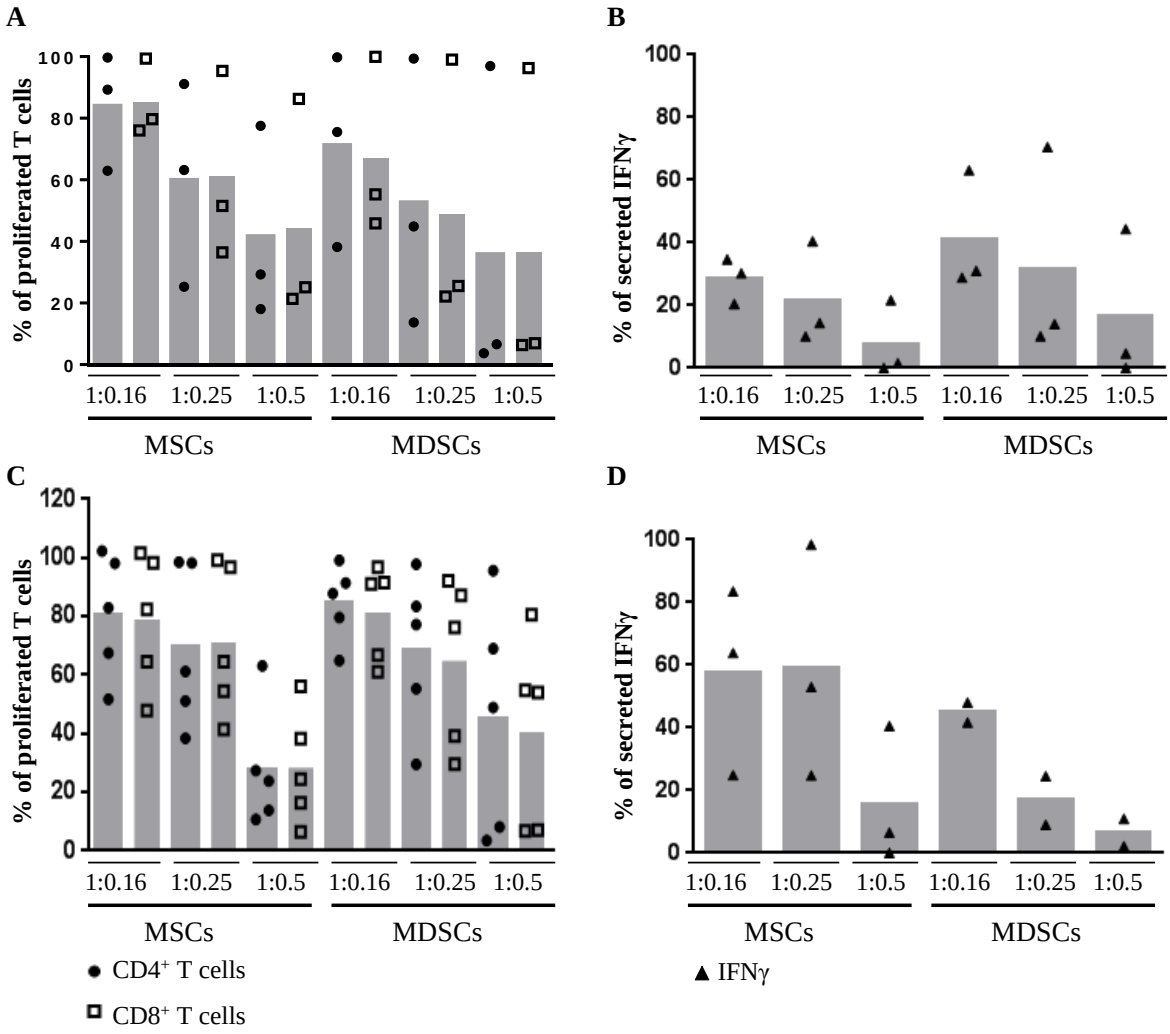

Figure 15: Comparison of MSCs and PMN-MDSCs from the same donor in an autologous and allogenic setting. (A and C) First, MSCs were isolated and cultured for up to 10 passages. PBMCs from heparinized fresh blood of the same donor were isolated by density gradient centrifugation. PMN-MDSCs were isolated from these PBMCs by magnetic separation with CD66b antibodies and appropriate MicroBeads. Additionally, responder PBMCs from that donor and another donor were labelled with CFSE, stimulated with anti-human CD3 antibody and IL-2. Stimulated PBMCs were cultured with MSCs or PMN-MDSCs in different ratios of 1:0.16, 1:0.25 or 1:0.5. After 4 days of incubation, the proliferation of T cells was analyzed by flow cytometry. Each donor of responder PBMCs is presented by ● for $CD4^+$ and by □ for $CD8^+$ T cells. (B and D) Supernatants from the co-cultured PBMCs with MSCs or PMN-MDSCs were collected after 4 days and the secretion of IFNγ was measured by ELISA. Each ▲ indicates the level of IFNγ from a single donor of responder PBMCs. In Figure 15 A+B, the autologous experimental setting is presented with responder PBMCs, MSCs, and PMN-MDSCs from the same donor, whereas in Figure 15 C+D the allogenic setting is shown with stimulated PBMCs from another donor, but MSCs and PMN-MDSCs were both obtained from the same donor.

Using MSCs and freshly isolated PMN-MDSCs from the same donor in an allogenic experimental setting containing stimulated PBMCs from another donor, both immuno-

modulatory cell types suppressed T-cell proliferation and the secretion of IFNγ in a concentration-dependent way (Figure 15 C+D). At the ratio 1:0.5, MSCs inhibited T-cell proliferation slightly more than PMN-MDSCs, but this was not significant. The data of this experimental setting showed a big variance between different donors. The small number of replicates was due to limited access to MSC donors, who agreed to also donate blood for this experiment.

Overall, the inhibitory effect of MSCs and PMN-MDSCs from the same donor showed similar results as the effect from different donors of the cell types.

5.1.5 Cell yield of freshly isolated PMN-MDSCs and $CD4^+CD25^+$ Tregs

For treatment of patients, the amount of immunomodulatory cells is crucial. The *in vitro* expansion of MSCs is already routinely done in our clinic and the cell yield is sufficient for treatment of patients. However, both PMN-MDSCs and $CD4^+CD25^+$ Tregs are rare in the peripheral blood of healthy humans. We isolated these cells by magnetic separation from PBMCs with a percentage of 0.37 ± 0.16 % and 0.46 ± 0.23 %, respectively (Table 12).

Isolated cells in percent of PBMCs	Mean ± SD
PMN-MDSCs (n=15)	0.37 ± 0.16
$CD4^+CD25^+$ Tregs (n=15)	0.46 ± 0.23

Table 12: Percentage of freshly isolated PMN-MDSCs and $CD4^+CD25^+$ Tregs in percent of PBMCs

These available cell numbers are too low for clinical application. Due to the higher suppression of T-cell proliferation of PMN-MDSCs, the *in vitro* generation of MDSCs derived from PBMCs was investigated to increase the cell yield.

5.2 Comparison of T-cell suppressive effect of cytokine-induced MDSCs from mononuclear cells

To raise the available cell number, PBMCs were first isolated and cultured *in vitro* with different cytokine stimulations to generate sufficient amounts of PMN-MDSCs. Based on the protocols from Lechner *et al.* 2010, PBMCs were stimulated with 10 ng/ml granulocyte/ macrophage colony-stimulating factor (GM-CSF) alone or in combination with 10 ng/ml human IL-6 for 7 days.

5.2.1 Characterization of PBMC-derived, cytokine-induced MDSCs

To ensure that the cytokine stimulations led to the generation of MDSCs, the cells were phenotypically characterized by flow cytometric analysis of surface markers.

As seen in Figure 16, the cytokine-induced, *in vitro* generated PMN-MDSCs derived from PBMCs showed a high expression of CD33, CD11b, and CD16, an intermediate expression of CXCR4 and HLA-DR, but CD14 and CD66b were absent. Further, these PBMC-derived PMN-MDSCs were also SSC^{high} in the forward/sideward scatter dot plot. In addition, these cultured cells were negative for CD3, CD56 and CD19 that are typical lineage markers of T, NK, and B cells, respectively. Both, the cells generated by stimulation with GM-CSF alone and the cells stimulated with GM-CSF and IL-6 demonstrated the same expression profile of surface markers, thus, only cells stimulated with GM-CSF are shown in Figure 16. To distinguish these PBMC-derived, cytokine-induced cells from neutrophilic granulocytes, expression of CCR2 was analyzed and confirmed for the PBMC-derived, cytokine-induced cells.

Overall, the PBMC-derived, cytokine-stimulated cells showed a very similar phenotypical expression of surface markers as freshly isolated PMN-MDSCs except of CD66b and HLA-DR.

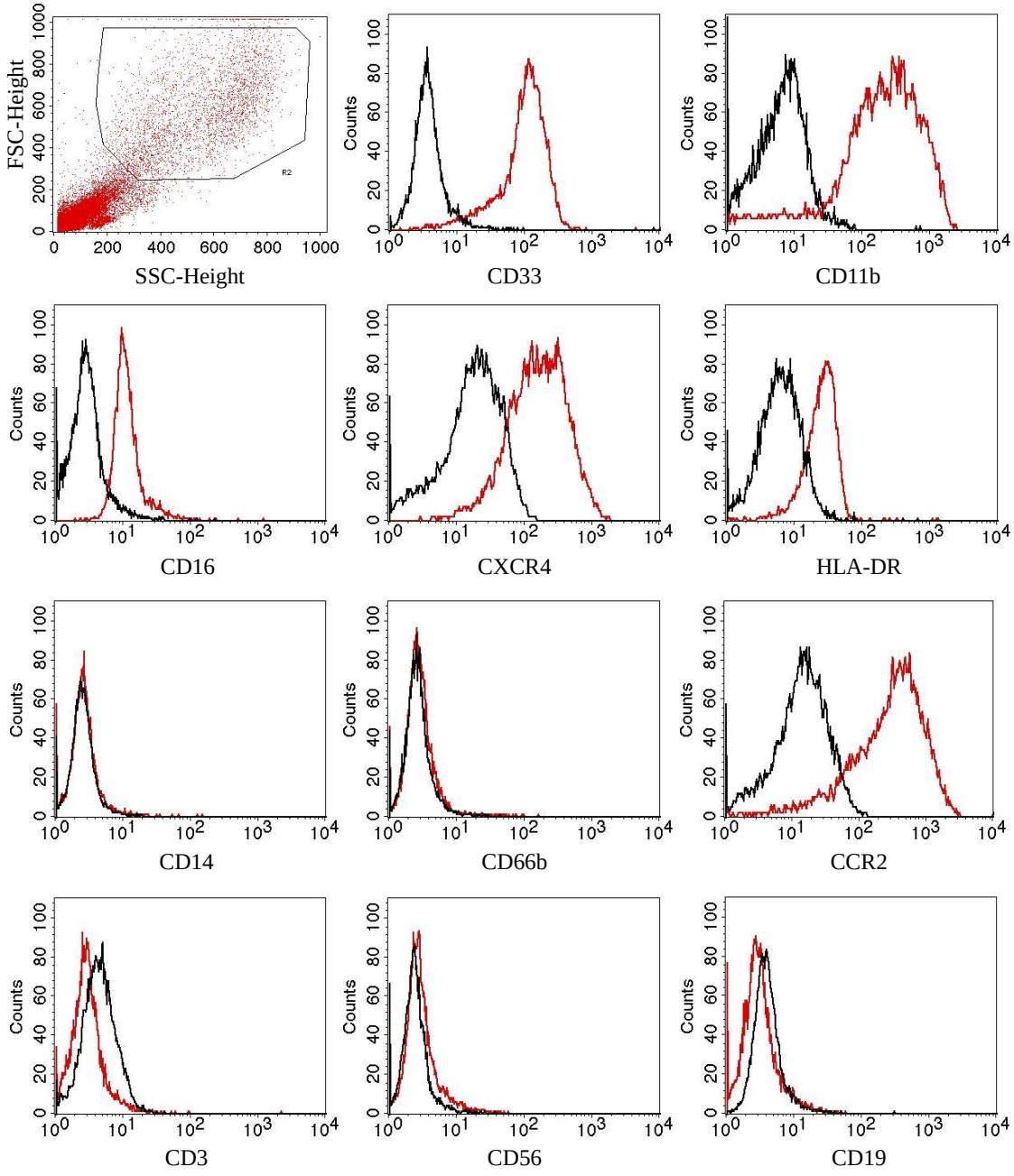

Figure 16: Characterization of PBMC-derived, cytokine-induced MDSCs. PBMCs were cultured in complete medium with 10 ng/ml GM-CSF for 7 days. Cytokine-induced MDSCs from PBMCs were identified as SSC^{high}, $CD33^{+}$, $CD11b^{+}$, $CD16^{+}$, $CXCR4^{inter}$, $HLA\text{-}DR^{inter}$ as well as $CD14^{-}$ $CD66b^{-}$, $CCR2^{+}$, and negative lineage markers (CD3, CD19, CD56). In the representative histograms, surface markers are shown in red and isotype controls in black.

5.2.2 Functional assessment of the T-cell suppressive effect of cytokine-induced MDSCs derived from PBMCs

To evaluate the suppressive potential of the PBMC-derived, cytokine-induced $CD33^+$ cells, the same co-culture experiments were performed as previously described.

Both types of stimulated, PBMC-derived $CD33^+$ cells suppressed proliferation of allogenic $CD4^+$ and $CD8^+$ T cells in a dose-dependent manner, as seen in Figure 17 A. This T-cell suppressive data together with the characterization (Figure 16) demonstrated that PBMC-derived, cytokine-induced cells were MDSCs. However, this inhibition of PBMC-derived, cytokine-induced $CD33^+$ MDSCs was lower in the allogenic setting containing PBMCs stimulated with anti-human CD3 antibody and IL-2 than detected by Lechner *et al*. 2010 in the autologous setting containing isolated T cells stimulated with anti-CD3/CD28 beads and IL-2. At the ratio 1:0.5, the PBMC-derived, GM-CSF-induced PMN-MDSCs suppressed the proliferation of $CD4^+$ T cells by 66.5 ± 19.3 % and for $CD8^+$ T cells by 69.5 ± 14.8 % compared with 62.6 ± 21.9 % for $CD4^+$ and 60.3 ± 16.5 % for $CD8^+$ T cells by PBMC-derived MDSCs induced by GM-CSF and IL-6. This showed that *in vitro* generated, PBMC-derived $CD33^+$ PMN-MDSCs had a lower suppressive effect than the freshly isolated PMN-MDSCs as shown in Figure 13 A.

Furthermore, a concentration-dependent decrease of secreted IFNγ was observed in the supernatants (Figure 17 B). At the ratio 1:0.5, the suppression of IFNγ release by cytokine-induced, PBMC-derived PMN-MDSCs was in a similar range than the one by freshly isolated PMN-MDSCs. But at lower concentrations, the inhibitory effect of cytokine-induced, PBMC-derived MDSCs was reduced to the effect of freshly isolated PMN-MDSCs. In addition, a high variance between different experiments was detected.

In order to investigate if these PBMC-derived, cytokine-induced PMN-MDSCs require cell-to-cell contact, the immunomodulatory cells were separated from stimulated PBMCs during T-cell suppression assays by a semipermeable membrane.

In the transwell system, PBMC-derived, cytokine-induced PMN-MDSCs also suppressed T-cell proliferation and secretion of IFNγ in a concentration-dependent manner (Figure 17 C+D) but to a lesser extent than with cell-to-cell contact. Again, the inhibitory effects of GM-CSF and GM-CSF with IL-6 stimulated, PBMC-derived $CD33^+$ MDSCs were similar except the inhibition of IFNγ at the ratio of 1:0.5, which was stronger by GM-CSF stimulated cells than the inhibition mediated by GM-CSF and IL-6 stimulated cells.

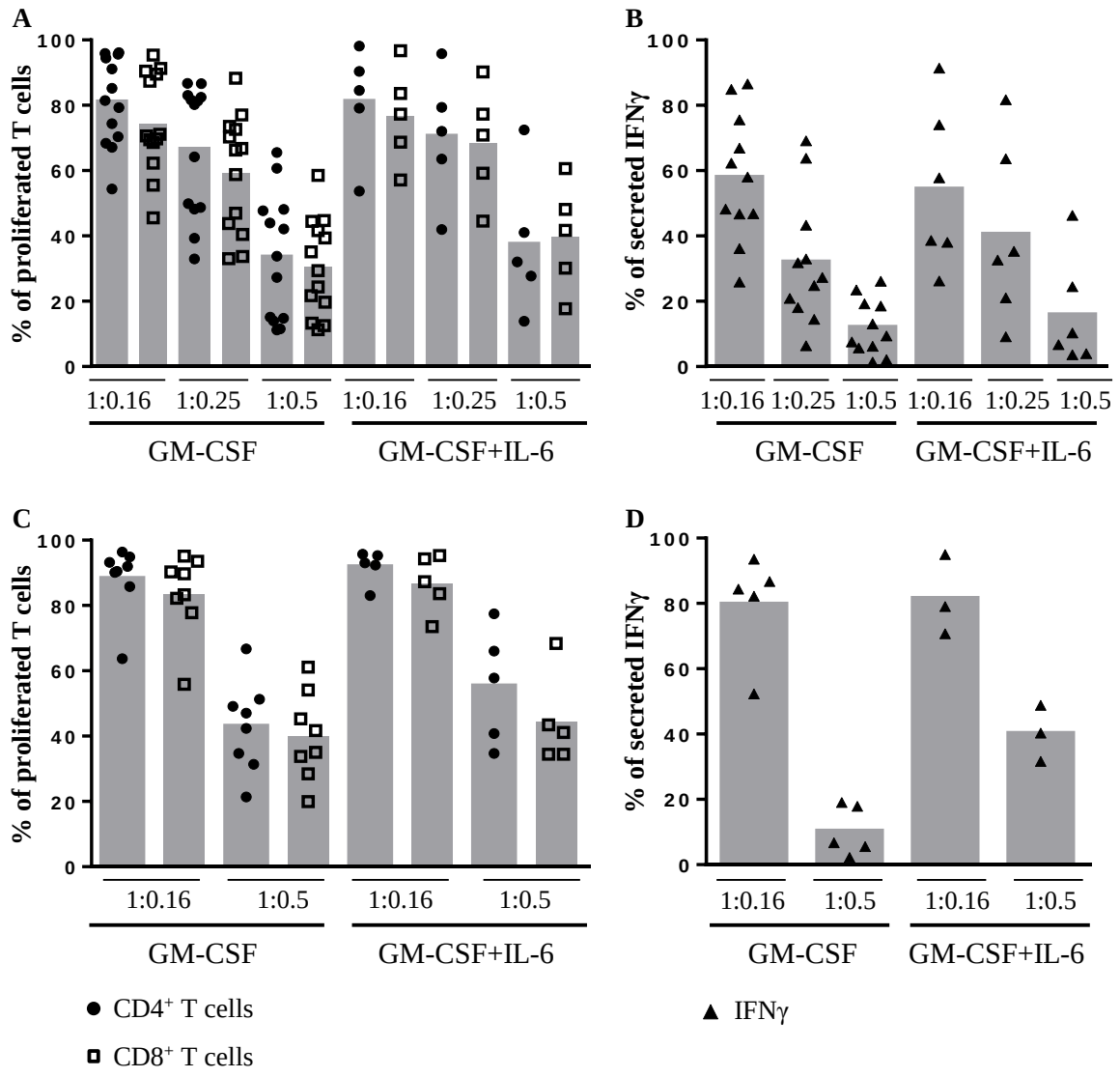

Figure 17: Suppressive effects on T-cell proliferation and secretion of Interferon-γ by PBMC-derived, cytokine-induced CD33$^+$ MDSCs. (A) PBMCs were isolated and cultured with GM-CSF alone or in combination with IL-6 for 7 days followed by CD33$^+$ magnetic selection of cytokine-induced CD33$^+$ MDSCs. On day 7, responder PBMCs from another healthy donor were isolated, labeled with CFSE and stimulated with anti-human CD3 antibody and IL-2. These PBMCs were co-cultured with PBMC-derived, cytokine-induced CD33$^+$ MDSCs in different ratios of 1:0.16, 1:0.25 or 1:0.5. After 4 days of incubation, the T-cell proliferation was assessed by flow cytometry. Each donor of responder PBMCs is presented by ● for CD4$^+$ and by □ for CD8$^+$ T cells. CD33$^+$ MDSCs of 10 different PBMC donors stimulated with GM-CSF alone and CD33$^+$ MDSCs of 4 PBMC donors stimulated with GM-CSF and IL-6 were examined. (B) After co-culture, the supernatants were collected and secreted IFNγ was analyzed by ELISA. Each ▲ indicates the level of IFNγ from a single donor of responder PBMCs after co-culture with the indicated cell type. (C-D) Same procedures as in A and B but cells were cultured in a transwell system without cell-to-cell contact in ratio 1:0.16 or 1:0.5. All measurements were normalized to the control of untreated PBMCs as 100 %. Each donor of responder PBMCs is presented by ● for CD4$^+$ and by □ for CD8$^+$ T cells or by ▲ for the level of IFNγ. CD33$^+$ MDSCs of 6 different PBMC donors stimulated with GM-CSF alone and CD33$^+$ MDSCs of 3 PBMC donors stimulated with GM-CSF and IL-6 were examined.

5.2.3 Cell yield of PBMC-derived, cytokine-induced MDSCs

In vitro generation of PMN-MDSCs from PBMCs by stimulation with GM-CSF alone led to an isolation rate of 0.40 ± 0.16 % of cultured PBMCs and 0.37 ± 0.28 % after stimulation with GM-CSF and IL-6 in combination (Table 13). Thus, the cell yields of both types of

stimulated PBMC-derived PMN-MDSCs were in the same range as the cell numbers of freshly isolated PMN-MDSCs (Table 12).

Isolated cells in percent of cultured PBMCs	Mean ± SD
GM-CSF stimulated PMN-MDSCs (n=11)	0.40 ± 0.16
GM-CSF and IL-6 stimulated PMN-MDSCs (n=5)	0.37 ± 0.28

Table 13: Percentage of isolated, ctokine-induced PMN-MDSCs derived from PBMCs

Taken together, the reduced immunosuppressive effect as well as the low cell number of $CD33^+$ MDSCs derived from PBMCs required further investigations and improvements of the *in vitro* generation of MDSCs for any clinical application.

5.2.4 Characterization of cytokine-induced MDSCs derived from bone marrow mononuclear cells

Due to the lower suppression of T-cell proliferation of PBMC-derived, cytokine-induced PMN-MDSCs compared to freshly isolated PMN-MDSCs, we investigated the *in vitro* generation of MDSCs from BMMCs. The idea was that the immature cells from the bone marrow could lead to a more T-cell suppressive and immature population of MDSCs, because it is known that MDSCs consist of a heterogeneous mixture of immature cells from the myeloid cell lineage (Gabrilovich and Nagaraj 2009).

Based on the protocols from Lechner *et al.,* 2010 for the generation of MDSCs derived from PBMCs, BMMCs were isolated and cultured with 10 ng/ml GM-CSF, or with both 10 ng/ml GM-CSF and 10 ng/ml IL-6 for 7 days (see 4.2.5.1). After incubation time, the harvested cells were stained with fluorochrom-labeled antibodies and analyzed by flow cytometry (see 4.2.7.1) to investigate if under this treatment MDSCs were generated.

The flow cytometric analysis showed in the forward/sideward scatter dot plot that the cytokine-induced, BMMC-derived cells were SSC^{high}, but also cell debris was contained in the unselected cell solution (Figure 18). Further, the cells expressed CD33, CD11b, $CD16^{inter}$, $CXCR4^{inter}$, and HLA-DR^{inter} on their surface, whereas the surface markers of CD14, CD66b and the lineage markers (CD3, CD56, CD19) were absent. The expression of CCR2 was analyzed to distinguish these cells from neutrophilic granulocytes and BMMC-derived cells expressed CCR2.

No difference was found regarding the expression of surface markers between the two types of stimulation. Thus, stimulation with GM-CSF alone as well as stimulation with GM-CSF

and IL-6 resulted in the generation of $CD33^+$ cells, which had a similar phenotypical expression of surface markers as freshly isolated PMN-MDSCs.

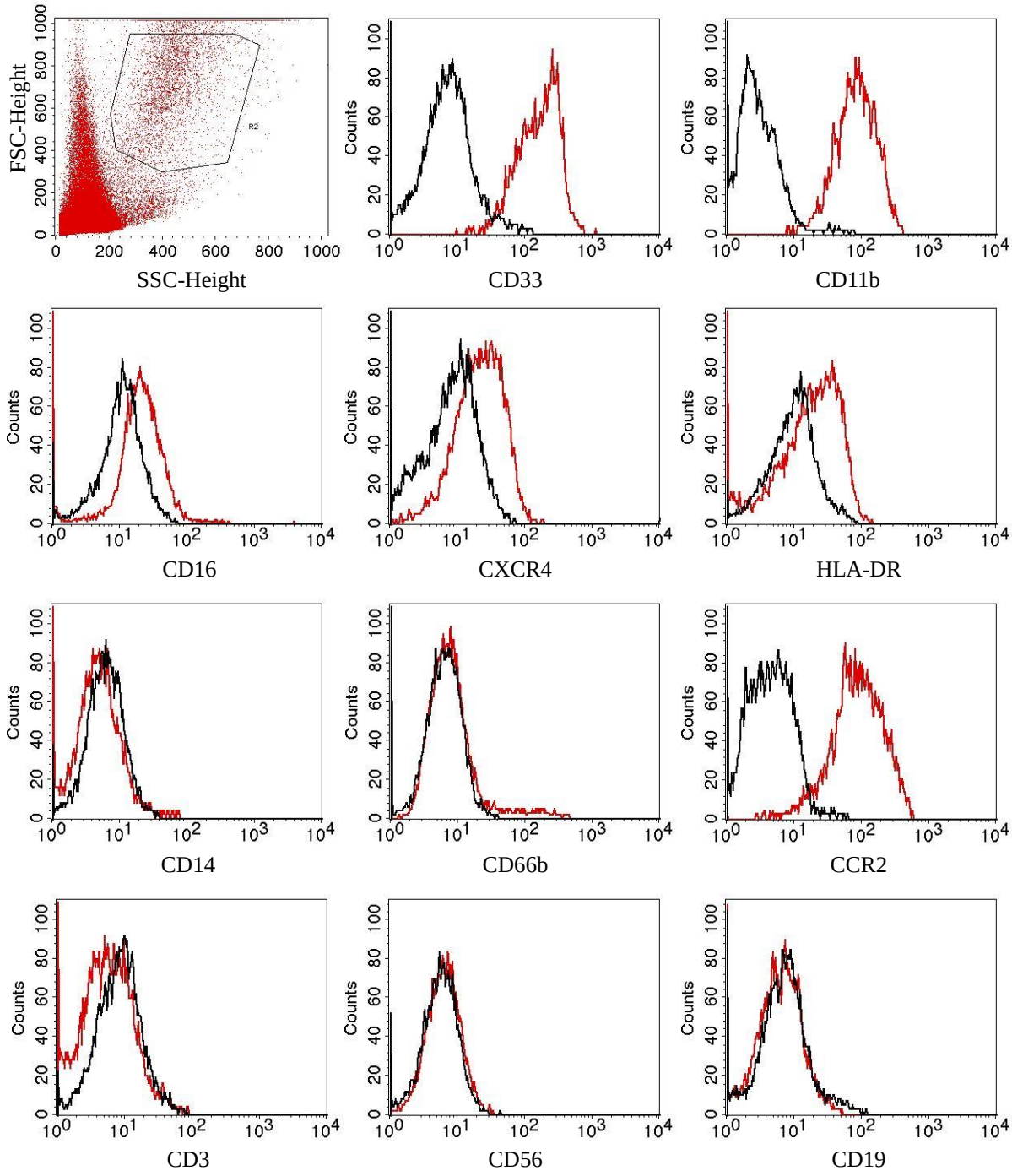

Figure 18: Characterization of BMMC-derived, cytokine-induced MDSCs. After density gradient centrifugation of bone marrow aspirates, BMMCs were cultured in complete medium with 10 ng/ml GM-CSF for 7 days. Cytokine-induced MDSCs from BMMCs were determined as SSC^{high}, $CD33^+$, $CD11b^+$, $CD16^+$, $CXCR4^{inter}$, $HLA\text{-}DR^{inter}$, and additionally $CD14^-$, $CD66b^-$, and negative lineage markers (CD3, CD19, CD56). In order to distinct these cells from neutrophils, the expression of CCR2 was analyzed and the BMMC-derived, cytokine-induced cells expressed CCR2. Representative histograms are shown with surface markers in red and isotype controls in black.

5.2.5 Functional assessment of the T-cell suppressive effect of BMMC-derived, cytokine-induced MDSCs

Equal co-culture conditions as for the other immunomodulatory cell types during T-cell suppression assay were used to investigate the T-cell suppressive capacity of the *in vitro* generated, BMMC-derived and $CD33^+$-selected cells.

Both types of cytokine-stimulated, BMMC-derived $CD33^+$ cells suppressed T-cell proliferation in a concentration-dependent manner. This T-cell suppression together with the phenotype characterization demonstrated that these BMMC-derived, cytokine-induced cells were MDSCs. The inhibitory effect of BMMC-derived $CD33^+$ cells induced by the combination of GM-CSF and IL-6 was on average slightly smaller compared to cells stimulated by GM-CSF alone, but this was not significant. At a ratio of 1:0.5, both $CD4^+$ and $CD8^+$ T-cell proliferation was reduced around 90 % by BMMC-derived $CD33^+$ MDSCs with both types of stimulation (Figure 19 A). Thereby, BMMC-derived, GM-CSF-induced MDSCs showed a significantly greater inhibition of T-cell proliferation (p=0.0006 at $CD4^+$ T cells and p=0.0008 at $CD8^+$ T cells) compared to $CD33^+$ MDSCs derived from GM-CSF-stimulated PBMCs (Figure 17 A). The suppression of BMMC-derived, cytokine-induced $CD33^+$ MDSCs was in the same range as the suppressive effect of freshly isolated PMN-MDSCs (Figure 13 A).

Furthermore, both stimulated BMMC-derived $CD33^+$ cells types strongly inhibited the release of IFNγ by around 90 % compared to the level of IFNγ of the untreated control (Figure 19 B). The secretion of IFNγ was also significantly lower after co-culture with BMMC-derived $CD33^+$ MDSCs compared to PBMC-derived MDSCs (p=0.006). At the ratio 1:0.5, BMMC-derived MDSCs suppressed the release of IFNγ on average more than freshly isolated PMN-MDSCs.

In order to analyze if cell-to-cell contact is required for the inhibitory effect of cytokine-induced BMMC-derived $CD33^+$ MDSCs, these cells were separated from the stimulated PBMCs by a semipermeable membrane in a transwell system.

In this experimental setting, $CD33^+$ MDSCs generated from BMMCs also suppressed T-cell proliferation and secretion of IFNγ in a dose-dependent manner (Figure 19 C+D). Again, both types of cytokine-induced, BMMC-derived MDSCs showed a reduction of T-cell function in the same range. This demonstrated that both types of stimulation are equally useful for the *in vitro* generation of $CD33^+$ MDSCs from BMMCs. Furthermore, the T-cell suppressive effect of these cells without direct contact was also in a similar range as with cell-to-cell contact.

This data showed that BMMC-derived, cytokine-induced cells were MDSCs, which had a great potential to suppress T cells and which could be used in cell therapies against overwhelming immune reactions.

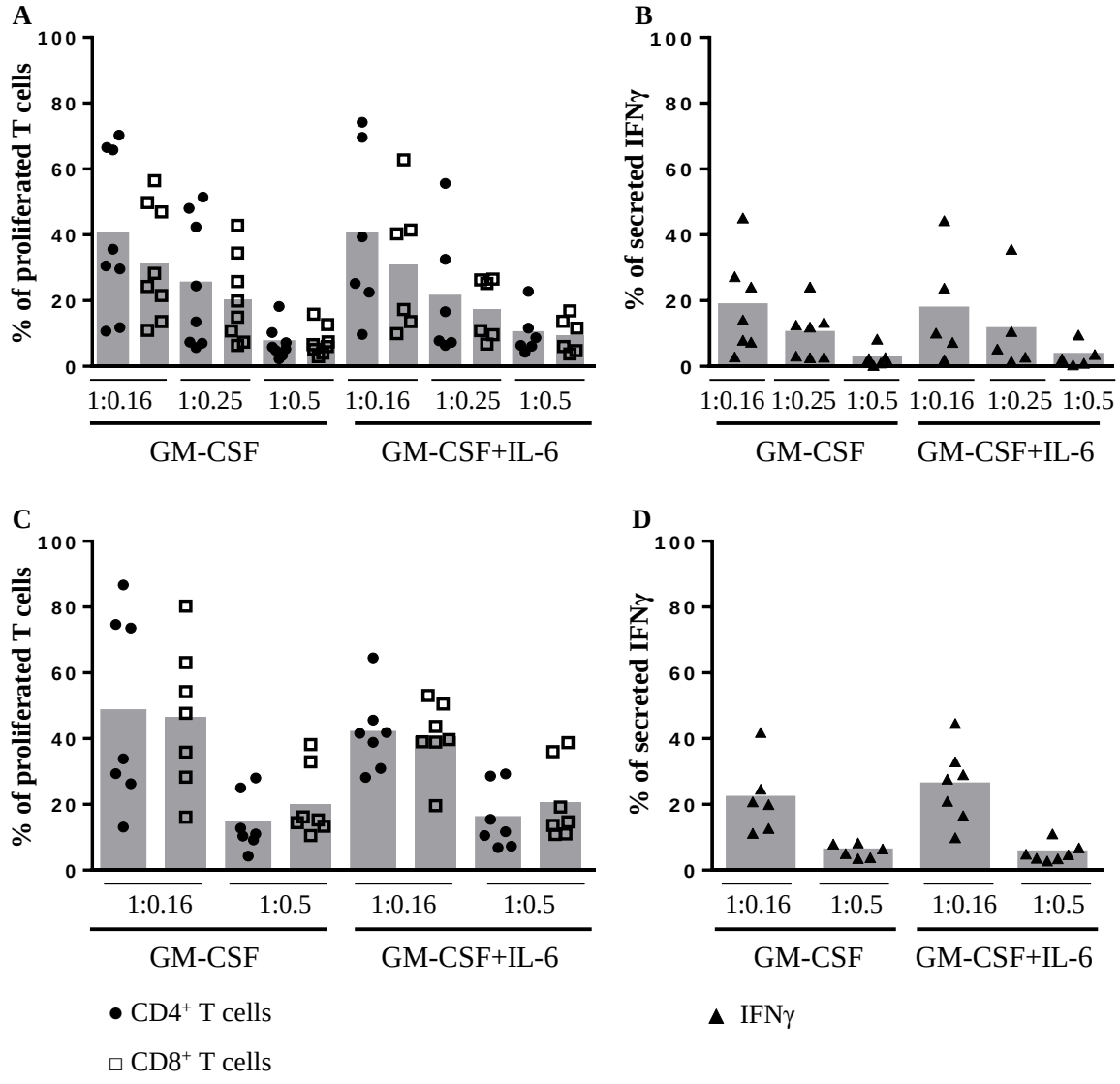

Figure 19: Suppressive effects on T-cell proliferation and secretion of Interferon-γ by BMMC-derived, cytokine-induced CD33$^+$ MDSCs. (A) BMMCs were isolated and cultured for 7 days with either only GM-CSF or both GM-CSF and IL-6 followed by CD33$^+$ selection of cytokine-induced MDSCs. On day 7, responder PBMCs from another healthy donor were isolated, labeled with CFSE and stimulated with OKT3 and IL-2. These PBMCs and CD33$^+$ MDSCs from BMMCs were co-cultured in different ratios of 1:0.16, 1:0.25 or 1:0.5. After 4 days of incubation the T cell proliferation was determined by flow cytometry. Each donor of responder PBMCs is presented by ● for CD4$^+$ and by □ for CD8$^+$ T cells. CD33$^+$ MDSCs of 6 different BMMC donors stimulated with GM-CSF alone and CD33$^+$ MDSCs of 5 BMMC donors stimulated with both GM-CSF and IL-6 were examined. (B) After co-culture, the supernatants were collected and analyzed by IFNγ ELISA. Each ▲ indicates the level of IFNγ from a single donor of responder PBMCs after co-culture with the indicated cell type. (C+D) Same procedures as in A and B, but cells were cultured in a transwell system without cell-to-cell contact in ratio 1:0.16 or 1:0.5. Each donor of responder PBMCs is presented by ● for CD4$^+$ and by □ for CD8$^+$ T cells or by ▲ for the level of IFNγ. CD33$^+$ MDSCs of 5 different BMMC donors stimulated with GM-CSF alone and CD33$^+$ MDSCs of 5 BMMC donors stimulated with both GM-CSF and IL-6 were examined. All measurements were normalized to the control of untreated PBMCs as 100 %.

5.2.6 Cell yield of BMMC-derived, cytokine-induced MDSCs

Besides the suppressive effect, the amount of immunomodulatory cells represents a key issue for potential later clinical application.

Isolated cells in percent of cultured BMMCs	Mean ± SD
GM-CSF stimulated PMN-MDSCs (n=11)	1.01 ± 0.48
GM-CSF and IL-6 stimulated PMN-MDSCs (n=11)	0.96 ± 0.33

Table 14: Percentage of isolated $CD33^+$ MDSCs generated from BMMCs

The amount of $CD33^+$ MDSCs derived from BMMCs reaches around 1.0 % by both types of stimulation (Table 14), which indicates a higher amount of MDSCs and their precursors in the bone marrow than in the peripheral blood. But still, this available cell number of BMMC-derived, cytokine-induced $CD33^+$ MDSCs was too low for any clinical use.

5.3 T-cell suppressive effects of a combination of two types of immuno-modulatory cells

The low number of available immunomodulatory cells led to the idea of combining two cell types to get an increased T-cell suppressive effect at lower cell concentrations.

Isolation of the immunomodulatory cells, and if necessary cell culture was performed as previously described. MSCs were seeded one day before the T-cell suppression assay. Allogenic responder PBMCs were isolated, stained with CFSE, and stimulated by anti-human CD3 antibody and IL-2 as usual. Besides the usual controls of unstimulated and stimulated responder PBMCs, also each type of immunomodulatory cells were seeded alone in the ratios 1:0.16 and 1:0.5 to detect their suppressive potential. In the combination approaches, two types of immunomodulatory cells were added in the ratio of 1:0.16 or 1:0.5, respectively, which led to ratios of responder PBMCs to all immunomodulatory cells of 1:0.32 and 1:1, respectively.

First, each MSCs and freshly isolated PMN-MDSCs were analyzed alone as a control and both in combination as seen in Figure 20. In the controls, MSCs and PMN-MDSCs respectively demonstrated a concentration-dependent suppression of T-cell proliferation in these experiments, but to a lesser extent than before in Figure 13 A. The combination of MSCs and PMN-MDSCs also reduced T-cell proliferation in a concentration-dependent manner. Even though the total concentration of immunomodulatory cells was higher at the

combined cell types, the suppression of the T-cell proliferation was lower compared to the control of PMN-MDSCs alone (Figure 20 A).

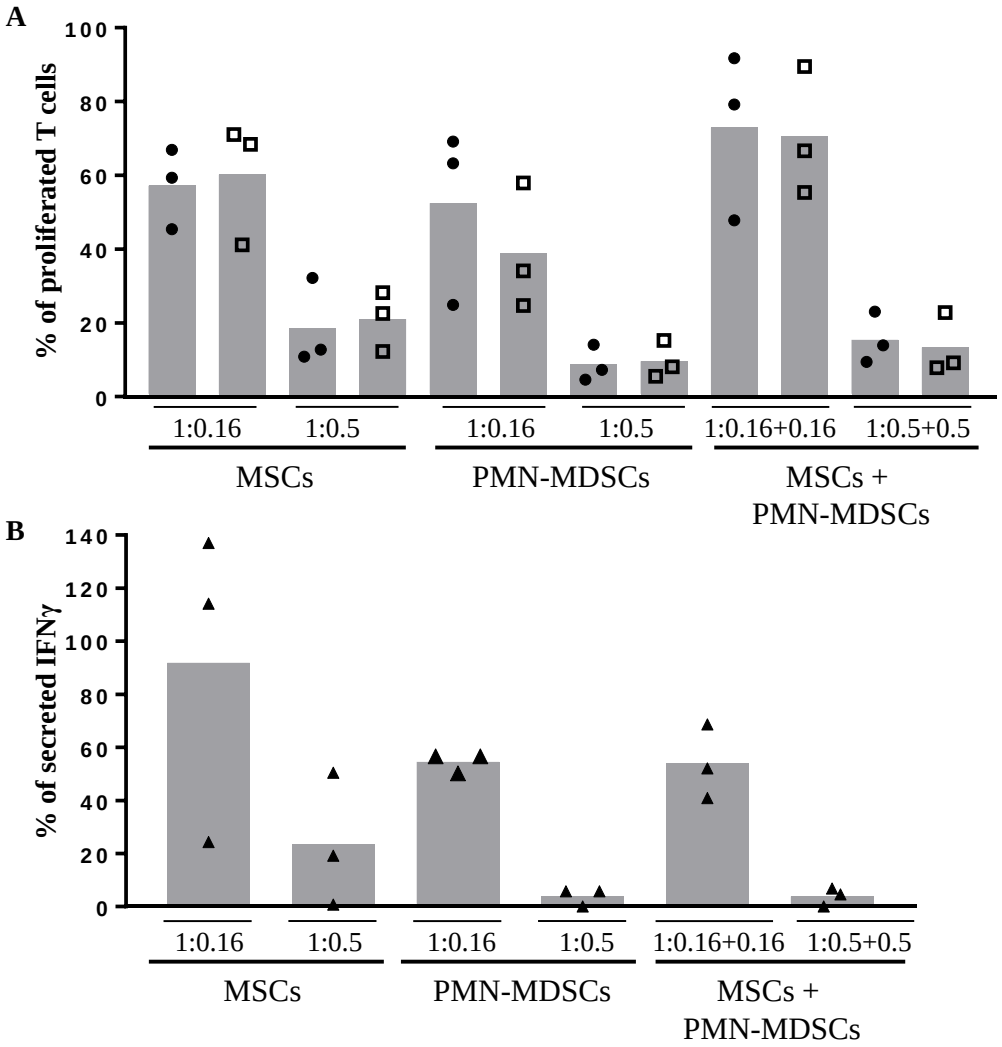

Figure 20: Suppressive effects of combined MSCs and freshly isolated PMN-MDSCs. (A+B) Responder PBMCs were labelled with CFSE, stimulated with anti-CD3 antibody and IL-2. PMN-MDSCs were isolated from another donor by magnetic separation with CD66b antibodies and appropriate MicroBeads. Stimulated PBMCs were cultured with MSCs or PMN-MDSCs or both MSCs and PMN-MDSCs in different ratios as indicated. After 4 days of incubation, supernatants were collected and (A) the proliferation of T cells was analyzed by flow cytometry. Each donor of responder PBMCs is presented by ● for $CD4^+$ T cells and by □ for $CD8^+$ T cells. (B) The level of secreted IFNγ was detected by ELISA and it is shown by ▲ for each donor. All measurements were normalized to the control of stimulated PBMCs as 100 %.

For the cytokine analysis, the secretion of IFNγ during co-culture was examined from supernatants of stimulated responder PBMCs with each immunomodulatory cell type separately or with the combined MSCs and freshly isolated PMN-MDSCs (Figure 20 B). In this experiment, MSCs showed in two of three cases no suppression of IFNγ at the ratio 1:0.16. At the ratio 1:0.5, MSCs demonstrated on average a lower suppression than in former experiments (Figure 13 B). Freshly isolated PMN-MDSCs suppressed the release of IFNγ in a

dose-dependent manner; but, compared to Figure 13 B, the effect of PMN-MDSCs alone was decreased at the ratio 1:0.16 and it was increased at 1:0.5. The combination of MSCs and PMN-MDSCs reduced the secretion of IFNγ by stimulated responder PBMCs in the same range as PMN-MDSCs alone (Figure 20 B).

Second, MSCs and BMMC-derived, cytokine-induced $CD33^+$ MDSCs were evaluated as single cell types as controls and in combination as shown in Figure 21. MSCs alone reduced T-cell proliferation in a similar range as before (Figure 13 A), whereas BMMC-derived MDSCs showed a slightly lower suppression than before (Figure 19 A). At a total ratio of 1:0.32 of responder PBMCs to combined MSCs and BMMC-derived MDSCs, the T-cell proliferation was reduced to 13.9 ± 5.7 % for $CD4^+$ and 20.5 ± 12.1 % for $CD8^+$ T cells and at the ratio 1:1, it was 5.9 ± 2.5 % for $CD4^+$ and 9.0 ± 7.0 % $CD8^+$ T cells. In this experiment, the combined cell types reduced T-cell proliferation at the ratio 1:0.32 in a similar extent as each cell type alone at the ratio 1:0.5 (Figure 21 A). This demonstrated that a combination of MSCs and BMMC-derived MDSCs had an increased suppressive effect on T-cell proliferation compared to each cell type alone.
The cytokine analysis showed that MSCs alone, BMMC-derived $CD33^+$ MDSCs alone and the combination of these two cell types effectively reduced the secretion of IFNγ (Figure **21** B). Due to the strong IFNγ suppression by each cell type alone, the combination did not show a greater reduction of IFNγ secretion.

However, the cell yield of BMMC-derived, cytokine-induced $CD33^+$ MDSCs was still low. Further improvements to increase the available cell number are required in order to use cell combinations of MSCs and BMMC-derived, cytokine-induced $CD33^+$ MDSCs for therapeutic approaches.

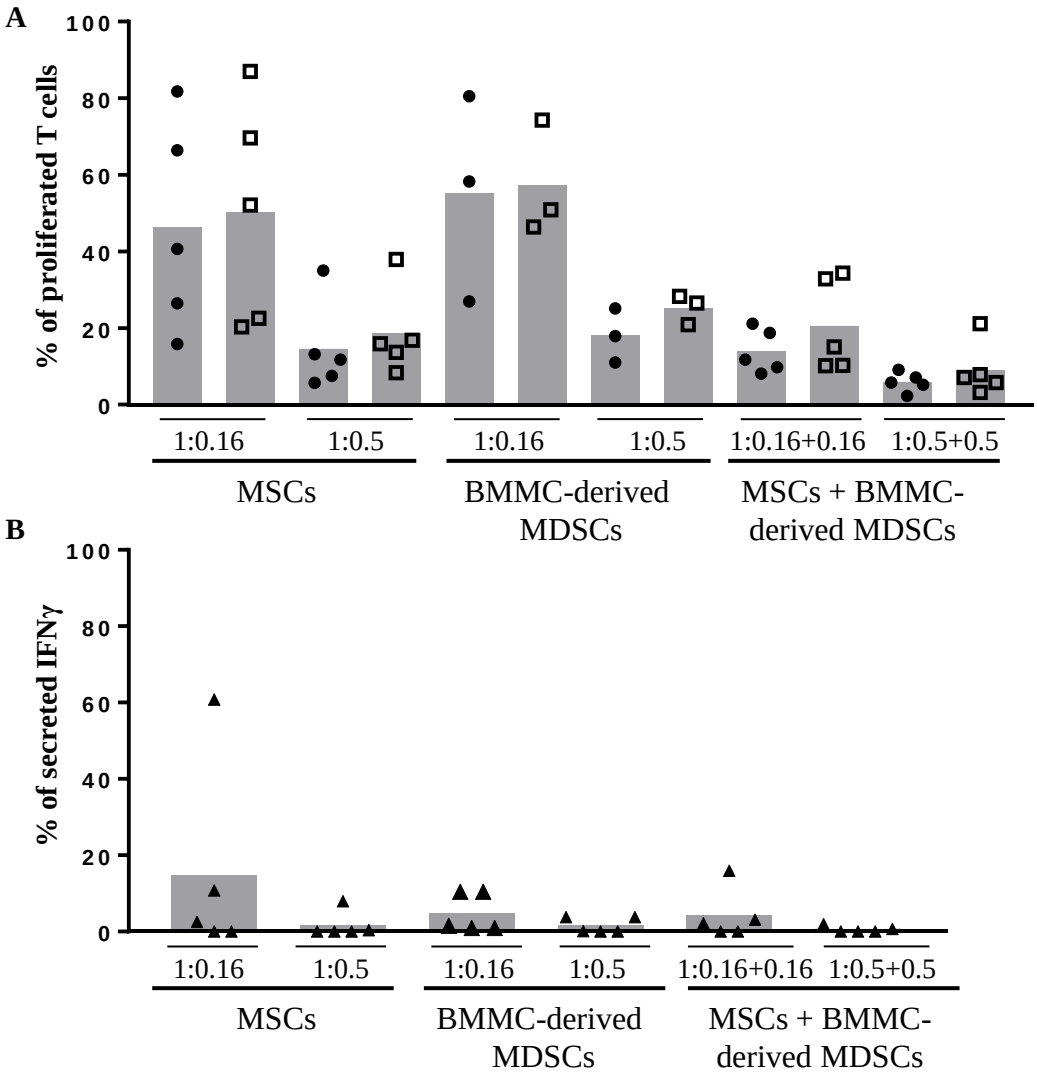

Figure 21: T-cell suppressive effects of combined MSCs and BMMC-derived, cytokine-induced MDSCs. (A+B) BMMCs were isolated by density centrifugation, cultured with 10 ng/ml GM-CSF for 7 days and CD33+ cells were isolated by magnetic separation. Responder PBMCs were isolated from another donor, labelled with CFSE, stimulated with anti-CD3 antibody and IL-2. Stimulated PBMCs were cultured with MSCs or/and BMMC-derived MDSCs in different ratios as indicated. After 4 days of incubation, supernatants were collected and (A) the proliferation of T cells was analyzed by flow cytometry. Each donor of responder PBMCs is presented by ● for CD4+ T cells and by □ for CD8+ T cells. (B) The secretion of IFNγ was measured by ELISA. Each ▲ indicates the level of IFNγ from a single donor. All measurements were normalized with T cell proliferation of stimulated PBMCs as 100 %.

5.4 Suppressive effect of cytokine induced MDSCs from CD34$^+$ HSCs

The cell yield of cytokine-induced MDSCs was increased with BMMCs as source material compared to PBMCs. Thus, the more immature cells have a greater potential for the cytokine-induced generation of MDSCs. With this knowledge and a protocol of Casacuberta-Serra *et al*. 2017, CD34$^+$ HSCs were used for the generation of MDSCs.

5.4.1 Characterization of cytokine-induced MDSCs derived from CD34$^+$ HSCs

After *in vitro* stimulation of CD34$^+$ HSCs for 20 days, the cells were harvested (see 4.2.5.2), CD33$^+$ cells were isolated by magnetic separation (see 4.2.6.4) and these cells were stained with fluorochrom-labeled antibodies and analyzed by flow cytometry (see 4.2.7.1).

This flow cytometric analysis demonstrated that the CD33$^+$ cell fraction still contained a certain amount of dead cells and debris; nevertheless, in the selected gate were over 95 % of cells CD33-positive and PI-negative (Figure 24). These cells were, however, not SSC^{high} (Figure 22) as the freshly isolated PMN-MDSCs (Figure 10). The flow cytometric analysis showed also that the selected gate contained a mixture of cells as seen in Figure 22 by the different expression levels of the surface markers CD11b, CD14, and CCR2. All cells in the gate were positive for CD11b and CCR2 markers; however, for each marker, one population demonstrated a low and another one a high expression level. Further, most cells were CD16$^+$, and CD66b$^-$, only a few cells showed a low expression of CD66b. In line with this were some cells negative for the expression of CD14 and another smaller cell population expressed CD14. Almost all cells expressed HLA-DR at low levels and CXCR4 at an intermediate level, and only a few cells show a high expression of these markers. In the selected gate, all cells were negative for the lineage markers of CD3, CD19, and CD56 (Figure 22).

No difference appeared between the cells of the two different stimulation types. Thus, IL-3 had no clear effect on the differentiation of CD34$^+$ HSCs into a certain cell type. Small distinctions were seen between different donors of the CD34$^+$ HSCs, but again, independent of the addition of IL-3.

Overall, the stimulation during 20 days of cell culture of CD34$^+$ HSCs resulted in a heterogeneous mixture of non-adherent cells containing a large population of lineage negative, CD33$^+$, CD11b$^+$, HLA-DR^{low}, which are probably MDSCs.

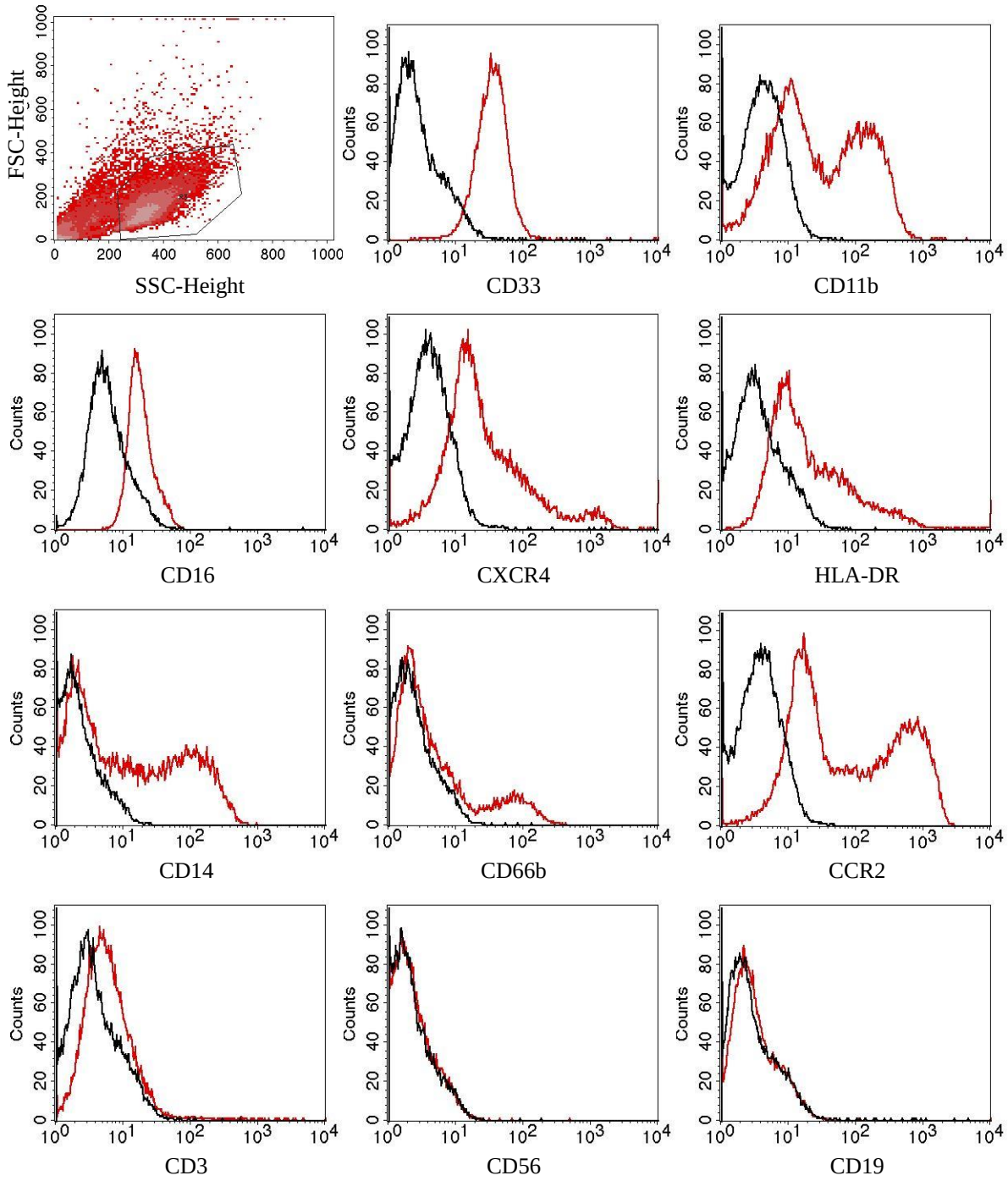

Figure 22: Characterization of CD34$^+$ HSC-derived, cytokine-induced MDSCs. After isolation from bone marrow aspirates, CD34$^+$ HSCs were cultured for 20 days in gMDSC medium without IL-3. After cell culture, CD34$^+$ HSC-derived, cytokine-induced MDSCs were isolated by magnetic separation of CD33$^+$ cells and analyzed by flow cytometry. The cells in Gate 2 were determined as CD33$^+$, CD11b$^+$, CD16$^+$, CXCR4^{inter}, HLA-DR^{inter}, additional CD14$^-$ or CD14^{low}, CD66b$^-$, and negative lineage markers (CD3, CD19, CD56). The expression of CCR2 was analyzed to distinguish these cells from neutrophils. CD34$^+$ HSC-derived, cytokine-induced MDSCs expressed CCR2 at low or high expression levels. Representative histograms are shown with surface markers in red and isotype controls in black.

5.4.2 Functional assessment of T-cell suppressive effect of MDSCs derived from CD34$^+$ HSCs

To investigate the T-cell suppressive effect of *in vitro* generated MDSCs derived from CD34$^+$ HSCs, the T-cell suppression assay and cytokine analysis were performed as previously with the other immunomodulatory cell types.

HSC-derived MDSCs from both types of stimulation (with or without IL-3) suppressed effectively the proliferation of CD4$^+$ and CD8$^+$ T cells in a dose-dependent manner (Figure **23** A). At a ratio of 1:0.5, 89.5 % of CD4$^+$ and 86.9 % of CD8$^+$ T-cell proliferation were inhibited by HSC-derived MDSCs without IL-3 stimulation during *in vitro* generation and 89.0 % of CD4$^+$ and 87.9 % of CD8$^+$ T-cell proliferation by IL-3 stimulated, HSC-derived MDSCs.

No difference was seen between the two stimulation types of HSC-derived MDSCs at the ratio 1:0.16 and 1:0.5. At the ratio 1:0.08, MDSCs generated without IL-3 from CD34$^+$ HSCs showed a slightly greater reduction of T-cell proliferation than IL-3-stimulated HSC-derived MDSCs, but this ratio was only studied with two donors of responder PBMCs, thereby just demonstrating a tendency. At the ratio 1:0.5, HSC-derived MDSCs inhibited around 90 % of CD4$^+$ and CD8$^+$ T-cell proliferation compared to the control. However, freshly isolated PMN-MDSCs suppressed CD4$^+$ and CD8$^+$ T-cell proliferation significantly more than HSC-derived MDSCs (with $p \leq 0.01$ for each analysis). At the ratio 1:0.16, the suppression of T-cell proliferation by HSC-derived MDSCs was slightly greater as the one of BMMC-derived MDSCs, and at the ratio 1:0.5, the suppression of these differently generated MDSCs was in the same range.

The supernatants from the T-cell suppression assay were used for the detection of secreted IFNγ after co-culture of stimulated responder PBMCs with *in vitro* generated MDSCs derived from CD34$^+$ HSCs. These cells suppressed effectively the secretion of IFNγ, as seen in Figure 23 B. At the ratio 1:0.5, the level of IFNγ was 2.0 ± 3.8 % with HSC-derived MDSCs without IL-3 stimulation and 0.6 ± 0.5 % with IL-3-stimulated HSC-derived MDSCs compared to the control. The IFNγ reduction by HSC-derived MDSCs with IL-3 stimulation was slightly greater than by those without IL-3, but no clear difference was detected. Both types of HSC-derived MDSCs suppressed significantly more the secretion of IFNγ than freshly isolated PMN-MDSCs (p=0.005 with IL-3 and p=0.02 without IL-3) (Figure 13 B). After addition of HSC-derived MDSCs (Figure 23 B) to the stimulated responder PBMCs, the level of IFNγ

was in the same range as after addition of MSCs (Figure 13 B) or BMMC-derived MDSCs (Figure 19 B).

To sum up, at the ratio 1:0.5, HSC-derived MDSCs showed a strong suppressive effect on T-cell proliferation comparable to the effect of freshly isolated PMN-MDSCs, and the inhibition of IFNγ secretion by HSC-derived MDSCs was even stronger than by freshly isolated PMN-MDSCs.

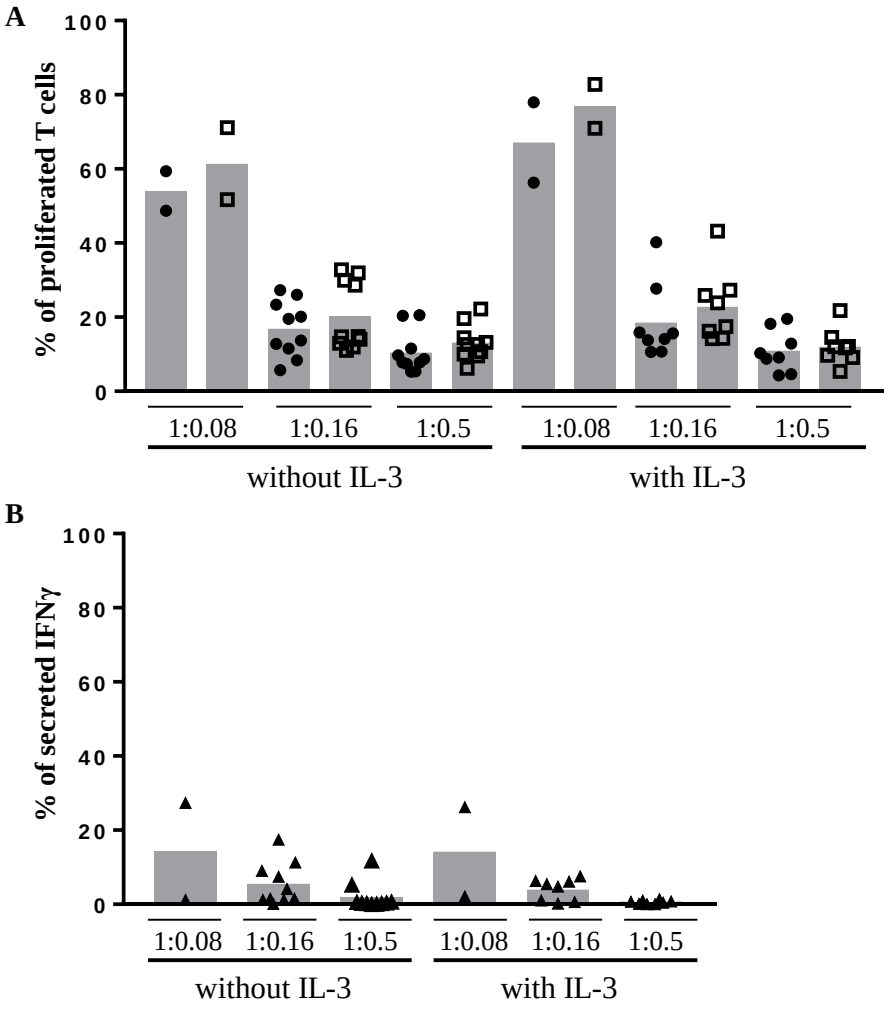

Figure 23: Suppressive effects on T-cell proliferation and secretion of Interferon-γ by $CD34^+$ HSC-derived, cytokine induced MDSCs. CD34+ HSCs were cultured for 20 days with in gMDSC medium containing 20 ng/ml IL-3 where indicated. After cell culture, CD33+ cells were isolated by magnetic separation. (A) Responder PBMCs were isolated, labelled with CFSE, and stimulated with anti-CD3 antibody and IL-2. Stimulated PBMCs were cultured with CD34+ HSC-derived, cytokine-induced MDSCs in different ratios of 1:0.08, 1:0.16 or 1:0.5 as indicated. After 4 days of incubation, the proliferation of T cells was analyzed by flow cytometry. Each donor of responder PBMCs is presented by ● for CD4+ T cells and by □ for CD8+ T cells. (B) Supernatants from the co-cultured cells were collected after 4 days and assessed for the secretion of IFNγ by ELISA. Each ▲ indicates the level of IFNγ from one donor of responder PBMCs. All measurements were normalized by setting T-cell proliferation or secretion of IFNγ of stimulated PBMCs as 100 %.

5.4.3 Cell yield and magnetic separation of cytokine-induced MDSCs generated from CD34$^+$ HSCs

HSC-derived MDSCs demonstrated a strong suppressive effect on T-cell proliferation and on IFNγ secretion. For a clinical application, the cell yield is important and the available cell number of freshly isolated PMN-MDSCs as well as BMMC-derived MDSCs was yet not enough. The *in vitro* cytokine-stimulation of CD34$^+$ HSCs led to a greater cell proliferation, seen by the cell count on day 0 and on day 20 (Table 16) and consequently on the n-fold increase during cell culture (Table 15). The output of CD33$^+$ cells was low compared to the high cell number, which was used for the magnetic separation (Table 16).

Experiment number	n-fold increase during cell culture	Cell yield of CD33$^+$ separation (in %)	n-fold increase during cell culture	Cell yield of CD33$^+$ separation (in %)
	Without IL-3 stimulation		With IL-3 stimulation	
1	26.1	5.2	13.8	8.0
2	51.2	4.5	-	-
3	142.5	1.4	111.3	2.1
4	136.0	1.9	125.0	2.9
5	80.0	11.9	189.0	4.8
6	68.6	4.6	61.4	4.7
7	2.9	20.0	3.4	23.3
Mean	72.5	7.1	84.0	7.6
SD	52.4	6.7	71.3	8.0

Table 15: *In vitro* generation of cytokine-induced MDSCs from CD34$^+$ HSCs and cell yield of CD33$^+$ cells by magnetic separation

The average increase of cells during stimulation and culture time of 20 days was 72.5 ± 52.0 without IL-3 stimulation, and 84.0 ± 71.3 with IL-3 (Table 15). The yield of CD33$^+$ cells was 7.1 ± 6.7 % without, respectively 7.6 ± 8.0 % with IL-3 stimulation during cell culture. This showed on average a higher cell proliferation with addition of IL-3 during cell culture than without IL-3, but only a slightly higher yield of CD33$^+$ cells.

But, by comparing the single experiments in Table 15 and the counted cell numbers in Table 16, a very high variance was seen between the different runs with each time a different donor of CD34$^+$ HSCs, and furthermore, the variances between different donors of CD34$^+$ HSCs were much higher than the differences between stimulation without or with IL-3. In addition, the cell yield of CD33$^+$ cells in percent was higher when lower cell numbers were used for the magnetic separation, as seen in Table 16, experiment number 7.

Experiment number	Cell count d0	Cell count d20	Number of $CD33^+$ cells	Cell count d0	Cell count d20	Number of $CD33^+$ cells
	Without IL-3 stimulation			With IL-3 stimulation		
1	$8.0 \cdot 10^5$	$2.1 \cdot 10^7$	$1.1 \cdot 10^6$	$8.0 \cdot 10^5$	$1.1 \cdot 10^7$	$8.8 \cdot 10^5$
2	$2.5 \cdot 10^5$	$1.3 \cdot 10^7$	$5.7 \cdot 10^5$	-	-	-
3	$4.0 \cdot 10^5$	$5.7 \cdot 10^7$	$8.0 \cdot 10^5$	$4.0 \cdot 10^5$	$4.5 \cdot 10^7$	$9.4 \cdot 10^5$
4	$2.0 \cdot 10^5$	$2.7 \cdot 10^7$	$5.2 \cdot 10^5$	$2.0 \cdot 10^5$	$2.5 \cdot 10^7$	$7.2 \cdot 10^5$
5	$2.0 \cdot 10^5$	$1.6 \cdot 10^7$	$1.9 \cdot 10^6$	$2.0 \cdot 10^5$	$3.8 \cdot 10^7$	$1.8 \cdot 10^6$
6	$7.0 \cdot 10^5$	$4.8 \cdot 10^7$	$2.2 \cdot 10^6$	$7.0 \cdot 10^5$	$4.3 \cdot 10^7$	$2.0 \cdot 10^6$
7	$3.5 \cdot 10^5$	$1.0 \cdot 10^6$	$2.0 \cdot 10^5$	$3.5 \cdot 10^5$	$1.2 \cdot 10^6$	$2.8 \cdot 10^5$

Table 16: Cell numbers from *in vitro* generation and magnetic separation of $CD34^+$ HSC-derived MDSCs

As demonstrated by the big difference between the output of cultured cells and the yield of $CD33^+$ cells, the magnetic separation caused a big loss of cells. An additional flow cytometric analysis of both cell fractions was performed after magnetic separation of stimulated $CD34^+$ HSCs. In the positive cell fraction that contained the selected $CD33^+$ cells expressed over 95 % of cells in gate 2 CD33 and all cells were negative for PI; however, gate 1 showed around 40 % of PI-positive, dead cells (Figure 24 A-C). Furthermore, the negative fraction also contained a high cell number of $CD33^+$ cells with over 90 % in gate 2 (Figure 24 D-F).

Thus, the cell numbers increased during *in vitro* generation of MDSCs from $CD34^+$ HSCs, which was contrary to the decreased cell numbers after cell culture of PBMCs as well as BMMCs for 7 days. Overall, the large expansion of $CD33^+$ MDSCs during cell culture of $CD34^+$ HSCs seems to have potential for a clinical application.

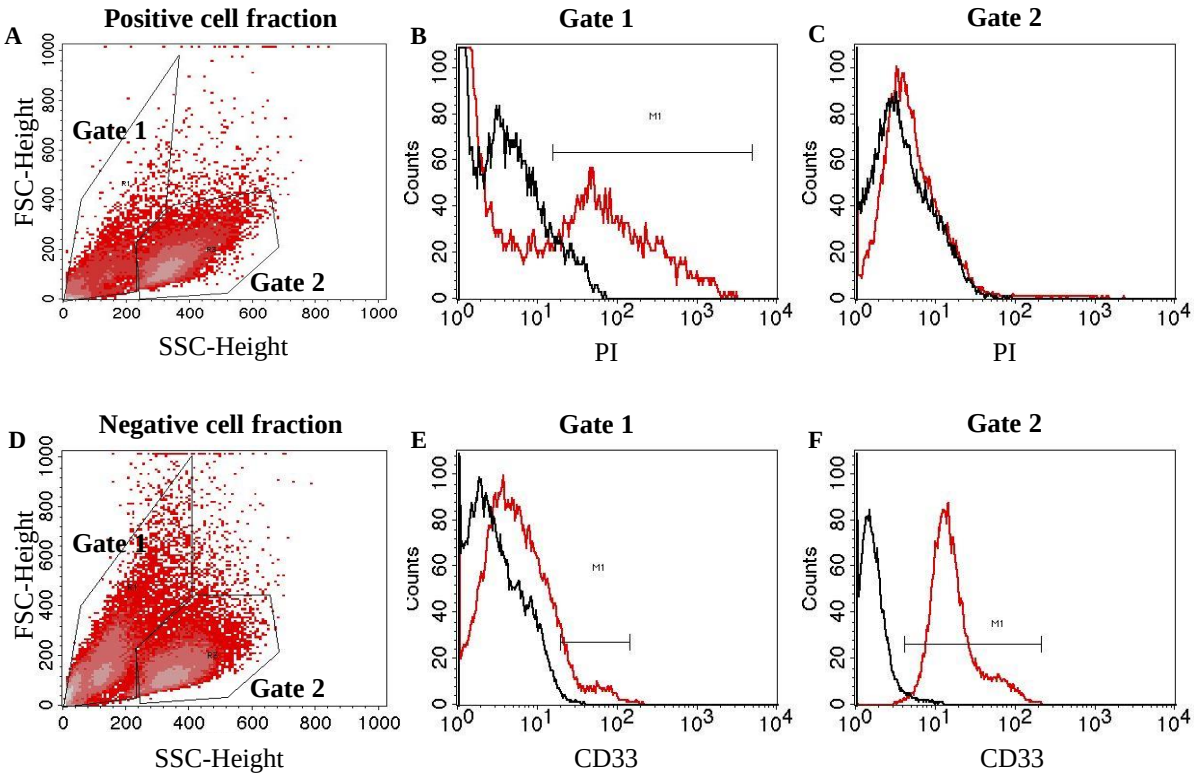

Figure 24: Flow cytometric analysis of CD33 cell fractions after magnetic separation of CD34$^+$ HSC-derived, cytokine-induced MDSCs. CD34$^+$ HSCs were isolated and cultured with gMDSC medium for 20 days as previously described. After magnetic separation, the expression of surface marker CD33 and binding of PI was analyzed by flow cytometry. Representative dot plots and histograms are shown with surface marker CD33 or PI in red and isotype control or unstained cells in black. (A) Dot plot of CD33$^+$ cell fraction showed two distinct populations. (B) Histogram of PI staining from CD33$^+$ selected cells of Gate 1 indicated that these cells were mainly positive for PI, therefore dead. (C) Histogram from CD33$^+$ cells of Gate 2 showed no PI-positive cells. (D) Dot plot of CD33$^-$ cell fraction showed also two distinct populations. (E+F) Histograms of CD33 staining from this cell fraction demonstrated in Gate 1 very few CD33$^+$ cells, whereas in Gate 2 expressed over 95 % of cells CD33.

6 Discussion

The central aim of this study was to systematically compare the T-cell suppressive effect of different immunomodulatory cells and their available cell number in regard to a clinical application for patients with GvHD. So far, several cell types suppressing T cells have been described, however it was still not clear which cell type provides the greatest potential for cell therapy approaches.

6.1 MSCs, freshly isolated MDSCs, and Tregs

The detected expression profiles of surface markers from each cell type fits to the described minimal phenotypical criteria of MSCs (Figure 9), PMN-MDSCs (Figure 10), and Tregs (Figure 11), respectively (Dominici *et al.* 2006; Santegoets *et al.* 2015; Bronte *et al.* 2016). The suppression of T-cell proliferation is also required for the characterization of MDSCs, as shown in Figure 13 for the freshly isolated PMN-MDSCs (Bronte *et al.* 2016).

Direct comparison of human MSCs, Tregs and freshly isolated PMN-MDSCs showed that all three cell types inhibited T-cell proliferation in a concentration-dependent manner (Figure **13**). PMN-MDSCs had the strongest suppressive effect on T-cell proliferation, nevertheless MSCs and Tregs also demonstrated a clear suppression of T-cell proliferation. Moreover, MSCs reduced the secretion of IFNγ stronger than PMN-MDSCs and Tregs; however these cell types also suppressed the release of IFNγ in a similar range (Figure 13).

The strong T-cell suppressive effect and the feasibility of *in vitro* expansion of MSCs are the main reasons for their application in multiple clinical trials. However, in the co-culture experiments for the analysis of combined immunomodulatory cell types, an increase of IFNγ secretion was detected in two cases of the control of MSCs alone (Figure 20), which is in contrast to previous findings showing a strong suppression of IFNγ secretion by MSCs (Figure 13). These contradictory results regarding the release of IFNγ were also found by different groups depending on the lymphocyte population and their stimulation (Castro-Manrezza 2015). Due to production stop of the T-cell stimulation antibody from clone OKT3, the anti-human CD3 antibody had to be switched to clone HIT3a. In preliminary experiments (not shown), there were no differences detectable for the PBMCs response, while stimulated by the two different anti-human CD3 antibodies. But the difference between the antibodies' clones, potentially inducing slightly different stimulation could be a reason for these contradictory measurements and therefore explain the increased secretion of IFNγ in presence of MSCs in Figure 20. There are also a few inconsistent results of MSCs regarding T-cell

proliferation, which were detected in experiments with mice and rats (Zinöcker *et al.* 2012; Sudres *et al.* 2006). Furthermore, MSCs seem to require an exposure to IFNγ as an activation stimulus, which increased MSC suppression of GvHD in murine experiments (Polchert *et al.* 2008). Thus, another hypothesis could be that in these two cases, the activation of MSCs was taken more time and that a potential suppression could have followed later.

In order to analyze the requirement of cell-to-cell contact, transwell experiments were performed with immunomodulatory cells separated by a semipermeable membrane from stimulated responder PBMCs. Each immunomodulatory cell type demonstrated also in the transwell system suppression of T-cell proliferation and secretion of IFNγ, however to a lesser extent than with direct cell contact (Figure 13). This shows that each immunomodulatory cell type uses several mechanisms for their T-cell suppression, which are partly based on cell contact and partly on soluble factors. Diverse results regarding the dependency of cell contact are published for MSCs and PMN-MDSCs (Castro-Manrreza and Montesinos 2015; Rieber *et al.* 2013; Gabrilovich and Nagaraj 2009), which also indicates that both cell types can suppress other immune cells by various mechanisms, just depending on the surrounding and the stimulation.

However, the suppression of T-cell proliferation and IFNγ secretion mediated by Tregs in the transwell system (Figure 13) was unexpectedly strong since two studies from 1998 reported that murine Tregs require cell-to-cell contact for the suppression of effector T cells (Thornton and Shevach 1998; Takahashi *et al.* 1998). One explanation could be that during magnetic separation of $CD4^+CD25^+$ Tregs, it is not possible to differentiate between cells with high or intermediate expression of CD25; therefore isolated cells consist of a heterogeneous population of $CD4^+$ T cells, including type 1 Tregs (Tr1) and Th3. These cells display immunosuppressive effects towards T cells by soluble factors, such as IL-10 and TGF-ß (Jonuleit and Schmitt 2003). Or Tr1 cells are induced from $CD4^+$ T cells in the lower compartment of the transwell containing allogenic stimulated PBMCs that also might contain a few Tregs (Dieckmann *et al.* 2002). In addition, it is clear that secretion of cytokines is a mode of action mediated by Tregs (Sojka *et al.* 2008; Sakaguchi *et al.* 2013; Schmidt *et al.* 2012) and the Vignalis group also reported that Tregs were able to suppress effector T cells without cell-to-cell contact in a transwell system when Tregs had cell-to-cell contact with effector T cells in the other compartment of the transwell system (Collison *et al.* 2009). The detected T-cell suppression mediated by Tregs in our experiments could be due to cell-to-cell contact, because we could only achieve a purity of $CD4^+CD25^+$ Tregs of 90-95 % during magnetic separation. This T-cell suppression mediated by Tregs in the transwell system

should be further analyzed; however, several reports describing the plasticity of Tregs, able to convert into effector T cells, raised questions regarding the general use of Tregs for the uncontrolled immune reactions in GvHD patients.

Several studies with murine and human Tregs as well as *in vivo* experiments demonstrated that Tregs downregulate the expression of FoxP3 over time and that Tregs even express pro-inflammatory cytokines, such as IL-17, especially in an inflammatory surrounding (Zhou *et al.* 2009; Koenen *et al.* 2008). On the other side, Rubtsov *et al.* reported a strong stability of murine Tregs *in vivo*, even in an inflammatory environment (Rubtsov *et al.* 2010). One major aspect regarding the stability of Tregs is the methylation status of conserved noncoding sequence 2 in the *FOXP3* locus, which is also known as Treg cell-specific demethylated region. Demethylation of this region leads to stable *FOXP3* expression and changes in this epigenetic pattern of cells result in loss of *FOXP3* expression and conversion into $FoxP3^-$ non-Tregs (Zheng *et al.* 2010; Sakaguchi *et al.* 2013). For clinical application, instability of Tregs is a high risk factor; however there are reports that low doses of IL-2 stimulation could prevent such conversion. Furthermore, the plasticity of single cells is not a problematic issue, only plasticity of large cell populations is hazardous for patients (Sakaguchi *et al.* 2013).

The first clinical trials showed successful expansion of Tregs *ex vivo* and after administration of these cells in HSCT patients, lower incidence of GvHD was detected, indicating that Tregs could prevent the development of GvHD (Brunstein *et al.* 2011; Di Ianni *et al.* 2011). The studies for the treatment of GvHD patients have only demonstrated positive effects in patients with chronic, but not with the acute form of the complication (Trzonkowski *et al.* 2009; Gliwiński *et al.* 2017). The encouraging results lead to more laboratory and clinical investigations, which will hopefully demonstrate positive results and report a possible administration into the patients. Before that, further studies are required, keeping in mind the various unknown aspects of Tregs such as: subtype characterization, stability, expansion, timing of administration and dosing (Gliwiński *et al.* 2017; Safinia *et al.* 2013).

The direct comparison of MSCs and freshly isolated PMN-MDSCs from the same donor demonstrated great variances between different donors and their immune reactions (e.g. for one donor immunomodulatory cells suppressed $CD4^+$ more than $CD8^+$ T cells while we observed the opposite effect for another donor) (Figure 15). Furthermore, the secretion inhibition of IFNγ in all donors, even though one donor showed no suppression of T-cell proliferation, indicates clearly that the immunomodulatory cells have an effect not only on T cells, but also on other IFNγ-producing immune cells, such as NK cells (Figure 15).

The T-cell suppression mediated by freshly isolated PMN-MDSCs was in the autologous and allogenic experimental setting in a similar range, and just showed again the variances between the immune reactions of different donors (Figure 14).

Overall, the strong suppression of T-cell proliferation mediated by freshly isolated PMN-MDSCs and the so far untapped potential of this cell type, led us to continue our studies in respect with a potential clinical application of MDSCs.

6.2 *In vitro* generated MDSCs derived from mononuclear cells of peripheral blood or bone marrow

The characterization of MDSCs is difficult, similar as the characterization of Tregs, because both cell types lack a unique cell marker. The current criteria for the characterization of MDSCs differentiate them in three subtypes: early MDSCs, M-MDSCs, and PMN-MDSCs. The latter are described as $CD11b^+$ or equivalent $CD33^+$, $CD14^-$, $CD66b^+$ or $CD15^+$. But, PMN-MDSCs share the same markers with neutrophils and M-MDSCs with monocytes (Bronte *et al.* 2016). May-Grünwald-Giemsa staining of the morphology and gene expression profiling are described to distinguish PMN-MDSCs from neutrophils in mice (Greifenberg *et al.* 2009; Youn *et al.* 2012; Fridlender *et al.* 2012). However, these methods cannot be used for isolation of cells. At the moment, the only method for separation of human PMN-MDSCs from neutrophils is a gradient centrifugation with polysaccharide solution of 1.077 g/l density, as realized during this work. PMN-MDSCs are in the low density fraction containing all PBMCs, whereas neutrophils are in the lower fraction together with the red blood cells. But probably, some activated neutrophils with reduced granularity can pass through the polysaccharide and contaminate the PBMC fraction (Bronte *et al.* 2016; Bryk *et al.* 2010). Therefore, the current criteria of MDSCs require not only phenotypical staining of surface markers, also functional assessment of the T-cell suppression (Bronte *et al.* 2016). The used isolation strategy as well as the results of the characterization and T-cell suppression assays of freshly isolated PMN-MDSCs fit to these criteria (Figure 10, Figure 13). The *in vitro* generated MDSCs derived from PBMCs by cytokine induction were $CD33^+$, $CD11b^+$, $HLA\text{-}DR^{inter}$, $CD14^-$, and lineage negative, so that the expression of surface markers also fit to these minimal criteria, except for the absence of CD66b expression (Figure 16). However, an expression of CD16 was detected, and CD16 is also a specific marker of polymorphonuclear neutrophils (Fernandes *et al.* 2006; Davoine *et al.* 2002), just as CD66b (Lakschevitz *et al.* 2016). In this study, the absence of CD66b expression of these cytokine-induced PBMC-

derived MDSCs is in contrast to the high expression of CD66b reported by Lechner *et al.*, 2010. The only difference in the generation methods is that Lechner and colleagues refreshed the media every 2-3 days, whereas we refreshed the media every 3-4 days. In addition to the similar characterization of the cytokine-induced PBMC-derived cells, is that they suppressed T-cell proliferation and thereby, qualified for a major criterion of MDSCs.

However, the cytokine-induced $CD33^+$ MDSCs generated from PBMCs showed a lower suppression of T-cell proliferation and of IFNγ-secretion (Figure 17) compared to the results of Lechner *et al*., 2010. Further, no statistical relevant difference was noticed in this study between the induction with GM-CSF alone and GM-CSF combined with IL-6 (Figure 17). This finding is also in contrast to the results of Lechner *et al.* with greater T-cell suppression by MDSCs stimulated with GM-CSF and IL-6 than by those stimulated with GM-CSF alone. Furthermore, relatively large variances were detected between single cell donors within both groups testing cytokine-induced PBMC-derived MDSCs. The main reason for these discrepancies could be due to the fact that in this study, allogenic PBMCs were stimulated to induce polyclonal T-cell proliferation, whereas Lechner *et al*. used isolated autologous T cells (Lechner *et al.* 2010). It could indicate that the various cell types in the PBMC fraction reduce the T-cell suppressive effect or/and that the cytokine-induced PBMC-derived MDSCs have a stronger effect in the autologous rather than in the allogenic setting. In addition, a T-cell suppressive effect mediated by PBMC-derived cytokine-induced $CD33^+$ MDSCs was detected with direct cell-to-cell contact as well as in the transwell system without cell contact (Figure 17), once more contrasting with the contact dependency described by Lechner *et al.*, 2010. One explanation could be that the cytokine-induced $CD33^+$ MDSCs secrete soluble factors that interfere with T-cell activation by APCs, followed by reduced T-cell proliferation. Such an interaction would not be recognized in an experimental setting with isolated T cells without APCs as used by Lechner *et al.*, 2010. Additionally in this study, PBMCs were isolated from buffy coats for the generation of MDSCs, which could explain the reduced inhibition of T-cell proliferation with cell contact and the increased suppression without cell contact compared to the results of Lechner *et al.*, 2010. It cannot be excluded that the precursors of MDSCs as well as all included leukocytes might have been already stimulated or damaged by the buffy coat preparation on the previous day or by the storage, so that fewer MDSCs were generated by cytokine induction. A reduced viability was reported for granulocytes from buffy coats (van de Geer *et al.* 2017). However, no activation of leukocytes was shown so far, only increased activation of platelets was noticed after storage of buffy coats for more than 12 hours (Kluter *et al.* 1997). Moreover, the moderate inhibition of T-cell

proliferation could be due to the already matured state of the precursors of MDSCs in the PBMC fraction. Taken together, the immunosuppressive capacity of PBMC-derived cytokine-induced $CD33^+$ MDSCs was moderate in this allogenic setting and the available cell numbers (Table 13) were too low for clinical applicability.
Further cytokines or chemokines need to be tested for their potential to generate MDSCs out of PBMCs *in vitro*, for example, cytokines from the IL-1 family (Ballbach *et al.* 2016). Combinations of several factors during PBMC culture could also increase the induction of MDSCs, such as GM-CSF, IL-6, and Finasteride (Zhang, Wu, *et al.* 2016).

The generation of MDSCs derived from human BMMCs was successful with the used protocol, based on the one from Lechner *et al.* 2010, as seen by the cell characterization (Figure 18) and the T-cell suppressive effect (Figure 19). Particularly, the generation of MDSCs derived from BMMCs was effective with both types of cytokine stimulation, on the one side GM-CSF alone and on the other side GM-CSF combined with IL-6. It was previously reported that a long-term treatment of murine BM cells with low doses of GM-CSF results in the generation of MDSCs (Lutz *et al.* 2000; Ribechini *et al.* 2010). This group also reported that this treatment generated a mixture of immature cells that induce T-cell unresponsiveness *in vitro* and even prolonged allograft survival *in vivo* (Lutz *et al.* 2000). This group used a lower concentration of GM-CSF (20 U/ml) and a longer incubation time of 8-10 days for the murine BM cells compared to the generation of cytokine-induced BMMC-derived MDSCs used in the present study (10 ng/ml GM-CSF). Marigo and colleagues presented in 2010 the generation of MDSCs derived from human BM cells, by GM-CSF alone or combined with either IL-6 or G-CSF in higher concentrations (each 40 ng/ml), and with shorter incubation time of 4 days. They demonstrated that MDSCs generated with GM-CSF and IL-6 out of human BM cells have the greatest T-cell suppressive effect *in vitro* (Marigo *et al.* 2010). Consequently, the protocol used in this study for the generation of MDSCs from BMMCs is not only based on the protocol from Lechner *et al.* 2010 established for PBMCs, but includes as well key parts of the protocols from Lutz *et al.* 2000 and Marigo *et al.* 2010 established for BM cells.

The generated $CD33^+$ MDSCs from human BMMCs suppressed T-cell proliferation and secretion of IFNγ (Figure 19) more efficiently than $CD33^+$ MDSCs generated from PBMCs (Figure 17), both with cell-to-cell contact as well as without direct contact. This greater T-cell suppression by BMMC-derived MDSCs compared to PBMC-derived ones strengthens the

hypothesis that more immature cells are required for the effective generation of MDSCs. Furthermore, the inhibition of T-cell proliferation by BMMC-derived $CD33^+$ MDSCs was more prominent in this setting than previously shown for human BM-derived MDSCs by Marigo *et al*. 2010, therefore demonstrating that this method results in the generation of more effective MDSCs. However, the cellular yield of $CD33^+$ MDSCs obtained after incubation and isolation was lower, reaching only around 1% of the initial BMMCs (Table 14) compared to 70-80 % recovery without any selection, as performed by Marigo *et al*. 2010. Beside different concentrations, incubation times and initial cell populations, the magnetic separation of $CD33^+$ MDSCs from stimulated BMMCs provides a potential explanation for these discrepant cell yields. But with respect to any clinical application, an isolation of the functional cell population and a removal of contaminating cells (such as T cells) need to be considered in the experimental setting. Nevertheless, even without magnetic separation, the cell yield was highly reduced after 7 days of culture and one explanation for the reduced cell viability of the BMMCs could be that the BM aspirates used for these experiments were stored for several days at 4 °C before the generation started. No differences in T-cell suppression were detected between the BMMC-derived cytokine-induced MDSCs of both types of stimulation (Figure **19**), similar to the results showed for PBMC-derived MDSCs (Figure 17). The discrepant findings in this study compared to Lechner *et al*. 2010 and Marigo *et al*. 2010 should be analyzed, mainly to find the reason for the lower cell yield compared to the levels reported by other studies.

Overall, BMMC-derived $CD33^+$ MDSCs showed robust immunosuppressive capacity, encouraging to search for further improvements aiming to increase the cellular yield. Furthermore, a combination of several immunosuppressive cell types could represent a promising therapeutic approach, similar as shown previously for MSCs combined with Tregs in mice (Lim *et al.* 2014).

6.3 Cell combinations

In 2014, Lim and colleagues demonstrated the combined cell transfer of MSCs and Tregs in an animal model of GvHD. This cell combination showed improved clinical GvHD scores and prolonged survival of mice treated with MSCs and Tregs. In addition, the levels of endogenous Tregs were increased and transferred Tregs had prolonged survival in the recipients (Lee *et al.* 2015; Lim *et al.* 2014). The idea of such cell combinations is that two immunomodulatory cell types at the same time have a synergistically increased suppressive effect

with lower concentrations of each cell type. However, in this study, MSCs combined with freshly isolated PMN-MDSCs showed a lower or only similar suppression of T-cell proliferation as PMN-MDSCs alone (Figure 20). It seems that the combined cells weakened or compensated the T-cell suppressive effect of each other, instead of amplifying it.

The combination of MSCs with BMMC-derived cytokine-induced MDSCs demonstrated an increased inhibition of T-cell proliferation at lower concentrations of each cell type. Furthermore, the suppression of the secretion of IFNγ was very strong while using both cell types in combination, but each cell type independently also induced a decrease of IFNγ release in a similar range (Figure 21). To get a comparable effect, the combination reduced the need of BMMC-derived cytokine–induced MDSCs of around one third. Unfortunately, the cell yield of the *in vitro* generation of BMMC-derived MDSCs was still very low (Table 14) and definitely not sufficient for clinical applications.

6.4 Generation of MDSCs derived from CD34$^+$ HSCs

The *in vitro* cytokine stimulation of CD34$^+$ HSCs resulted in the generation of a cell population that is CD33$^+$, CD11b$^+$, HLA-DR^{low}, and negative for the lineage markers (CD3, CD19, CD56), and thereby the cells fit to the phenotypical criteria of Bronte *et al.*, 2016. The generation led to cells that fulfill these current criteria of MDSCs as seen by the cell characterization (Figure 22) and the T-cell suppression (Figure 23). Furthermore, the staining of surface markers showed that the cells contain at least two populations as seen by the different expression levels of several markers. The HSC-derived cytokine-induced cells consist probably of both subtypes of MDSCs, PMN-MDSCs and M-MDSCs, just as described by Casacuberta-Serra *et al.*, 2017, who developed the generation protocol. Most of the cells were negative for CD14 and positive for CD16, with few CD66b positive cells, representing the PMN-MDSC population. Fewer cells were positive for CD14 and negative for CD16 and CD66b, characterizing the M-MDSCs. A small quantity of cells expressed HLA-DR at high levels and could be further assimilated with a phenotype of CD33$^+$, HLA-DR^{high}, such as DCs or monocytes/macrophages. In general, no phenotypical differences were detected between the generated HSC-derived MDSCs stimulated in presence or absence of IL-3, in contrast to the findings of Casacuberta-Serra *et al.*, 2017; however the exact percentage of M- and PMN-MDSCs was not analyzed in this study. A few phenotypical differences were measured between the HSC-derived MDSCs of different donors, such as the percentage of cells with a high expression of HLA-DR. These results are probably caused by the differences in time

periods required for the differentiation and maturation of the cells from different donors, also due to varied activation status.

The HSC-derived MDSCs suppressed T-cell proliferation and the secretion of IFNγ in a concentration-dependent manner (Figure 23). The inhibition of IFNγ release by both types of HSC-derived MDSCs was greater than the reduction by freshly isolated PMN-MDSCs or BMMC-derived MDSCs. The secretion of IFNγ was suppressed by HSC-derived MDSCs in a similar range as by MSCs. This indicates that HSC-derived MDSCs interact not only with T cells, also with NK cells and other IFNγ-producing cells, such as activated MSCs inhibit secretion of IFNγ by T cells and by NK cells (Castro-Manrreza and Montesinos 2015).
The suppression of T-cell proliferation by HSC-derived MDSCs reached around 87-90 % reduction at the ratio 1:0.5, which is in a similar range as the one by BMMC-derived MDSCs. The reduction by both types of HSC-derived MDSCs was much stronger in this experimental setting of the T-cell suppression assay than the suppression detected by Casacuberta-Serra *et al*., 2017. It is not clear if this disparity is just caused by different experimental settings or by a stronger T-cell suppressive effect of these HSC-derived MDSCs. Furthermore, the T-cell suppression by HSC-derived MDSCs could probably increase to a level similar to the strong effect induced by freshly isolated PMN-MDSCs (with around 95 % suppression), if the selected $CD33^+$ fraction after magnetic separation would contain less cell debris and dead cells, as seen in Figure 24 A+B. It is well described that macrophages are involved in the removal of dead cells and cell debris, thereby activating them, which in turn activate T cells (Mosser and Edwards 2008). Such an activation of APCs, followed by T-cell proliferation could be reduced or abrogated, if the $CD33^+$ fraction would contain only MDSCs without any contaminations of dead cells and debris. In addition, the contaminating cell debris affect probably the efficiency of the magnetic separation, through unspecific binding to the CD33 MicroBeads, which results in less MicroBeads for the cell suspension. As seen in Figure 24 D-F, the negative fraction of CD33 separation also contained $CD33^+$ MDSCs. This demonstrates that further improvements of the magnetic separation are required to get all $CD33^+$ MDSCs out of the $CD34^+$ HSC-derived cytokine-induced cells. According to the manufacturer, the CD33 MicroBeads are designed to a content of around one third of positive cells. However, the cytokine-induced generation derived from $CD34^+$ HSCs led to a much higher content of $CD33^+$ MDSCs, with a high rate of dead cells and debris. One way to increase the isolation of the $CD33^+$ MDSCs could be adjustment of the labeling protocol, for which the manufacturer suggested to increase the volume of CD33 MicroBeads within the

same volume of cell suspension. Indeed, the total cell number and/or its volume affect the efficiency of the magnetic separation, as it can be seen in experiment number 7 in Table 15 and Table 16 (the lowest total cell number associated with the highest cell yield in percent by magnetic separation). Overall, Table 15 and Figure 24 demonstrate that the isolation of MDSCs should be further improved for clinical application purposes. Another way to get a pure cell population of $CD33^+$ MDSCs without dead cells could be the use of a cell sorter instead of magnetic separation, as done by Casacuberta-Serra *et al*., 2017. Cell sorters have already been used for clinical studies with Tregs (Trzonkowski *et al.* 2009) and demonstrating the feasibility of this isolation method. While cell sorters are known to isolate cells with higher purity, magnetic separation is in contrast easy to handle experimentally and clinically according to good manufacturing practice (Gliwiński *et al.* 2017). Finally, Tregs isolated by magnetic separation resulted in well-tolerated and promising outcomes in clinical studies (Brunstein *et al.* 2011; Di Ianni *et al.* 2011), demonstrating that isolation and purification through this method can be sufficient.

In addition to the strong T-cell suppressive effect, the average increase of the total cell numbers during *in vitro* stimulation of $CD34^+$ HSCs was also higher in these experiments than the expansion described by Casacuberta-Serra *et al*., 2017. However, big variances were detected in cell expansion regarding the different donors (ranging from 2.9 to 189.0 fold increases during 20 days of cell culture). Until now, the reasons for such different expansion rates are not clear. Even tough, cryopreservation of $CD34^+$ HSCs was performed in a standardized way; it is a critical step with a high influence on cell viability that could explain the variability observed in the expansion rates. Especially, small differences in the freezing rate as well as the concentration of dimethylsulfoxide seem to have an effect on cell viability (Berz *et al.* 2007). Further investigations are required, as for example examine the cell population composition during cell culture at various time points. Also the influence of extra media exchanges or additions should be analyzed in the fast growing cells. Such extra media was required by the fast growing cells in this study, as seen by color change of the media (see 4.2.5.2). Unfortunately, no analysis regarding its influence on cell viability or differentiation was performed during this study and this should be further explored. Brunstein *et al.* detected an even greater range in the *in vitro* expansion rate of Tregs, and the authors speculated that the variation is mainly due to inherent factors of cells by different donors (Brunstein *et al.* 2011). The variation in the expansion rate of MDSCs derived from $CD34^+$ HSCs could also be caused by the use of HSCs from different donors. The aim of subsequent studies could be

to get a constant and high expansion rate of MDSCs derived from $CD34^+$ HSCs since they have the highest expansion rate and T-cell suppressive effect.

Overall, the increasing cell numbers and the strong T-cell suppressive effect of $CD34^+$ HSC-derived cytokine-induced MDSCs describe their great potential for clinical application for patients with overwhelming immune reactions, such as GvHD.

6.5 MDSCs as immunosuppressive therapy?

Several studies demonstrated so far that *in vitro* generated MDSCs alleviated or prevented GvHD in murine transplantation models (Highfill *et al.* 2010; Messmann *et al.* 2015; Zhou *et al.* 2010; Yang *et al.* 2016). Each group used different combinations of cytokines for the induction of MDSCs derived from murine BM cells with incubation times varying between 4 and 7 days. Highfill *et al.* detected after adoptive transfer of MDSCs that donor T-cell proliferation, activation and cytokine production were reduced via arginase-1-dependent mechanisms. Besides, Messmann *et al.* measured no reduction of T-cell numbers in their study, but a skewing towards Th2 cells. Yang *et al.* reported that the induced M-MDSCs increased transplant tolerance via high generation of NO via iNOS. So far, it is not clear which mechanism is used by $CD34^+$ HSC-derived cytokine-induced MDSCs to reduce T-cell proliferation and the secretion of IFNγ *in vitro*. However, the mechanism of HSC-derived MDSCs should be analyzed before using in clinical applications to estimate its effect on other cell types and the whole body.

In addition, the stability of the T-cell suppressive effect by MDSCs is challenged. Drujont *et al.* generated *in vitro* MDSCs from murine BM cells by stimulation with GM-CSF and IL-6 with the protocol of Marigo *et al.* 2010. These MDSCs strongly suppressed $CD8^+$ T-cell proliferation *in vitro*, but they didn't reduced proliferation or cytotoxicity of T cells *in vivo.* The infusion of MDSCs prolonged allograft survival in mice after skin transplantation by over-activation of T cells and APCs (Drujont *et al.* 2014). Koehn *et al.* reported after adoptive transfer of MDSCs that the cells rapidly lose the suppressive capacity in the inflammatory setting of mice with acute GvHD, but still partially suppressed GvHD. This suppressive effect could be increased by genetic alteration of transferred MDSCs in order to disable inflammasome activation, resulting in improved survival of mice treated with altered MDSCs compared to wild-type MDSCs (Koehn *et al.* 2015). This demonstrates that *in vivo* experiments are still useful to investigate the complex interactions during development and course of diseases. The HSC-derived cytokine-induced MDSCs should also be analyzed in a more complex model of

acute GvHD, maybe even an animal model, to investigate if these cells have a stable T-cell suppressive effect, even under inflammatory conditions.

In addition, animal studies modeling allograft transplantations and GvHD could advice in many other open issues regarding cell therapies with immunosuppressive cells. In regards to clinical applications of immunosuppressive cells, further developments and standardizations are required assessing not only cell preparations but also, the timing and site of injection, as well as doses (number of cells and/or number of injections), similar as within the field of Treg therapies (Safinia *et al.* 2013).

In this study, Tregs as well as freshly isolated or cytokine-induced MDSCs demonstrated *in vitro* strong T-cell suppression in ratios between 1:0.16 and 1:0.5 with stimulated responder PBMCs to immunosuppressive cells. However, *in vivo* experiments demonstrated that Tregs required ratios of 1:1 or 1:3 of effector T cells to Tregs to reduce murine GvHD (Ramlal and Hildebrandt 2017). Highfill *et al.* reported that MDSCs prevented GvHD lethality in the ratio 1:3 of donor T cells to MDSCs in murine experiments, whereas Zhou *et al.* applied MDSCs in the ratio 1:4 (Highfill *et al.* 2010; Zhou *et al.* 2010). So far, higher numbers of MDSCs were used *in vivo* to detect a reduction in GvHD lethality than during *in vitro* experiments. In addition, in both studies, MDSCs were administrated together with the transplantation of BM cells, which represents prevention and not a treatment of ongoing GvHD. This demonstrates that further investigations regarding cell ratios and time points of injections are required before MDSCs can be used in clinical applications. Especially in humans, the use of cell therapies is more acceptable in patients with severe GvHD without any other treatment option instead of patients undergoing allogenic HSCT without increased risks.

Another treatment option could be the induction of autologous MDSCs *in vivo* by stimulating drugs. Adeegbe *et al.* described that the combined administration of human G-CSF with IL-2 complex induced MDSCs and Tregs in high frequencies in multiple tissues of treated mice. Furthermore, skin graft rejection was delayed in mice treated with these drugs (Adeegbe *et al.* 2011). Turnquist *et al.* reported that administration of IL-33 increased MDSCs and Tregs in mice and prolonged graft tolerance after allogenic heart transplantation (Turnquist *et al.* 2011). Further studies showed that the number of MDSCs can be increased in different disease models in mice by administration of cannabidiol (Hegde *et al.* 2015), lipopolysaccharide (LPS) (De Wilde *et al.* 2009) or the JAK inhibitor tofacitinib (Nishimura *et al.* 2015). However, all these substances have broader effects on the immune system than just the induction of MDSCs, which should be carefully considered. In a murine model of GvHD after haploidentical BM transplantation, post-transplant administration of

bendamustine increased the number of MDSCs, alleviated GvHD and improved survival without reducing the GvT effect (Stokes *et al.* 2016). Furthermore, Rieber *et al.* demonstrated at the same hospital that patients with GvHD have increased levels of PMN-MDSCs compared to healthy people or patients after HSCT without GvHD and that treatment with extracorporeal photopheresis further raised the percentage of PMN- MDSCs in patients with GvHD (Rieber *et al.* 2014).

Overall, this study demonstrates that MDSCs strongly suppressed T-cell proliferation and the secretion of the pro-inflammatory cytokine IFNγ *in vitro.* So far, the available cell number of MDSCs is a limiting factor for a clinical application of MDSCs, because of the paucity of MDSCs in healthy persons and the difficulties to generate functional human MDSCs. However, the generation of MDSCs derived from $CD34^+$ HSCs showed a great potential of expansion. Therefore, we are working on a protocol for the *in vitro* generation of HSC-derived MDSCs with respect to cell preparation, according to good manufacturer practice. This could pave the way to adoptive transfer of MDSCs into patients with overwhelming immune reactions, such as GvHD.

7 References

Abumaree, M. H., Al Jumah, M. A., Kalionis, B., Jawdat, D., Al Khaldi, A., Abomaray, F. M., Fatani, A. S., Chamley, L. W., and Knawy, B. A. 2013. 'Human Placental Mesenchymal Stem Cells (pMSCs) Play a Role as Immune Suppressive Cells by Shifting Macrophage Differentiation from Inflammatory M1 to Anti-inflammatory M2 Macrophages', *Stem Cell Reviews and Reports*, 9: 620-41.

Adeegbe, D., Serafini, P., Bronte, V., Zoso, A., Ricordi, C., and Inverardi, L. 2011. 'In vivo induction of myeloid suppressor cells and CD4(+)Foxp3(+) T regulatory cells prolongs skin allograft survival in mice', *Cell Transplant*, 20: 941-54.

Aldinucci, A., Rizzetto, L., Pieri, L., Nosi, D., Romagnoli, P., Biagioli, T., Mazzanti, B., Saccardi, R., Beltrame, L., Massacesi, L., Cavalieri, D., and Ballerini, C. 2010. 'Inhibition of Immune Synapse by Altered Dendritic Cell Actin Distribution: A New Pathway of Mesenchymal Stem Cell Immune Regulation', *The Journal of Immunology*, 185: 5102-10.

Amorin, B., Alegretti, A. P., Valim, V., Pezzi, A., Laureano, A. M., da Silva, M. A. L., Wieck, A., and Silla, L. 2014. 'Mesenchymal stem cell therapy and acute graft-versus-host disease: a review', *Human Cell*, 27: 137-50.

Asseman, C., Read, S., and Powrie, F. 2003. 'Colitogenic Th1 Cells Are Present in the Antigen-Experienced T Cell Pool in Normal Mice: Control by CD4+ Regulatory T Cells and IL-10', *The Journal of Immunology*, 171: 971-78.

Balan, A., Lucchini, G., Schmidt, S., Schneider, A., Tramsen, L., Kuci, S., Meisel, R., Bader, P., and Lehrnbecher, T. 2014. 'Mesenchymal stromal cells in the antimicrobial host response of hematopoietic stem cell recipients with graft-versus-host disease--friends or foes?', *Leukemia*, 28: 1941-8.

Ballbach, M., Hall, T., Brand, A., Neri, D., Singh, A., Schaefer, I., Herrmann, E., Hansmann, S., Handgretinger, R., Kuemmerle-Deschner, J., Hartl, D., and Rieber, N. 2016. 'Induction of Myeloid-Derived Suppressor Cells in Cryopyrin-Associated Periodic Syndromes', *Journal of Innate Immunity*, 8: 493-506.

Barriga, F., Ramírez, P., Wietstruck, A., and Rojas, N. 2012. 'Hematopoietic stem cell transplantation: clinical use and perspectives', *Biological Research*, 45: 307-16.

Benvenuto, F., Ferrari, S., Gerdoni, E., Gualandi, F., Frassoni, F., Pistoia, V., Mancardi, G., and Uccelli, A. 2007. 'Human Mesenchymal Stem Cells Promote Survival of T Cells in a Quiescent State', *STEM CELLS*, 25: 1753-60.

Bernardo, M. E., and Locatelli, F. 2016. 'Mesenchymal Stromal Cells in Hematopoietic Stem Cell Transplantation', *Methods Mol Biol*, 1416: 3-20.

Bernardo, M. E., Locatelli, F., and Fibbe, W. E. 2009. 'Mesenchymal Stromal Cells', *Annals of the New York Academy of Sciences*, 1176: 101-17.

Berz, D., McCormack, E. M., Winer, E. S., Colvin, G. A., and Quesenberry, P. J. 2007. 'Cryopreservation of Hematopoietic Stem Cells', *American journal of hematology*, 82: 463-72.

Blazar, B. R., Murphy, W. J., and Abedi, M. 2012. 'Advances in graft-versus-host disease biology and therapy', *Nature reviews. Immunology*, 12: 443-58.

Bronte, V., Brandau, S., Chen, S.-H., Colombo, M. P., Frey, A. B., Greten, T. F., Mandruzzato, S., Murray, P. J., Ochoa, A., Ostrand-Rosenberg, S., Rodriguez, P. C., Sica, A., Umansky, V., Vonderheide, R. H., and Gabrilovich, D. I. 2016. 'Recommendations for myeloid-derived suppressor cell nomenclature and characterization standards', *Nat Commun*, 7.

Bronte, V., Kasic, T., Gri, G., Gallana, K., Borsellino, G., Marigo, I., Battistini, L., Iafrate, M., Prayer-Galetti, T., Pagano, F., and Viola, A. 2005. 'Boosting antitumor responses of T lymphocytes infiltrating human prostate cancers', *The Journal of Experimental Medicine*, 201: 1257-68.

Brunstein, C. G., Miller, J. S., Cao, Q., McKenna, D. H., Hippen, K. L., Curtsinger, J., DeFor, T., Levine, B. L., June, C. H., Rubinstein, P., McGlave, P. B., Blazar, B. R., and Wagner, J. E. 2011. 'Infusion of ex vivo expanded T regulatory cells in adults transplanted with umbilical cord blood: safety profile and detection kinetics', *Blood*, 117: 1061-70.

Bryk, J. A., Popovic, P. J., Zenati, M. S., Munera, V., Pribis, J. P., and Ochoa, J. B. 2010. 'Nature of myeloid cells expressing arginase 1 in peripheral blood after trauma', *J Trauma*, 68: 843-52.

Calmettes, C., Vigouroux, S., Labopin, M., Tabrizi, R., Turlure, P., Lafarge, X., Marit, G., Pigneux, A., Leguay, T., Bouabdallah, K., Dilhuydy, M.-S., Duclos, C., Mohr, C., Lascaux, A., Dumas, P.-Y., Dimicoli-Salazar, S., Saint-Lézer, A., and Milpied, N. 2015. 'Risk Factors for Steroid-Refractory Acute Graft-versus-Host Disease after Allogeneic Stem Cell Transplantation from Matched Related or Unrelated Donors', *Biology of Blood and Marrow Transplantation*, 21: 860-65.

Camisaschi, C., Casati, C., Rini, F., Perego, M., De Filippo, A., Triebel, F., Parmiani, G., Belli, F., Rivoltini, L., and Castelli, C. 2010. 'LAG-3 Expression Defines a Subset of CD4+CD25highFoxp3+ Regulatory T Cells That Are Expanded at Tumor Sites', *The Journal of Immunology*, 184: 6545-51.

Casacuberta-Serra, S., Pares, M., Golbano, A., Coves, E., Espejo, C., and Barquinero, J. 2017. 'Myeloid-derived suppressor cells can be efficiently generated from human hematopoietic progenitors and peripheral blood monocytes', *Immunol Cell Biol*.

Castro-Manrreza, M. E., and Montesinos, J. J. 2015. 'Immunoregulation by Mesenchymal Stem Cells: Biological Aspects and Clinical Applications', *Journal of Immunology Research*, 2015: 20.

Chaplin, D. D. 2010. 'Overview of the Immune Response', *The Journal of allergy and clinical immunology*, 125: S3-23.

Chiesa, S., Morbelli, S., Morando, S., Massollo, M., Marini, C., Bertoni, A., Frassoni, F., Bartolomé, S. T., Sambuceti, G., Traggiai, E., and Uccelli, A. 2011. 'Mesenchymal stem cells impair in vivo T-cell priming by dendritic cells', *Proceedings of the National Academy of Sciences of the United States of America*, 108: 17384-89.

Collison, L. W., Pillai, M. R., Chaturvedi, V., and Vignali, D. A. A. 2009. 'Regulatory T Cell Suppression Is Potentiated by Target T Cells in a Cell Contact, IL-35- and IL-10-Dependent Manner', *The Journal of Immunology*, 182: 6121-28.

Collison, L. W., Workman, C. J., Kuo, T. T., Boyd, K., Wang, Y., Vignali, K. M., Cross, R., Sehy, D., Blumberg, R. S., and Vignali, D. A. A. 2007. 'The inhibitory cytokine IL-35 contributes to regulatory T-cell function', *Nature*, 450: 566-69.

Crisan, M., Corselli, M., Chen, W. C. W., Péault, B., and Moldovan, N. I. 2012. 'Perivascular cells for regenerative medicine', *Journal of Cellular and Molecular Medicine*, 16: 2851-60.

Crisan, M., Yap, S., Casteilla, L., Chen, C.-W., Corselli, M., Park, T. S., Andriolo, G., Sun, B., Zheng, B., Zhang, L., Norotte, C., Teng, P.-N., Traas, J., Schugar, R., Deasy, B. M., Badylak, S., Bűhring, H.-J., Giacobino, J.-P., Lazzari, L., Huard, J., and Péault, B. 2008. 'A Perivascular Origin for Mesenchymal Stem Cells in Multiple Human Organs', *Cell Stem Cell*, 3: 301-13.

Cui, R., Rekasi, H., Hepner-Schefczyk, M., Fessmann, K., Petri, R. M., Bruderek, K., Brandau, S., Jäger, M., and Flohé, S. B. 2016. 'Human mesenchymal stromal/stem cells acquire immunostimulatory capacity upon cross-talk with natural killer cells and

might improve the NK cell function of immunocompromised patients', *Stem Cell Research & Therapy*, 7: 88.

Davoine, F., Lavigne, S., Chakir, J., Ferland, C., Boulay, M.-È., and Laviolette, M. 2002. 'Expression of FcγRIII (CD16) on human peripheral blood eosinophils increases in allergic conditions', *Journal of Allergy and Clinical Immunology*, 109: 463-69.

De Wilde, V., Van Rompaey, N., Hill, M., Lebrun, J. F., Lemaître, P., Lhommé, F., Kubjak, C., Vokaer, B., Oldenhove, G., Charbonnier, L. M., Cuturi, M. C., Goldman, M., and Le Moine, A. 2009. 'Endotoxin-Induced Myeloid-Derived Suppressor Cells Inhibit Alloimmune Responses via Heme Oxygenase-1', *American Journal of Transplantation*, 9: 2034-47.

Di Ianni, M., Falzetti, F., Carotti, A., Terenzi, A., Castellino, F., Bonifacio, E., Del Papa, B., Zei, T., Ostini, R. I., Cecchini, D., Aloisi, T., Perruccio, K., Ruggeri, L., Balucani, C., Pierini, A., Sportoletti, P., Aristei, C., Falini, B., Reisner, Y., Velardi, A., Aversa, F., and Martelli, M. F. 2011. 'Tregs prevent GVHD and promote immune reconstitution in HLA-haploidentical transplantation', *Blood*, 117: 3921-28.

Di Nicola, M., Carlo-Stella, C., Magni, M., Milanesi, M., Longoni, P. D., Matteucci, P., Grisanti, S., and Gianni, A. M. 2002. 'Human bone marrow stromal cells suppress T-lymphocyte proliferation induced by cellular or nonspecific mitogenic stimuli', *Blood*, 99: 3838-43.

Dieckmann, D., Bruett, C. H., Ploettner, H., Lutz, M. B., and Schuler, G. 2002. 'Human CD4+CD25+ Regulatory, Contact-dependent T Cells Induce Interleukin 10–producing, Contact-independent Type 1-like Regulatory T Cells', *The Journal of Experimental Medicine*, 196: 247-53.

Dilek, N., Vuillefroy de Silly, R., Blancho, G., and Vanhove, B. 2012. 'Myeloid-derived suppressor cells: mechanisms of action and recent advances in their role in transplant tolerance', *Frontiers in Immunology*, 3.

Dominici, M., Le Blanc, K., Mueller, I., Slaper-Cortenbach, I., Marini, F., Krause, D., Deans, R., Keating, A., Prockop, D., and Horwitz, E. 2006. 'Minimal criteria for defining multipotent mesenchymal stromal cells. The International Society for Cellular Therapy position statement', *Cytotherapy*, 8: 315-17.

DRST. 2015. *Deutsches Register für Stammzelltransplantationen - Jahresbericht 2015* (Essen & Ulm). http://www.drst.de/download/jb2015.pdf.

Drujont, L., Carretero-Iglesia, L., Bouchet-Delbos, L., Beriou, G., Merieau, E., Hill, M., Delneste, Y., Cuturi, M. C., and Louvet, C. 2014. 'Evaluation of the Therapeutic Potential of Bone Marrow-Derived Myeloid Suppressor Cell (MDSC) Adoptive Transfer in Mouse Models of Autoimmunity and Allograft Rejection', *PLoS ONE*, 9: e100013.

Fernandes, Maria J G., Rollet-Labelle, E., Paré, G., Marois, S., Tremblay, M.-L., Teillaud, J.-L., and Naccache, Paul H. 2006. 'CD16b associates with high-density, detergent-resistant membranes in human neutrophils', *Biochemical Journal*, 393: 351-59.

Ferrara, J. L., Levine, J. E., Reddy, P., and Holler, E. 2009. 'Graft-versus-host disease', *Lancet*, 373: 1550-61.

Flowers, M. E. D., Inamoto, Y., Carpenter, P. A., Lee, S. J., Kiem, H.-P., Petersdorf, E. W., Pereira, S. E., Nash, R. A., Mielcarek, M., Fero, M. L., Warren, E. H., Sanders, J. E., Storb, R. F., Appelbaum, F. R., Storer, B. E., and Martin, P. J. 2011. 'Comparative analysis of risk factors for acute graft-versus-host disease and for chronic graft-versus-host disease according to National Institutes of Health consensus criteria', *Blood*, 117: 3214-19.

Franquesa, M., Mensah, F. K., Huizinga, R., Strini, T., Boon, L., Lombardo, E., DelaRosa, O., Laman, J. D., Grinyó, J. M., Weimar, W., Betjes, M. G. H., Baan, C. C., and Hoogduijn, M. J. 2015. 'Human Adipose Tissue-Derived Mesenchymal Stem Cells

Abrogate Plasmablast Formation and Induce Regulatory B Cells Independently of T Helper Cells', *STEM CELLS*, 33: 880-91.

Fridlender, Z. G., Sun, J., Mishalian, I., Singhal, S., Cheng, G., Kapoor, V., Horng, W., Fridlender, G., Bayuh, R., Worthen, G. S., and Albelda, S. M. 2012. 'Transcriptomic Analysis Comparing Tumor-Associated Neutrophils with Granulocytic Myeloid-Derived Suppressor Cells and Normal Neutrophils', *PLoS ONE*, 7: e31524.

Friedenstein, A. J., Petrakova, K. V., Kurolesova, A. I., and Frolova, G. P. 1968. 'HETEROTOPIC TRANSPLANTS OF BONE MARROW', *Transplantation*, 6: 230-47.

Gabrilovich, D. I. 2017. 'Myeloid-Derived Suppressor Cells', *Cancer Immunology Research*, 5: 3-8.

Gabrilovich, D. I., and Nagaraj, S. 2009. 'Myeloid-derived suppressor cells as regulators of the immune system', *Nat Rev Immunol*, 9: 162-74.

Geneugelijk, K., Thus, K. A., and Spierings, E. 2014. 'Predicting Alloreactivity in Transplantation', *Journal of Immunology Research*, 2014: 12.

Gieseke, F., Böhringer, J., Bussolari, R., Dominici, M., Handgretinger, R., and Müller, I. 2010. 'Human multipotent mesenchymal stromal cells use galectin-1 to inhibit immune effector cells', *Blood*, 116: 3770-79.

Glennie, S., Soeiro, I., Dyson, P. J., Lam, E. W.-F., and Dazzi, F. 2005. 'Bone marrow mesenchymal stem cells induce division arrest anergy of activated T cells', *Blood*, 105: 2821-27.

Gliwiński, M., Iwaszkiewicz-Grześ, D., and Trzonkowski, P. 2017. 'Cell-Based Therapies with T Regulatory Cells', *BioDrugs*.

Greifenberg, V., Ribechini, E., Rößner, S., and Lutz, M. B. 2009. 'Myeloid-derived suppressor cell activation by combined LPS and IFN-γ treatment impairs DC development', *European Journal of Immunology*, 39: 2865-76.

Grossman, W. J., Verbsky, J. W., Barchet, W., Colonna, M., Atkinson, J. P., and Ley, T. J. 2004. 'Human T Regulatory Cells Can Use the Perforin Pathway to Cause Autologous Target Cell Death', *Immunity*, 21: 589-601.

Haddad, R., and Saldanha-Araujo, F. 2014. 'Mechanisms of T-Cell Immunosuppression by Mesenchymal Stromal Cells: What Do We Know So Far?', *BioMed Research International*, 2014: 14.

Handgretinger, R., Chen, X., Pfeiffer, M., Mueller, I., Feuchtinger, T., Hale, G. A., and Lang, P. 2007. 'Feasibility and Outcome of Reduced-Intensity Conditioning in Haploidentical Transplantation', *Annals of the New York Academy of Sciences*, 1106: 279-89.

Hanson, E. M., Clements, V. K., Sinha, P., Ilkovitch, D., and Ostrand-Rosenberg, S. 2009. 'Myeloid-Derived Suppressor Cells Down-Regulate L-Selectin Expression on CD4+ and CD8+ T Cells', *The Journal of Immunology*, 183: 937-44.

Hegde, V. L., Singh, U. P., Nagarkatti, P. S., and Nagarkatti, M. 2015. 'Critical Role of Mast Cells and Peroxisome Proliferator-Activated Receptor gamma in the Induction of Myeloid-Derived Suppressor Cells by Marijuana Cannabidiol In Vivo', *J Immunol*, 194: 5211-22.

Henden, A. S., and Hill, G. R. 2015. 'Cytokines in Graft-versus-Host Disease', *The Journal of Immunology*, 194: 4604-12.

Highfill, S. L., Rodriguez, P. C., Zhou, Q., Goetz, C. A., Koehn, B. H., Veenstra, R., Taylor, P. A., Panoskaltsis-Mortari, A., Serody, J. S., Munn, D. H., Tolar, J., Ochoa, A. C., and Blazar, B. R. 2010. 'Bone marrow myeloid-derived suppressor cells (MDSCs) inhibit graft-versus-host disease (GVHD) via an arginase-1–dependent mechanism that is up-regulated by interleukin-13', *Blood*, 116: 5738-47.

Höchst, B., Schildberg, F. A., Sauerborn, P., Gäbel, Y. A., Gevensleben, H., Goltz, D., Heukamp, L. C., Türler, A., Ballmaier, M., Gieseke, F., Müller, I., Kalff, J., Kurts, C., Knolle, P. A., and Diehl, L. 2013. 'Activated human hepatic stellate cells induce myeloid derived suppressor cells from peripheral blood monocytes in a CD44-dependent fashion', *Journal of Hepatology*, 59: 528-35.

Hoechst, B., Ormandy, L. A., Ballmaier, M., Lehner, F., Kruger, C., Manns, M. P., Greten, T. F., and Korangy, F. 2008. 'A new population of myeloid-derived suppressor cells in hepatocellular carcinoma patients induces CD4(+)CD25(+)Foxp3(+) T cells', *Gastroenterology*, 135: 234-43.

Holtan, S. G., Pasquini, M., and Weisdorf, D. J. 2014. 'Acute graft-versus-host disease: a bench-to-bedside update', *Blood*, 124: 363-73.

Horwitz, E. M., Le Blanc, K., Dominici, M., Mueller, I., Slaper-Cortenbach, I., Marini, F. C., Deans, R. J., Krause, D. S., and Keating, A. 2005. 'Clarification of the nomenclature for MSC: The International Society for Cellular Therapy position statement', *Cytotherapy*, 7: 393-95.

Hsu, W.-T., Lin, C.-H., Chiang, B.-L., Jui, H.-Y., Wu, K. K.-Y., and Lee, C.-M. 2013. 'Prostaglandin E2 Potentiates Mesenchymal Stem Cell–Induced IL-10+IFN-γ+CD4+ Regulatory T Cells To Control Transplant Arteriosclerosis', *The Journal of Immunology*, 190: 2372-80.

Introna, M., Lucchini, G., Dander, E., Galimberti, S., Rovelli, A., Balduzzi, A., Longoni, D., Pavan, F., Masciocchi, F., Algarotti, A., Mico, C., Grassi, A., Deola, S., Cavattoni, I., Gaipa, G., Belotti, D., Perseghin, P., Parma, M., Pogliani, E., Golay, J., Pedrini, O., Capelli, C., Cortelazzo, S., D'Amico, G., Biondi, A., Rambaldi, A., and Biagi, E. 2014. 'Treatment of graft versus host disease with mesenchymal stromal cells: a phase I study on 40 adult and pediatric patients', *Biol Blood Marrow Transplant*, 20: 375-81.

Ivanova, E. A., and Orekhov, A. N. 2015. 'T Helper Lymphocyte Subsets and Plasticity in Autoimmunity and Cancer: An Overview', *BioMed Research International*, 2015: 327470.

Jonuleit, H., and Schmitt, E. 2003. 'The Regulatory T Cell Family: Distinct Subsets and their Interrelations', *The Journal of Immunology*, 171: 6323-27.

Jonuleit, H., Schmitt, E., Kakirman, H., Stassen, M., Knop, J., and Enk, A. H. 2002. 'Infectious Tolerance: Human CD25(+) Regulatory T Cells Convey Suppressor Activity to Conventional CD4(+) T Helper Cells', *The Journal of Experimental Medicine*, 196: 255-60.

Kekre, N., and Antin, J. H. 2014. 'Hematopoietic stem cell transplantation donor sources in the 21st century: choosing the ideal donor when a perfect match does not exist', *Blood*, 124: 334-43.

Kluter, H., Schlenke, P., Muller-Steinhardt, M., Paulsen, M., and Kirchner, H. 1997. 'Impact of buffy coat storage on the generation of inflammatory cytokines and platelet activation', *Transfusion*, 37: 362-7.

Koehn, B. H., Apostolova, P., Haverkamp, J. M., Miller, J. S., McCullar, V., Tolar, J., Munn, D. H., Murphy, W. J., Brickey, W. J., Serody, J. S., Gabrilovich, D. I., Bronte, V., Murray, P. J., Ting, J. P.-Y., Zeiser, R., and Blazar, B. R. 2015. 'GVHD-associated, inflammasome-mediated loss of function in adoptively transferred myeloid-derived suppressor cells', *Blood*, 126: 1621-28.

Koenen, H. J. P. M., Smeets, R. L., Vink, P. M., van Rijssen, E., Boots, A. M. H., and Joosten, I. 2008. 'Human CD25highFoxp3pos regulatory T cells differentiate into IL-17–producing cells', *Blood*, 112: 2340-52.

Lakschevitz, F. S., Hassanpour, S., Rubin, A., Fine, N., Sun, C., and Glogauer, M. 2016. 'Identification of neutrophil surface marker changes in health and inflammation using high-throughput screening flow cytometry', *Experimental Cell Research*, 342: 200-09.

Le Blanc, K., Frassoni, F., Ball, L., Locatelli, F., Roelofs, H., Lewis, I., Lanino, E., Sundberg, B., Bernardo, M. E., Remberger, M., Dini, G., Egeler, R. M., Bacigalupo, A., Fibbe, W., and Ringdén, O. 2008. 'Mesenchymal stem cells for treatment of steroid-resistant, severe, acute graft-versus-host disease: a phase II study', *The Lancet*, 371: 1579-86.

Lechner, M. G., Liebertz, D. J., and Epstein, A. L. 2010. 'Characterization of Cytokine-Induced Myeloid-Derived Suppressor Cells from Normal Human Peripheral Blood Mononuclear Cells', *The Journal of Immunology*, 185: 2273-84.

Lee, E.-S., Lim, J.-Y., Im, K.-I., Kim, N., Nam, Y.-S., Jeon, Y.-W., and Cho, S.-G. 2015. 'Adoptive Transfer of Treg Cells Combined with Mesenchymal Stem Cells Facilitates Repopulation of Endogenous Treg Cells in a Murine Acute GVHD Model', *PLoS ONE*, 10: e0138846.

Lelis, F. J. N. 2017. *Myeloid-derived suppressor cells regulate B-cell responses* (Eberhard Karls Universitaet Tuebingen). http://dx.doi.org/10.15496/publikation-15786.

Lim, J.-Y., Park, M.-J., Im, K.-I., Kim, N., Jeon, E.-J., Kim, E.-J., Cho, M.-L., and Cho, S.-G. 2014. 'Combination Cell Therapy Using Mesenchymal Stem Cells and Regulatory T-Cells Provides a Synergistic Immunomodulatory Effect Associated With Reciprocal Regulation of Th1/Th2 and Th17/Treg Cells in a Murine Acute Graft-Versus-Host Disease Model', *Cell Transplantation*, 23: 703-14.

Luttmann, W., Bratke, K., Küpper, M., and Myrtek, D. 2008. *Der Experimentator: Immunologie* (Spektrum Akademischer Verlag: Heidelberg).

Lutz, M. B., Suri, R. M., Niimi, M., Ogilvie, A. L., Kukutsch, N. A., Rossner, S., Schuler, G., and Austyn, J. M. 2000. 'Immature dendritic cells generated with low doses of GM-CSF in the absence of IL-4 are maturation resistant and prolong allograft survival in vivo', *Eur J Immunol*, 30: 1813-22.

Lyons, A. B. 2000. 'Analysing cell division in vivo and in vitro using flow cytometric measurement of CFSE dye dilution', *Journal of Immunological Methods*, 243: 147-54.

Mandapathil, M., Hilldorfer, B., Szczepanski, M. J., Czystowska, M., Szajnik, M., Ren, J., Lang, S., Jackson, E. K., Gorelik, E., and Whiteside, T. L. 2010. 'Generation and Accumulation of Immunosuppressive Adenosine by Human CD4(+)CD25(high)FOXP3(+) Regulatory T Cells', *The Journal of Biological Chemistry*, 285: 7176-86.

Marigo, I., Bosio, E., Solito, S., Mesa, C., Fernandez, A., Dolcetti, L., Ugel, S., Sonda, N., Bicciato, S., Falisi, E., Calabrese, F., Basso, G., Zanovello, P., Cozzi, E., Mandruzzato, S., and Bronte, V. 2010. 'Tumor-Induced Tolerance and Immune Suppression Depend on the C/EBPβ Transcription Factor', *Immunity*, 32: 790-802.

Markey, K. A., MacDonald, K. P. A., and Hill, G. R. 2014. 'The biology of graft-versus-host disease: experimental systems instructing clinical practice', *Blood*, 124: 354-62.

Martelli, M. F., Di Ianni, M., Ruggeri, L., Falzetti, F., Carotti, A., Terenzi, A., Pierini, A., Massei, M. S., Amico, L., Urbani, E., Del Papa, B., Zei, T., Iacucci Ostini, R., Cecchini, D., Tognellini, R., Reisner, Y., Aversa, F., Falini, B., and Velardi, A. 2014. 'HLA-haploidentical transplantation with regulatory and conventional T-cell adoptive immunotherapy prevents acute leukemia relapse', *Blood*, 124: 638-44.

Martino, R., Iacobelli, S., Brand, R., Jansen, T., van Biezen, A., Finke, J., Bacigalupo, A., Beelen, D., Reiffers, J., Devergie, A., Alessandrino, E., Mufti, G. J., Barge, R., Sierra, J., Ruutu, T., Boogaerts, M., Falda, M., Jouet, J.-P., Niederwieser, D., and de Witte, T. 2006. 'Retrospective comparison of reduced-intensity conditioning and conventional high-dose conditioning for allogeneic hematopoietic stem cell transplantation using HLA-identical sibling donors in myelodysplastic syndromes', *Blood*, 108: 836-46.

Melief, S. M., Schrama, E., Brugman, M. H., Tiemessen, M. M., Hoogduijn, M. J., Fibbe, W. E., and Roelofs, H. 2013. 'Multipotent stromal cells induce human regulatory T

cells through a novel pathway involving skewing of monocytes toward anti-inflammatory macrophages', *STEM CELLS*, 31: 1980-91.

Messmann, J. J., Reisser, T., Leithäuser, F., Lutz, M. B., Debatin, K.-M., and Strauss, G. 2015. 'In vitro-generated MDSCs prevent murine GVHD by inducing type 2 T cells without disabling antitumor cytotoxicity', *Blood*, 126: 1138-48.

Millrud, C. R., Bergenfelz, C., and Leandersson, K. 2017. 'On the origin of myeloid-derived suppressor cells', *Oncotarget*, 8: 3649-65.

Miltenyi Biotec GmbH. 2017. *MACS cell separation - MACS technology* (Miltenyi Biotec GmbH: Bergisch Gladbach). http://www.miltenyibiotec.com/en/products-and-services/macs-cell-separation/macs-technology/microbeads_dp.aspx.

Mosmann, T. R., Li, L., Hengartner, H., Kagi, D., Fu, W., and Sad, S. 1997. 'Differentiation and functions of T cell subsets', *Ciba Found Symp*, 204: 148-54; discussion 54-8.

Mosser, D. M., and Edwards, J. P. 2008. 'Exploring the full spectrum of macrophage activation', *Nature reviews. Immunology*, 8: 958-69.

Müller, I., Kordowich, S., Holzwarth, C., Isensee, G., Lang, P., Neunhoeffer, F., Dominici, M., Greil, J., and Handgretinger, R. 2008. 'Application of multipotent mesenchymal stromal cells in pediatric patients following allogeneic stem cell transplantation', *Blood Cells, Molecules, and Diseases*, 40: 25-32.

Müller, I., Kordowich, S., Holzwarth, C., Spano, C., Isensee, G., Staiber, A., Viebahn, S., Gieseke, F., Langer, H., Gawaz, M. P., Horwitz, E. M., Conte, P., Handgretinger, R., and Dominici, M. 2006. 'Animal serum-free culture conditions for isolation and expansion of multipotent mesenchymal stromal cells from human BM', *Cytotherapy*, 8: 437-44.

Murphy, K. M. 2011. *Janeway's Immunobiology* (Taylor & Francis Group). https://books.google.de/books?id=WDMmAgAAQBAJ.

Nagaraj, S., Schrum, A. G., Cho, H.-I., Celis, E., and Gabrilovich, D. I. 2010. 'Mechanism of T Cell Tolerance Induced by Myeloid-Derived Suppressor Cells', *The Journal of Immunology*, 184: 3106-16.

Nakamura, K., Kitani, A., Fuss, I., Pedersen, A., Harada, N., Nawata, H., and Strober, W. 2004. 'TGF-β1 Plays an Important Role in the Mechanism of CD4+CD25+ Regulatory T Cell Activity in Both Humans and Mice', *The Journal of Immunology*, 172: 834-42.

Nishimura, K., Saegusa, J., Matsuki, F., Akashi, K., Kageyama, G., and Morinobu, A. 2015. 'Tofacitinib facilitates the expansion of myeloid-derived suppressor cells and ameliorates arthritis in SKG mice', *Arthritis Rheumatol*, 67: 893-902.

Norkin, M., and Wingard, J. R. 2017. 'Recent advances in hematopoietic stem cell transplantation', *F1000Research*, 6: 870.

Ostrand-Rosenberg, S. 2010. 'Myeloid-derived suppressor cells: more mechanisms for inhibiting antitumor immunity', *Cancer immunology, immunotherapy : CII*, 59: 1593-600.

Pandiyan, P., Zheng, L., Ishihara, S., Reed, J., and Lenardo, M. J. 2007. 'CD4+CD25+Foxp3+ regulatory T cells induce cytokine deprivation-mediated apoptosis of effector CD4+ T cells', *Nat Immunol*, 8: 1353-62.

Polchert, D., Sobinsky, J., Douglas, G. W., Kidd, M., Moadsiri, A., Reina, E., Genrich, K., Mehrotra, S., Setty, S., Smith, B., and Bartholomew, A. 2008. 'IFN-γ activation of mesenchymal stem cells for treatment and prevention of graft versus host disease', *European Journal of Immunology*, 38: 1745-55.

Qian, L., Wu, Z., and Shen, J. 2013. 'Advances in the treatment of acute graft-versus-host disease', *Journal of Cellular and Molecular Medicine*, 17: 966-75.

Ramlal, R., and Hildebrandt, G. C. 2017. 'Advances in the Use of Regulatory T-Cells for the Prevention and Therapy of Graft-vs.-Host Disease', *Biomedicines*, 5.

Rasmusson, I., Le Blanc, K., Sundberg, B., and Ringdén, O. 2007. 'Mesenchymal Stem Cells Stimulate Antibody Secretion in Human B Cells', *Scandinavian Journal of Immunology*, 65: 336-43.

Ribechini, E., Greifenberg, V., Sandwick, S., and Lutz, M. B. 2010. 'Subsets, expansion and activation of myeloid-derived suppressor cells', *Medical Microbiology and Immunology*, 199: 273-81.

Rieber, N., Gille, C., Köstlin, N., Schäfer, I., Spring, B., Ost, M., Spieles, H., Kugel, H. A., Pfeiffer, M., Heininger, V., Alkhaled, M., Hector, A., Mays, L., Kormann, M., Zundel, S., Fuchs, J., Handgretinger, R., Poets, C. F., and Hartl, D. 2013. 'Neutrophilic myeloid-derived suppressor cells in cord blood modulate innate and adaptive immune responses', *Clinical and Experimental Immunology*, 174: 45-52.

Rieber, N., Wecker, I., Neri, D., Fuchs, K., Schafer, I., Brand, A., Pfeiffer, M., Lang, P., Bethge, W., Amon, O., Handgretinger, R., and Hartl, D. 2014. 'Extracorporeal photopheresis increases neutrophilic myeloid-derived suppressor cells in patients with GvHD', *Bone Marrow Transplant*, 49: 545-52.

Riera Romo, M., Pérez-Martínez, D., and Castillo Ferrer, C. 2016. 'Innate immunity in vertebrates: an overview', *Immunology*, 148: 125-39.

Rodríguez, P. C., and Ochoa, A. C. 2008. 'Arginine regulation by myeloid derived suppressor cells and tolerance in cancer: mechanisms and therapeutic perspectives', *Immunological Reviews*, 222: 180-91.

Rosado, M. M., Bernardo, M. E., Scarsella, M., Conforti, A., Giorda, E., Biagini, S., Cascioli, S., Rossi, F., Guzzo, I., Vivarelli, M., Dello Strologo, L., Emma, F., Locatelli, F., and Carsetti, R. 2015. 'Inhibition of B-Cell Proliferation and Antibody Production by Mesenchymal Stromal Cells Is Mediated by T Cells', *Stem Cells and Development*, 24: 93-103.

Rubtsov, Y. P., Niec, R. E., Josefowicz, S., Li, L., Darce, J., Mathis, D., Benoist, C., and Rudensky, A. Y. 2010. 'Stability of the Regulatory T Cell Lineage in Vivo', *Science*, 329: 1667-71.

Safinia, N., Leech, J., Hernandez-Fuentes, M., Lechler, R., and Lombardi, G. 2013. 'Promoting transplantation tolerance; adoptive regulatory T cell therapy', *Clinical & Experimental Immunology*, 172: 158-68.

Sakaguchi, S., Miyara, M., Costantino, C. M., and Hafler, D. A. 2010. 'FOXP3+ regulatory T cells in the human immune system', *Nat Rev Immunol*, 10: 490-500.

Sakaguchi, S., Vignali, D. A. A., Rudensky, A. Y., Niec, R. E., and Waldmann, H. 2013. 'The plasticity and stability of regulatory T cells', *Nature Reviews Immunology*, 13: 461.

Santegoets, S. J. A. M., Dijkgraaf, E. M., Battaglia, A., Beckhove, P., Britten, C. M., Gallimore, A., Godkin, A., Gouttefangeas, C., de Gruijl, T. D., Koenen, H. J. P. M., Scheffold, A., Shevach, E. M., Staats, J., Taskén, K., Whiteside, T. L., Kroep, J. R., Welters, M. J. P., and van der Burg, S. H. 2015. 'Monitoring regulatory T cells in clinical samples: consensus on an essential marker set and gating strategy for regulatory T cell analysis by flow cytometry', *Cancer Immunology, Immunotherapy*, 64: 1271-86.

Schmetterer, K. G., Neunkirchner, A., and Pickl, W. F. 2012. 'Naturally occurring regulatory T cells: markers, mechanisms, and manipulation', *The FASEB Journal*, 26: 2253-76.

Schmidt, A., Oberle, N., and Krammer, P. H. 2012. 'Molecular Mechanisms of Treg-Mediated T Cell Suppression', *Frontiers in Immunology*, 3: 51.

Schmidt, A., Oberle, N., Weiß, E.-M., Vobis, D., Frischbutter, S., Baumgrass, R., Falk, C. S., Haag, M., Brügger, B., Lin, H., Mayr, G. W., Reichardt, P., Gunzer, M., Suri-Payer, E., and Krammer, P. H. 2011. 'Human Regulatory T Cells Rapidly Suppress T

Cell Receptor–Induced Ca2+, NF-κB, and NFAT Signaling in Conventional T Cells', *Science Signaling*, 4: ra90-ra90.

Schoenborn, J. R., and Wilson, C. B. 2007. 'Regulation of interferon-gamma during innate and adaptive immune responses', *Adv Immunol*, 96: 41-101.

Sojka, D. K., Huang, Y.-H., and Fowell, D. J. 2008. 'Mechanisms of regulatory T-cell suppression – a diverse arsenal for a moving target', *Immunology*, 124: 13-22.

Sotiropoulou, P. A., Perez, S. A., Gritzapis, A. D., Baxevanis, C. N., and Papamichail, M. 2006. 'Interactions Between Human Mesenchymal Stem Cells and Natural Killer Cells', *STEM CELLS*, 24: 74-85.

Squillaro, T., Peluso, G., and Galderisi, U. 2016. 'Clinical Trials With Mesenchymal Stem Cells: An Update', *Cell Transplantation*, 25: 829-48.

Srivastava, M. K., Sinha, P., Clements, V. K., Rodriguez, P., and Ostrand-Rosenberg, S. 2010. 'Myeloid-Derived Suppressor Cells Inhibit T-Cell Activation by Depleting Cystine and Cysteine', *Cancer Research*, 70: 68-77.

Stokes, J., Hoffman, E. A., Zeng, Y., Larmonier, N., and Katsanis, E. 2016. 'Post-transplant bendamustine reduces GvHD while preserving GvL in experimental haploidentical bone marrow transplantation', *Br J Haematol*, 174: 102-16.

Strauss, L., Bergmann, C., and Whiteside, T. L. 2009. 'Human Circulating CD4+CD25high Foxp3+ Regulatory T Cells Kill Autologous CD8+ but Not CD4+ Responder Cells by Fas-Mediated Apoptosis', *The Journal of Immunology*, 182: 1469-80.

Sudres, M., Norol, F., Trenado, A., Grégoire, S., Charlotte, F., Levacher, B., Lataillade, J.-J., Bourin, P., Holy, X., Vernant, J.-P., Klatzmann, D., and Cohen, J. L. 2006. 'Bone Marrow Mesenchymal Stem Cells Suppress Lymphocyte Proliferation In Vitro but Fail to Prevent Graft-versus-Host Disease in Mice', *The Journal of Immunology*, 176: 7761-67.

Sung, A. D., and Chao, N. J. 2013. 'Concise Review: Acute Graft-Versus-Host Disease: Immunobiology, Prevention, and Treatment', *Stem Cells Translational Medicine*, 2: 25-32.

Takahashi, T., Kuniyasu, Y., Toda, M., Sakaguchi, N., Itoh, M., Iwata, M., Shimizu, J., and Sakaguchi, S. 1998. 'Immunologic self-tolerance maintained by CD25+CD4+ naturally anergic and suppressive T cells: induction of autoimmune disease by breaking their anergic/suppressive state', *International Immunology*, 10: 1969-80.

Thornton, A. M., and Shevach, E. M. 1998. 'CD4(+)CD25(+) Immunoregulatory T Cells Suppress Polyclonal T Cell Activation In Vitro by Inhibiting Interleukin 2 Production', *The Journal of Experimental Medicine*, 188: 287-96.

Ting, C., Alterovitz, G., Merlob, A., and Abdi, R. 2013. 'Genomic studies of GVHD[mdash]lessons learned thus far', *Bone Marrow Transplant*, 48: 4-9.

Toren, A., Barak, V., Novick, D., and Nagler, A. 1997. 'Soluble interferon-gamma receptor and interferon-gamma in patients undergoing allogeneic bone marrow transplantation for hematological malignancies', *Cytokines Cell Mol Ther*, 3: 153-8.

Trzonkowski, P., Bieniaszewska, M., Juścińska, J., Dobyszuk, A., Krzystyniak, A., Marek, N., Myśliwska, J., and Hellmann, A. 2009. 'First-in-man clinical results of the treatment of patients with graft versus host disease with human ex vivo expanded CD4+CD25+CD127− T regulatory cells', *Clinical Immunology*, 133: 22-26.

Turnquist, H. R., Zhao, Z., Rosborough, B. R., Liu, Q., Castellaneta, A., Isse, K., Wang, Z., Lang, M., Stolz, D. B., Zheng, X. X., Demetris, A. J., Liew, F. Y., Wood, K. J., and Thomson, A. W. 2011. 'IL-33 expands suppressive CD11b+ Gr-1(int) and regulatory T cells, including ST2L+ Foxp3+ cells, and mediates regulatory T cell-dependent promotion of cardiac allograft survival', *J Immunol*, 187: 4598-610.

Uccelli, A., and de Rosbo, N. K. 2015. 'The immunomodulatory function of mesenchymal stem cells: mode of action and pathways', *Annals of the New York Academy of Sciences*, 1351: 114-26.

Uccelli, A., Moretta, L., and Pistoia, V. 2008. 'Mesenchymal stem cells in health and disease', *Nat Rev Immunol*, 8: 726-36.

van de Geer, A., Gazendam, R. P., Tool, A. T. J., van Hamme, J. L., de Korte, D., van den Berg, T. K., Zeerleder, S. S., and Kuijpers, T. W. 2017. 'Characterization of buffy coat-derived granulocytes for clinical use: a comparison with granulocyte colony-stimulating factor/dexamethasone-pretreated donor-derived products', *Vox Sanguinis*, 112: 173-82.

Wang, H., and Yang, Y.-G. 2014. 'The complex and central role of interferon-γ in graft-versus-host disease and graft-versus-tumor activity', *Immunological Reviews*, 258: 30-44.

Welniak, L. A., Blazar, B. R., and Murphy, W. J. 2007. 'Immunobiology of Allogeneic Hematopoietic Stem Cell Transplantation', *Annual Review of Immunology*, 25: 139-70.

Yang, F., Li, Y., Wu, T., Na, N., Zhao, Y., Li, W., Han, C., Zhang, L., Lu, J., and Zhao, Y. 2016. 'TNFalpha-induced M-MDSCs promote transplant immune tolerance via nitric oxide', *J Mol Med (Berl)*, 94: 911-20.

Yatim, K. M., and Lakkis, F. G. 2015. 'A Brief Journey through the Immune System', *Clinical Journal of the American Society of Nephrology*, 10: 1274-81.

Youn, J.-I., Collazo, M., Shalova, I. N., Biswas, S. K., and Gabrilovich, D. I. 2012. 'Characterization of the nature of granulocytic myeloid-derived suppressor cells in tumor-bearing mice', *Journal of Leukocyte Biology*, 91: 167-81.

Zhang, S., Ma, X., Zhu, C., Liu, L., Wang, G., and Yuan, X. 2016. 'The Role of Myeloid-Derived Suppressor Cells in Patients with Solid Tumors: A Meta-Analysis', *PLoS ONE*, 11: e0164514.

Zhang, S., Wu, K., Liu, Y., Lin, Y., Zhang, X., Zhou, J., Zhang, H., Pan, T., and Fu, Y. 2016. 'Finasteride Enhances the Generation of Human Myeloid-Derived Suppressor Cells by Up-Regulating the COX2/PGE(2) Pathway', *PLoS ONE*, 11: e0156549.

Zhao, Y., Wu, T., Shao, S., Shi, B., and Zhao, Y. 2016. 'Phenotype, development, and biological function of myeloid-derived suppressor cells', *OncoImmunology*, 5: e1004983.

Zheng, Y., Josefowicz, S., Chaudhry, A., Peng, X. P., Forbush, K., and Rudensky, A. Y. 2010. 'Role of conserved non-coding DNA elements in the Foxp3 gene in regulatory T-cell fate', *Nature*, 463: 808.

Zhou, X., Bailey-Bucktrout, S. L., Jeker, L. T., Penaranda, C., Martínez-Llordella, M., Ashby, M., Nakayama, M., Rosenthal, W., and Bluestone, J. A. 2009. 'Instability of the transcription factor Foxp3 leads to the generation of pathogenic memory T cells in vivo', *Nature Immunology*, 10: 1000.

Zhou, Z., French, D. L., Ma, G., Eisenstein, S., Chen, Y., Divino, C. M., Keller, G., Chen, S.-H., and Pan, P.-Y. 2010. 'Development and Function of Myeloid-Derived Suppressor Cells Generated From Mouse Embryonic and Hematopoietic Stem Cells', *Stem cells (Dayton, Ohio)*, 28: 620-32.

Zinöcker, S., Wang, M. Y., Rolstad, B., and Vaage, J. T. 2012. 'Mesenchymal Stromal Cells Fail to Alleviate Experimental Graft-Versus-Host Disease in Rats Transplanted with Major Histocompatibility Complex-Mismatched Bone Marrow', *Scandinavian Journal of Immunology*, 76: 464-70.

Zoso, A., Mazza, E. M. C., Bicciato, S., Mandruzzato, S., Bronte, V., Serafini, P., and Inverardi, L. 2014. 'Human fibrocytic myeloid-derived suppressor cells express IDO and promote tolerance via Treg-cell expansion', *European Journal of Immunology*, 44: 3307-19.

8 Supplement

8.1 Index of abbreviations

APC	Allophycocyanin
APCs	Antigen-presenting cells
BM	Bone marrow
BMMC	Bone marrow mononuclear cell
CD	Cluster of differentiation
CFSE	Carboxyfluorescein succinimidyl (diacetate) ester
DC	Dendritic cell
DMEM	Dulbecco's modified eagle's medium
ELISA	Enzyme-linked immunosorbent assay
FITC	Fluorescein isothiocyanate
Flt3-Ligand	Fms-related tyrosine kinase 3 ligand
GI	Gastrointestinal
G-CSF	granulocyte colony-stimulating factor
GM-CSF	Granulocyte/macrophage colony-stimulating factor
GMP	Good manufacturer practice
GvHD	Graft-versus-host disease
GVT	Graft-versus-tumor
HLA	Human leukocyte antigen
HRP	horseradish peroxidase
HSC	Hematopoietic stem cell
HSCT	Hematopoietic stem cell transplantation
IDO	Indoleamine 2,3-dioxygenase
IFNγ	Interferon-γ
Ig	Immunglobulin
IL	Interleukin
iNOS	Inducible nitric oxide synthase
inter	Intermediate
IU	Internationale Einheit
JAK	Janus kinase
KIR	Killer cell immunoglobulin-like receptors
MDSC	Myeloid-derived suppressor cell

MHC	Major histocompatibility complex
min	Minutes
MSC	Mesenchymal stromal cell, also known as mesenchymal stem cell
NFκB	Nuclear factor kappa-light-chain-enhancer of activated B-cells
NK	Natural killer
NO	Nitric oxide
PBMC	Peripheral blood mononuclear cell
PBS	Phosphate-buffered saline
PerCP	Peridinin chlorophyll
PI	propidium iodide
PMN-MDSC	Polymorphonuclear MDSC
RIC	Reduced-intensity conditioning
ROS	Reactive oxygen species
RPMI	Roswell park memorial institute
RT	Room temperature
SCF	Stem cell factor
SD	Standard deviation
STAT3	Signal transducer and activator of transcription 3
TGF	Transforming growth factor
Th	T helper
TLR	Toll-like receptors
TNF	Tumor necrosis factor
TPO	Thrombopoietin
Treg	Regulatory T cell
TSG-6	TNF-stimulated gene 6 protein

8.2 List of figures

8.3 List of tables

8.4 Publication and poster presentations

Parts of this study were already presented:

Publication

Siegmund DM, Schäfer I, Koch R, Singh A, Handgretinger R, Rieber N, Hartl D, and Mezger M. *Functional Assessment of Myeloid-Derived Suppressor Cells, Mesenchymal Stromal Cells, and Regulatory T Cells for the Control of T Cell Function: Implications for Graft-versus-Host Disease.* Ann Hematol Oncol. 2017; 4(1): 1132.

Poster presentations

Siegmund DM, Schäfer I, Koch R, Singh A, Handgretinger R, Rieber N, Hartl D, and Mezger M. *Functional assessment of mesenchymal stromal cells, myeloid-derived suppressor cells, and regulatory T cells for the control of T-cell function: implications for graft-versus-host disease.*
Novel Concepts in Innate Immunity
Tübingen, Germany, March 27th – 29th 2017

Brosch DM, Schäfer I, Koch R, Döring M, Handgretinger R, Rieber N, Hartl D, and Mezger M. *Therapeutic relevance of mesenchymal stromal cells, myeloid-derived suppressor cells and regulatory T cells for the control of graft-versus-host disease.*
Novel Concepts in Innate Immunity
Tübingen, Germany, September 23rd – 25th 2015

Further publications during graduation:

Ballbach M, Dannert A, Singh A, Siegmund DM, Handgretinger R, Piali L, Rieber N, and Hartl D. *Expression of checkpoint molecules on myeloid-derived suppressor cells.* Immunology Letters 2017; 192C, pp. 1-6.

Katz M, Michaelis S, Siegmund DM, Koch R, Bethge W, Handgretinger R, and Mezger M. *Association analysis between SUFU polymorphism rs17114808 and acute graft versus host disease after hematopoietic stem cell transplantation,* in press at Bone Marrow Transplantation.

8.5 Contributions

- Iris Schäfer taught me the general methods used in this study and assisted me at the beginning.
- Renate Koch assisted me with culturing of MSCs and technical implementation of single ELISAs.
- Caroline Baden assisted me with the technical implementation of the analyses regarding T-cell suppression by cell combinations and by HSC-derived MDSCs.
- Kristina Ruhm helped during an internship with culturing of PBMC- and BMMC-derived MDSCs.

8.6 Declaration

I, Darina Marlena Siegmund, herewith declare that I myself wrote the PhD thesis. I made use of only the sources and auxiliary means in word or context mentioned as such, and which I listed up completely and marked as such. I declare that I adhered to the guidelines of securing good scientific practical experience of the University of Tübingen (conclusion of the Academic Senate of 25 May 2000). I hereby affirm in lieu of an oath (Eidesstattliche Versicherung) that all these declarations are true and that I did not conceal anything. I am well aware that false declarations made under oath will be punished by a prison sentence up to three years or by a monetary penalty.

Tübingen, 10th January 2018

Darina M. Siegmund